Carbon Nanomaterials based on Graphene in (Electro-) chemical Sensors: Characterization, Modification and Application

Dissertation zur Erlangung des Doktorgrades der Naturwissenschaften

(Dr. rer. nat.)

der Fakultät Chemie und Pharmazie

der Universität Regensburg

Deutschland

vorgelegt von

Alexander Zöpfl

aus Ingolstadt

im Jahr 2015

Die vorgelegte Dissertation entstand in der Zeit von März 2012 bis Juni 2015 am Institut für Analytische Chemie, Chemo- und Biosensorik der Universität Regensburg.

Die Arbeit wurde angeleitet von Prof. Dr. Frank-Michael Matysik.

Promotionsgesuch eingereicht am : 22. Juni 2015

Kolloquiumstermin: 20. Juli 2015

Prüfungsausschuss

Voritzender: Prof. Dr. Oliver Tepner

Erstgutachter: Prof. Dr. Frank-Michael Matysik

Zweitgutachter: Prof. Dr. Otto S. Wolfbeis

Drittprüfer: PD Dr. habil. Richard Weihrich

Acknowledgements

I am very grateful to Prof. Dr. Frank-Michael Matysik for giving me the possibility to work on this topic, the helpful comments, discussions and his support.

My very special thanks go to Dr. Thomas Hirsch for supervising me. Many thanks for the great help, good advices, scientific discussions and all the other tremendous support during this time. It is really a fantastic experience working (and visiting conferences) with you!

Furthermore, I thank all my colleges from the 4th floor (especially Michael) and all the other members of the Institute of Analytical Chemistry for the friendly working atmosphere, helpful comments and support. Thanks for the superb time we spend during, but also after working hours.

I also want to thank Dr. Günther Ruhl at Infineon for the opportunity to work on this topic, the great support and discussions. Further, I thank all the pleasant colleagues I met in this company for their support. My special thanks go to Infineon Technologies AG for the financial support.

I am very grateful to the people from the Department of Physics (especially Masoumeh Sisakthi, Prof. Dr. Christoph Strunk) for the great collaboration. In this connection, I thank the DFG Research Training Group GRK 1570 for the financial support enabling additional conference visits.

Finally, I want to thank my family for their never-ending support. You are the best!

Table of Contents

Curriculum Vitae

Person

Name	Zöpfl Alexander
Adresse	Unterislinger Weg 18b
	93053Regensburg
Geburtsdatum, -ort	14.06.1986 in Ingolstadt

Ausbildung

03/2012 – 07/2015	**Promotionsstudium an der Universität Regensburg** Doktorarbeit am Institut für Analytische Chemie, Chemo- und Biosensorik (Prof. Dr. F.-M. Matysik) in Kooperation mit Infineon Technologies AG
04/2010 – 01/2012	**Master of Science an der Universität Regensburg** Hauptfach: Bioanalytik; Nebenfächer: Organische Chemie, Biologie Masterarbeitarbeit in der Analytischen Chemie (Prof. Dr. O.S. Wolfbeis) in Kooperation mit Infineon Technologies AG: „Studies of Graphene and its Modifications for Sensor Applications“
10/2006 – 04/2010	**Bachelor of Science an der Universität Regensburg** Wahlfächer: Biochemie, Nanoschience Bachelorarbeit in der Organischen Chemie (Prof. Dr. O. Reiser): „Synthese fluoreszenzmarkierter magnetischer Nanopartikel für die magnetische Transfektion“
09/2005 – 06/2006	**Zivildienst bei Lebenshilfe Werkstätten der Region 10 GmbH in Ingolstadt**
09/1996 – 07/2005	**Allgemeine Hochschulreife am Apian-Gymnasium in Ingolstadt**

Publications and Patents

Q. M. Kainz, A. Schätz, **A. Zöpfl**, W.J. Stark, O. Reiser

Combined Covalent and Noncovalent Functionalization of Nanomagnetic Carbon Surfaces with Dendrimers and BODIPY Fluorescent Dye, Chem. Mater. **2011** 23: 3606-3613

P. Palatzky, **A. Zöpfl**, T. Hirsch, F.-M. Matysik

Electrochemically Assisted Injection in Combination with Capillary Electrophoresis-Mass Spectrometry (EAI-CE-MS) – Mechanistic and Quantitative Studies of the Reduction of 4-Nitrotoluene at Various Carbon-Based Screen-Printed Electrodes, Electroanalysis **2013** 25:117-122

A. Zöpfl, W. Patterson, Th. Hirsch

Graphene for Biosensor Applications, Handbook of Carbon Nano Materials, Graphene - Energy and Sensor Applications **2014** 6:83-145

A. Zöpfl, M. M. Lemberger, M. König, G. Ruhl, F.-M. Matysik, T. Hirsch

Reduced Graphene Oxide and Graphene Composite Materials for Improved Gas Sensing at Low Temperature, Faraday Discuss. **2014** 173:403-414

A. Zöpfl, T. Hirsch, G. Ruhl

Graphene Gas Sensor for Measuring the Concentration of Carbon Dioxide in Gas Environments, Deutsches Patent- und Markenamt **2014** 102014212282.1 Anmeldedatum: 26. Juni 2014

C. Fenzl, C. Genslein, **A. Zöpfl**, A.J. Baeumner, T. Hirsch

A photonic crystal based sensing scheme for acetylcholine and acetylcholinesterase inhibitors, J. Mater. Chem. B **2015** 3:2089-2095

A. Zöpfl, M. Sisakthi, J. Eroms, F.-M. Matysik, C. Strunk, T. Hirsch

Signal Enhancement in Amperometric Peroxide Detection by Using Graphene Materials with Low Number of Defects, *submitted* to Microchimica Acta

Presentations

04/2012	Poster presentation at **Graphene 2012 in Bussels, Belgium** „The Fluorescence Properties of Graphene Oxide"
06/2012	Oral presentation at **Infineon Innovation Week in Regensburg, Germany** "Studies of Graphene and its Modifications for Gas Sensor Applications"
02/2013	Oral presentation at **7. Interdisziplinäres Doktorandenseminar in Berlin, Germany** „Carbon Nanomaterials based on Graphene in Electrochemical Gas Sensors"
03/2013	Poster presentation at **ANAKON in Essen, Germany** "Studies of Graphene and its Modifications for Gas Sensor Application"
04/2013	Poster presentation at **International Graphene Workshop of RTG 1510 in Regensburg, Germany** "Chemically Derived Graphene for the Detection of NO_2"
04/2013	Poster presentation at **Graphene 2013 in Bilbao, Spain** "Comparison of different Graphene Materials and their Electrochemical Application"
03/2014	Oral presentation at **Mikrosystemtechnik Symposium in Landshut, Germany** „Chemisch hergestelltes Graphen als funktionalisierbares Sensormaterial zur Detektion von NO_2"
05/2014	Poster presentation at **Graphene 2014 in Toulouse, France** „Comparison of Different Graphene Materials in Amperometric Sensors"
07/2014	Demonstration device and poster presentation at **Infineon Innovation Week in Regensburg, Germany** "Gas Sensitive Chemiresistors Based on Chemically Reduced Graphene Oxide"
09/2014	Oral presentation at **Faraday Discussion 173 in London, England** "Reduced graphene oxide and graphene composite materials for improved gas sensing at low temperature"
11/2014	Poster presentation at **Infineon Innovation Week in Munich, Germany** "Demonstration of Graphene in Possible Fields of Application"
03/2015	Poster presentation at **ANAKON in Graz, Graz** "Graphene Nanocomposites for Gas Sensing at Ambient Temperature"
03/2015	Poster presentation at **MRS Spring Meeting 2015 in San Francisco, USA** "Graphene Modified Electrodes for Enzymatic Biosensing"

Declaration of Collaborations

Most of the experimental and theoretical work presented in this thesis was carried out solely by the author. However, some of the results were obtained together with other researchers. In accordance with § 8 Abs. 1 Satz 2 Punkt 7 of the "Ordnung zum Erwerb des akademischen Grades eines Doktors der Naturwissenschaften (Dr. rer. nat.) an der Universität Regensburg vom 18. Juni 2009", this section gives information about these collaborations.

Graphene in Biosensor Applications (section 3.3)

The review was written mainly by the author, as well as the literature search. Chapter 2 "Glucose" and chapter 3 "Nucleic Acids" were contributed by the co-authors Thomas Hirsch and Wendy Patterson, respectively.

Signal Enhancement in Amperometric Peroxide Detection by Using Graphene Materials with Low Number of Defects (section 5.1)

This project was in collaboration with the Department of Physics of the University of Regensburg (Masoumeh Sisakthi, Prof. Dr. Christoph Strunk, Dr Jonathan Eroms). Most of the experimental work was carried out by the author solely. Preparation of electrodes with CVD and mechanically exfoliated graphene was done by Masoumeh Sisakthi. The article was mainly written by the author.

Reduced Graphene Oxide and Graphene Composite Materials for Improved Gas Sensing at Low Temperature (section 5.2)

The experimental work was carried out mostly by the author. Synthesis of the graphene modification with octadecylamine war carried out by Michael Lemberger under the author's guidance. Characterization with EDS and SEM was carried out together with Matthias König at Infineon Technologies AG and TEM by Christoph Fenzl. The article was written by the author solely.

Graphene Gas Sensor for Measuring the Concentration of Carbon Dioxide in Gas Environments (section 5.3)

The experimental work was carried by the author solely. Characterization with EDS and SEM was carried out together with Matthias König at Infineon Technologies AG.

Abbreviations

AA	Ascorbic acid
ADH	Alcohol dehydrogenase
ATP	Adenosine triphosphate
CNT	Carbon nanotube
CVD	Chemical vapor deposition
CVDG	Graphene derived from chemical vapor deposistion
DA	Dopamine
DNA	Deoxyribonucleic acid
EDS	Energy-dispersive X-ray spectroscopy
EIS	Electrochemical impedance spectroscopy
ELISA	Enzyme-linked immunosorbent assay
erGO	Electrochemically reduced graphene oxide
GO	Graphene oxide
GOx	Glucose oxsidase
IR	Infrared
LOD	Limit of detection
NADH	Nicotinamide adenine dinucleotide
NP	Nanoparticle
ODA	Octadecylamine
PCA	Principal component analysis
ppb	Parts per billion
ppm	Parts per million
ppt	Parts per trillion
rGO	Reduced graphene oxide
sccm	Standard cubic centimeters per minute
SCE	Saturated calomel electrode
SEM	Scanning electron microscopy
SG	Single layer graphene obtained by mechanical exfoliation
ssDNA	Single-stranded DNA molecules
TEM	Transmission electron microscopy
TGA-FTIR	Thermogravimetric analysis coupled to IR spectroscopy
UA	Uric acid

1 Introduction and Objectives

Pioneering research by *K. Novoselov* and *A. Geim* of the University of Manchester led to the isolation and characterization of the single atom thick layer of the carbon nanomaterial graphene in 2004 [1]. It can be described as a monolayer of sp^2 bound carbon atoms arranged in a honeycomb lattice. In 2010, the two scientists also received the Nobel Prize in physics for their innovative and groundbreaking studies. Starting from this, it has become one of the most influential materials in science and technology in the last decade.

This is reinforced by the European Commission's choice of graphene as a future emerging technology. Research in Europe involving graphene will be funded in one of the first so-called Flagship initiatives with 1,000 million euros over the next ten years [2]. The scientific and technological roadmap of the graphene flagship describes graphene as a platform with many beneficial properties. The two-dimensional material comprises extraordinary strength (Young's modulus of 1050 GPa) [3], but also high flexibility, having unique electrical (charge carrier mobility at room temperature of up to 250,000 $cm^2V^{-1}s^{-1}$) [4] and optical (~98% transparency) [5] properties. Further exceptional characteristics are its high thermal conductivity of 5000 $Wm^{-1}K^{-1}$ and high surface to volume ratio of 2630 m^2g^{-1} [6].

First applications, which can be transferred from academic research to industrial products were proposed for 2015. Transistors were predicted to lead the commercial success of the graphene story, followed by spin valves, flexible displays, radio frequency identification tags, ultra-light batteries, solar cells, ultrafast lasers, composite materials, and prostheses. Up to now the nanomaterial can be found in only a few products like graphene based conductive inks and a portable lightweight flexible power source from Vorbeck® [7], stronger and lighter tennis rackets from HEAD [8], bicycle race wheels comprising graphene enhanced composite materials from Vittoria [9] or graphene enhanced cycling helmets from Catlike [10]. This gives a short impression about the current market situation and shows that graphene still has not reached the market completely in the way it was proposed. However, many prototypes have been demonstrated, e.g. a touch panels from Samsung [11] or further portable supercapacitors from Zap&Go [12], and are expected to hit the market soon. Sensors and biosensors based on graphene have been proposed by the Flagship initiative by 2018. For the preliminary phase, a ramp up of 30 months with a total budget of 75 million euros is planned

by the European Flagship, where about 3-5% will be spent on the development of sensor technologies. Not only in Europe, but also in Asia (mainly Singapore) and in the United States, graphene is proclaimed as an important key technology. Therefore, the question arises: Will graphene be smart enough to replace some of the materials currently used in sensor technology? [partially adapted from P1]

Graphene holds great promise as tunable sensor material in miniaturized chemiresistive gas sensing applications [13]. Simple and reliable monitoring of gas concentration is important in everyday-life. In industrial processes hazardous gases need to be controlled to guarantee safety. Controlling air quality can save energy in automated air conditioning. But also the detection of environmental pollution (like NO_x) is of great interest [14]. Up to now, solid-state gas sensors based on metal oxide chemiresistors are well established in the field of chemical sensors and widely used in detecting gases [15, 16]. They are operated at high temperature [17], which consumes excessive energy and limits their long-term stability, thus leading to the development of new gas sensor concepts which overcome these drawbacks. Similar to solid state gas sensors, gas adsorption on graphene leads to a change in its electrical resistance. Therefore, any kind of interaction between graphene sheets and adsorbates, influencing the electronic structure of graphene, leads to an altered charge carrier concentration or respectively electrical conductance of the material already at low operating temperature [18, 19]. One aim of this work was to study graphene in terms of gas adsorption and its potential for gas sensor applications. [partially adapted from P2]

Since its discovery, it was suggested as highly sensitive material, allowing even the detection of single molecules [20]. The ability to work as receptor and transducer, combined with the high surface-to volume ratio results in fast and sensitive sensor responses. As a two-dimensional material, all atoms can be considered as surface atoms providing a maximum of surface, making it a very promising building block for sensor applications. Nevertheless, experimentally measured surface areas (270-1500 m^2g^{-1}) [21, 22] are remarkable but a little lower than the theoretically predicted 2630 m^2g^{-1} [6]. Many different preparation methods for graphene are known so far, but only a few of them are applicable in terms of sensor preparation (chapter 3.1). Chemically derived graphene obtained by reduction of graphene oxide (GO) [23, 24] is inexpensive, the synthesis is easily scalable and was therefore chosen for sensor preparation. The electrical properties are not as outstanding as the ones of pristine graphene due to a more defective structure [18, 25, 26]. However, it is also described that graphene with a more defective structure shows an improved adsorption of gas molecules.

[27] Furthermore, reduced graphene oxide (rGO) can be dispersed in aqueous solutions, simplifying the transfer to a substrate by e.g. spraying, printing and casting methods [28, 29]. [partially adapted from P2]

This work was motivated by the question how graphene can be modified to get a selective receptor for a certain type of analyte, especially for discriminating individual gases. Application of rGO via spin coating onto pre-structured microelectrodes comprising an interdigital structure was optimized and resulted in consistent layers of reproducible quality in terms of the electrical properties. The electrical resistance of such modified electrodes was measured in the presence of various gases diluted in synthetic air (NO_2, CH_4, and H_2) at moderate temperatures (85 °C). Chemical modifications were applied by insertion of functional groups and by doping with metals and metal oxides. The resulting materials were characterized and tested for their gas sensing behavior. It was demonstrated that a combination of functionalization of rGO lead to sensors with different characteristics, suitable to detect an individual by pattern recognition. Hereby, data analysis based on principal component analysis (PCA) can help to classify the overall detection pattern and was therefore applied. [partially adapted from P2]

Proving the feasibility of this sensor concept, another goal was to develop graphene based sensors suitable for the room temperature detection of CO_2. Since rGO itself provides bad sensing performance towards the analyte gas, different graphene composite materials were screened. Decoration with metal oxide nanoparticles (NPs) turned out to be an effective strategy to improve the sensitivity towards CO_2. Corresponding wet chemical and electrochemical preparation methods were investigated for optimization of the sensors response. Potential fields of application can be demand-controlled ventilation in buildings, which is primarily based on CO_2 detection and basically reflects the presence of persons in a room [30, 31]. This can help to reduce power consumption but also can be used in terms of security issues.

Another broad field of research is the use of graphene as electrode material, particularly in biosensing applications. It has also been reported that carbon nanomaterials comprise electrocatalytic effects in electrochemical detection systems [32]. Therefore numerous studies deal with graphene as electrode material in (bio)sensing applications [33], but often these materials are not exactly defined in their chemical structure, shape, size, or number of layers [34]. To date, most graphene employed in electrochemical analysis is chemically synthesized via oxidative methods with subsequent reduction, introducing a lot of defects and

heteroatoms [23, 35]. These materials still incorporate oxygen containing groups, which tremendously influences the electrochemical properties. Graphene derived from other methods like chemical vapor deposition (CVD) [36, 37] contain also structural defects or impurities generated by its transfer from the metallic support to an insulating substrate. Many other methods have been developed so far which allow the preparation of graphene of various sizes, shapes and quality [38]. The methods most commonly used can be classified by mechanical [1] or chemical exfoliation [39]. All of these methods are advantageous in some ways, and except the mechanical exfoliation they allow to produce large quantities of graphene. The defects in the carbon nanomaterials do not only negatively influence the conductance [40] but also offer the possibility of functionalization with e.g. biomolecules and/or metal and metal oxide nanoparticles. This step is mandatory to introduce selectivity to the system with the perspective of creating sensor platforms in great variability. Tailoring the size and morphology of the graphene in combination with other nanomaterials, results in composite materials with enhanced sensing performance [41]. Hydrogen peroxide is one of the most studied analytes in the development of amperometric detection systems based on graphene materials. For example, an enzymatic system using horseradish peroxidase immobilized onto graphene-based electrodes led to a limit of detection (LOD) of 0.1 μM [42]. Up to now there are still drawbacks assigned to this approach like complex immobilization protocols, low temporal stability, and massive influence of pH, temperature, or humidity on the enzyme activity. Therefore, great efforts have been paid for developing of non-enzymatic peroxide detection systems, using noble metals [43, 44], metal oxides and sulfides [45], and carbon nanomaterials composites [46]. These materials have been chosen for its enhanced electron transfer rates and for catalytic activity, resulting in higher sensitivities. Lin *et al*. [47] recently presented an electrochemical detection of H_2O_2 based on a carbon nanotube MoS_2 composite, with an outstanding LOD of 5 nM. Nevertheless the role of the individual materials within these composites is not fully understood yet. Another goal of this work was to investigate the influence of the choice of the graphene material itself on the electrochemical properties in direct detection of H_2O_2. Different prepared graphene materials where compared in their ability to build an electrochemical biosensor. [adapted from P4]

2 The Author's own Publications and Patents

Parts in this thesis were adapted from the author's publications or patent. The adapted text parts are indicated with [P1] - [P4]. The abstracts of the original publications are listed in this section.

[P1]

Graphene for Biosensor Applications

A. Zöpfl, W. Patterson, T. Hirsch

in *Handbook of Carbon Nano Materials, Graphene - Energy and Sensor Applications*
2014 6:83-145

Abstract

During the last decade there have been numerous studies on biosensors employing graphene materials. In this chapter, the latest approaches reported on most relevant analytes such as glucose, nucleic acids, proteins, H_2O_2, lipids, pesticides, ions and even whole cells and viruses are summarized.

[P2]

Reduced Graphene Oxide and Graphene Composite Materials for Improved Gas Sensing at Low Temperature

A. Zöpfl, M. M. Lemberger, M. König, G. Ruhl, F.-M. Matysik, T. Hirsch

in *Faraday Discussions* **2014** 173:403-414

Abstract

Reduced graphene oxide (rGO) was investigated as a material for chemiresistive gas sensors. The carbon nanomaterial was transferred onto silicon wafer with interdigital gold electrodes. Spin coating turned out to be the most reliable transfer technique, resulting in consistent rGO layers of reproducible quality. Fast changes in the electrical resistance at a low operating temperature of 85 °C could be detected for the gases NO_2, CH_4 and H_2. Especially upon adsorption of NO_2 the high signal changes allowed a minimum detection of 0.3 ppm (S/N = 3). To overcome the poor selectivity, rGO was chemically functionalized with octadecylamine, or modified by doping with metal nanoparticles such as Pd and Pt, and also metal oxides such as MnO_2, and TiO_2. The different response patterns for six different materials allow discriminating all test gases by pattern recognition based on principal component analysis.

[P3]

Graphene Gas Sensor for Measuring the Concentration of Carbon Dioxide in Gas Environments

A. Zöpfl, T. Hirsch, G. Ruhl

Deutsches Patent- und Markenamt **2014** 102014212282.1 Anmeldedatum:26. Juni 2014

Summary of the Invention

In one aspect the invention provides a gas sensor for measuring a concentration of carbon dioxide in a gas environment, the gas sensor comprising: a graphene layer having a side facing towards the gas environment; an electrode layer comprising a plurality of electrodes electrically connected to the graphene layer; and a chalcogenide layer covering at least a part of the side facing towards the gas environment of the graphene layer.

Of all materials known, graphene has the largest specific surface area (2630 m^2/g) and changes its electrical conductance as a function of adsorbed gas molecules. Since graphene is a p semiconductor under ambient conditions, the adsorption of electron donators (e.g. NH_3) reduces its electrical conductance, the adsorption of electron acceptors (e.g. NO_2) increases its electrical conductance. The amount of the change in electrical conductance correlates with the concentration of gas molecules and returns to the initial value once the gas molecules desorb. This change in electrical conductance may be measured by means of 4 electrodes structure. If the sheet resistance is significantly higher than the contact resistance toward the electrodes, it is also possible to use a 2 electrodes configuration.

The invention uses graphene, functionalized with chalcogenide, as the active sensor material. Chalcogenide is a chemical compound consisting of at least one chalcogen anion and at least one more electropositive element. The term chalcogenide refers in particular to sulfides, selenides, tellurides, and to oxides.

The functionalization improve adsorption of the desired types of gas, namely carbon dioxide, e.g. by chemically selective bonds, as well as possibly the extent of the charge transfer. Surprisingly it has been found that a class of materials that can be advantageously used for binding CO_2 is the class of chalcogenides.

[P4]

Signal Enhancement in Amperometric Peroxide Detection by Using Graphene Materials with Low Number of Defects

A. Zöpfl[†], M. Sisakthi[†], J. Eroms, F.-M. Matysik, C. Strunk, T. Hirsch

submitted to *Microchimica Acta*

[†] These authors contributed equally to this work.

Abstract

Two-dimensional carbon nanomaterials ranging from single-layer graphene to defective structures such as chemically reduced graphene oxide were studied with respect to their use in electrodes and sensors. Their electrochemical properties and utility in terms of fabrication of sensing devices are compared. Specifically, the electrodes have been applied to reductive amperometric determination of hydrogen peroxide. Low-defect graphene (SG) was obtained through mechanical exfoliation of natural graphite, while higher-defect graphenes were produced by chemical vapor deposition (CVDG) and by chemical oxidation of graphite and subsequent reduction (rGO). The carbonaceous materials were mainly characterized by Raman microscopy. The electrochemical behavior of the modified electrodes deposited on a carbon disk electrode were investigated by chronocoulometry, cyclic voltammetry, electrochemical impedance spectroscopy and amperometry. It is shown that the quality of the graphenes has an enormous impact on the amperometric performance. The use of carbon materials with many defects (like rGO) does not result in a significant improvement in signal compared to a plain carbon disc electrode. The sensitivity is 173 $mA \cdot M^{-1} \cdot cm^{-2}$ in case of using CVDG which is about 50 times better than that of a plain carbon disc electrode and about 7 times better than that of rGO. The limit of detection for hydrogen peroxide is 15.1 μM (at a working potential of -0.3 V *vs* SCE) for CVDG. It is concluded that the application of two-dimensional carbon nanomaterials offers large perspectives in amperometric detection systems due to electrocatalytic effects that result in highly sensitive detection.

3 Background

3.1 Preparation Methods and Transfer Techniques of Graphene

Synthesis of uniform graphene sheets with consistent reproduction of high quality and in large scale is still one of the main challenges for bringing graphene to commercial applications [48]. In this chapter, the most popular and promising methods are displayed, ranging from bottom-up preparation to top-down exfoliation of graphite (Figure 1). Especially the transfer of graphene structures to the desired position in an application is a crucial issue limiting the direct applicability.

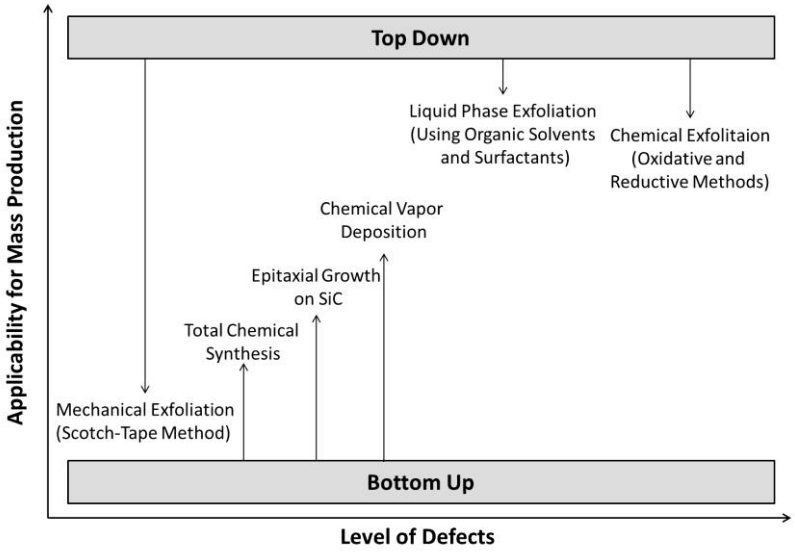

Figure 1. *Overview of preparation techniques of graphene and the influence on quality and applicability in terms of industrial production.*

The mechanical exfoliation of graphene as described by *A. Geim* and *K. Novoselov* [1] was performed by the so-called Scotch-tape method: A piece of adhesive tape is placed onto a piece of highly ordered pyrolytic graphite and is then removed. The graphite layers, which stick to the tape will be cleaved by repeating this procedure again and again. Graphite flakes are transferred from one piece of tape to another and in each step there is a chance that this layered material gets disrupted. In the last step, the transfer of the graphene to a substrate, the adhesive tape is placed onto and removed from a silicon wafer having a suitable oxide layer. The remaining graphene can be identified simply by interference contrast with an optical microscope [49]. This method allows single-, bi-, and multi-layer graphene to be

distinguished and gives access to the study of the physical properties of this unique carbon nanomaterial. Graphene obtained from this technique is of high quality and has a well ordered crystal structure [50]. For practical application, this synthesis is too laborious and inconvenient, since individual flakes of a size of few micrometers only can be produced. Two identical graphene flakes can never be obtained due to the imprecisely handling of the tape and diversity of the starting material. Therefore, nearly a dozen methods have been developed so far which allow the preparation of graphene of various dimensions, shapes and quality [38]. [partially adapted from P1]

Another method for the preparation of graphene is the epitaxial growth on SiC [51]. Single crystal SiC is annealed at 1500 °C evaporating Si atoms from the surface resulting in a formation of graphene on the SiC substrate. The crystallinity of these samples is very good, but this technique is also accompanied with several drawbacks. The starting material is very expensive and the transfer of the graphene is very difficult because of the interaction between graphene and substrate. Devices fabricated from this graphene are usually made directly on the substrate [52, 53].

One of the most promising approaches is the growth via CVD [36], utilizing the catalytic graphitization of hydrocarbon gases at a metal surface, namely Cu, Co and Ni. Here, a carbon feedstock decomposes at high temperatures of ~1000 °C and rearranges to form sp^2-carbon species [54]. The solubility of carbon in the metal is hereby of major importance. Copper provides only a low carbon solubility of ~0.03% and carbon atoms are only dissolved at the surface leading to the preferential growth of single layer graphene [55, 56]. This is a self-limiting process, since once the metal is covered with graphene the decomposition of the hydrocarbon precursor is terminated. With this technique 30-inch graphene films were realized in 2010 [57] and also prototype touch screens made out of this material have been presented in 2014 [58]. Despite the significant progress in this field, there are still some issues remaining for commercialization. Graphene grown on a metallic substrate has to be transferred for further use, usually involving wet chemical etching of the metal and stamping methods with a polymer support. This leads to contamination, but also to mechanical distortions and damage to the film and thereby has an impact on the performance in applications like touch panels [11]. Although the feasibility of such graphene applications has been shown, the material cannot yet compete with widely established materials like indium tin oxide and further improvements are needed.

The most popular concept for graphene production is the chemical exfoliation of graphite. Oxidation of graphite with strong oxidizing agents and under harsh conditions leads to a cleavage of the single carbon layers and single layers of graphene oxide (GO) are formed. Here, the Hummers method is most often used involving stirring and/or sonication of graphite in a solution of sulphuric acid and potassium permanganate [23]. The obtained product is stable in suspension and can be further reduced chemically [59], thermally [60] or electrochemically [61] forming rGO. Nevertheless, this material comprises a very defective and ill-defined structure and its electrical properties are not as outstanding as the ones of defect-free graphene. The oxidation leads to the insertion of hetero atoms like oxygen and also many topographic defects [62]. Still, these features are not always considered as a drawback. Functional groups like hydroxyl, epoxy and carboxyl groups are introduced, which enables further modification of this material. The method has the main advantages of being rapid, scalable and can be performed with basic requirements of equipment, but also the resulting product is obtained in suspension and simplifies further use. Different transfer techniques can be applied to generate graphene films and patterns, namely drop casting, spin coating, spray coating [63], Langmuir-Blodgett assembly [64] or inkjet printing [65].

Other methods for the liquid phase exfoliation of graphite have been studied and hold great promise for large-scale production [66]. A successful exfoliation requires the weakening of the van der Waals attraction between the carbon layers in graphite. The interfacial tension between liquid and solid should be low, hindering the exfoliated graphene sheets to agglomerate again. Organic solvents like *N*,*N*-dimethylformamide, *N*-methyl-2-pyrrolidone, or *ortho*-dichlorobenzene [67] and surfactants like pyrene derivatives [68] or sodium cholate [69] are suitable for this propose. Exfoliation is achieved during sonication or by introducing shearing forces. Recently, it has been shown that graphene can be prepared even with an ordinary kitchen blender in large scale, using this concept [70]. Still one major drawback is the residue of surfactant or organic solvent, which has to be eliminated after a transfer.

An interesting approach of a total bottom-up synthesis of graphene was presented by the group of *K. Müllen* [71, 72]. Polymerization of rationally designed monomers and solution mediated or surface assisted cyclodehydrogenation led to the formation of graphene nanoribbons of precise length, width, edge structure and degree of heteroatom doping. However, the solubility of the precursors is the main limiting factor and therefore the final graphene sheets are only small in dimension (length x width) ranging from 50 x 50 nm,

500 x 1.1 nm or 30 x 2 nm. Up to now, yields of this synthesis are rather low, disqualifying this method for industrial application.

All of these methods are advantageous in some ways, and most of them are able to produce large quantities of graphene. However, the resulting material does not always consist of well-defined, two-dimensional nanocrystals of unique chemical composition. Oftentimes, even within the same production technique, an ill-defined material will result and can have slightly different properties from batch to batch. The ideal graphene is characterized by a quasi-infinite size. This cannot be achieved by any preparation method. Graphene is comprised of only a surface, having no bulk phase, but there is always a border. At these edges the carbon atoms are chemically bound to hydrogen, hydroxyl, carboxyl and other impurities, influencing the characteristics of the material. So, as for every nanomaterial, the properties depend strongly on the dimensions of the material. The smaller an ideal single flake, the higher the ratio of carbon atoms located at the border to the ones within the two-dimensional crystal, and the more such a material will differ in its physical properties from pristine graphene. Furthermore, the structure itself can contain chemical functionalities or impurities, introduced by the synthesis or the transfer of this material. For rGO for example, elemental analysis showed that oxygen remains in this material. This has a tremendous influence on the behavior and the properties of rGO, which are no longer the same as found for graphene prepared by the Scotch-tape method. Additionally, many of the graphene materials synthesized have not been adequately classified and so the term "graphene" is often used for materials that differ significantly in chemical structure, shape, size, number of layers and, therefore, in their properties. This problem was previously addressed [73], but remains unresolved. The term graphene is often used without giving an exact characterization of the material. An urgent need for all carbon nanomaterials from graphene to graphite is to come to a consensus to describe this manifold of materials. Furthermore, standard characterization methods are required whereby any researcher can immediately evaluate the quality of the material, in terms of the number of layers, chemical doping, crystallite size, or presence of impurities. Practically most of this information can be obtained from Raman spectroscopy studies [74]. Therefore, it should be a mandatory first step for all works regarding graphene synthesis to present a Raman spectrum. [adapted from P1]

Despite all the advantages and drawbacks of different methods for preparing two-dimensional carbon nanomaterials, the final application of the material will always direct to the method of choice. Main issues are scaling, transfer, and reproducibility of the methods. Further possible

modifications of the material have also to be taken into account. The broad variety of graphene materials provides a versatile toolbox and therefore can be applied to many fields of application ranging from electrical devices like supercapacitors and solar cells to textiles and clothing; or ranging from flexible products like electronics to stiff lightweight applications like wind turbine blades or even cycling helmets; or large area applications like conductive paint and heating elements to nanoapplications in chemical sensors and electronic devices.

3.2 Graphene as Sensitive Material in Gas Detection Applications

3.2.1 Gas Sensing Fundamentals

Reliable detection of gaseous analytes is essential for many aspects of our everyday life. Applications are ranging from air quality control in cars or buildings for controlled ventilation [75–77], over quality control in food industry [78] to security and safety issues [79, 80]. Recognition of harmful, toxic and hazardous gases will improve quality of life. Gas sensors used so far can be principally divided in three big groups, namely spectroscopic methods, optical detection and electrochemical solid-state gas sensors. Spectroscopic methods are based on the direct analysis the vibrational spectrum or molecular mass of a target analyte enabling a quantitative detection with high precision. Optical sensors usually based on the adsorption measurements (particularly infrared adsorption) provide a characteristic fingerprint. Whereas both of these concepts are expensive and require a certain instrumental effort, sensing based on changes of the electrical properties of solid state devices can be miniaturized easily and therefore have a broader scope of application. In this context the analyte interacts with an active sensor material transducing an electrical signal that is most often potential, electrical conductance or capacitance. Depending on the measurement type, such sensors can be classified as potentiometric, amperometric or conductometric.

Especially conductometric or resistive type sensors hold great promise for the development of miniaturized chemical sensors. The change in electrical resistance due to the interaction of analyte with the sensor surface leads to changes in charge mobility or doping level of the material. Many metal oxides show response in their electrical conductance and are suitable for this propose [16]. Semiconductors like ZnO and SnO_2 are widely applied in this technology as thin-film or bulk resistor [81]. However, low electrical conductance and slow desorption characteristics limit the operation temperatures of these sensors to 250-600 °C [17], having negative effects on long term stability and power consumption [82]. A large surface area is highly desirable, to absorb as much target analyte as possible on the surface, giving a stronger response and better sensitivity. For all demands like fast response, large surface area and low operation temperature, graphene offers a possible solution. Another key issue and major challenge in the development of new sensitive materials is the cross sensitivity to other species or external influences like temperature or humidity. Gas sensors often respond to a broad variety of analytes limiting their potential fields of application. Multisensors, which consist of an array of different sensors, can be a solution for improving the selectivity. Each sensor element contributes to a dynamic response pattern helping to distinguish between

certain gases or even quantify concentrations in gas mixtures. Such sensor systems produce higher dimensional datasets, which have to be processed with multivariate statistics for evaluation. Here, PCA offers a tool to reduce the dimensions of the dataset into a manageable form enabling a simple readout.

3.2.2 Graphene in Gas Sensing Applications

Carbon based nanomaterials, are promising candidates for electrochemical gas detection at room temperature due to their intrinsic electrical properties, which are highly sensitive to changes in the chemical environment [83, 84]. Extensive research has been carried out on carbon nanotubes (CNTs) based chemical sensors [85]. A higher sensitivity compared to CNTs, but also better opportunities for device integration and low cost, make graphene a serious candidate for gas sensing devices in a commercial scenario [86].

The first graphene based gas sensor was presented by Schedin *et al.* [20] The device comprised a field effect transistor (FET) made of mechanically exfoliated graphene tailored and contacted by electron-beam lithography. Exposure to target gases like NO_2, H_2O, CO, and NH_3 led to a response which was attributed exclusively to gas adsorption and LODs in the ppb range, comparable to exiting technologies, were observed. In a complex Hall bar setup it was possible to display even the event of adsorption and desorption of a single NO_2 molecule. Nevertheless, the experimental conditions were far from reality, keeping the sensor under vacuum, applying only one gas species and recovering the sensor material at 150 °C. But they demonstrated the great potential of this material in gas sensing applications. The proof of concept inspired many other researchers to further investigate this behavior theoretically [27, 87, 88] and experimentally [89–101]. An electrochemical detection based on a resistive setup is here the most reasonable approach due to simplicity and applicability. The sensor concept is similar to metal oxide solid-state chemiresistors and was also used in the frame of this work (Figure 2). Graphene shows p-type semiconducting behavior, meaning that electron holes are the dominant species involved in the charge transport [84]. Therefore, adsorbates on the surface acting as electron donors lead to an increase of electrical resistance, whereas electron acceptors result in a decrease, respectively.

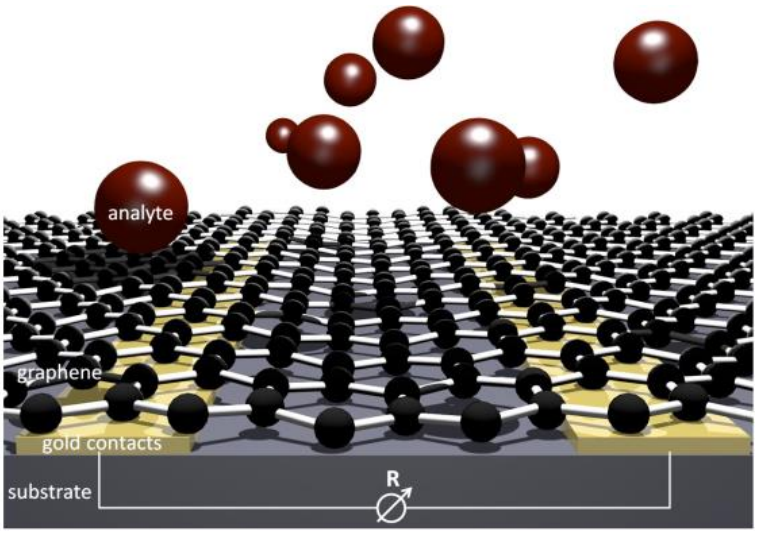

Figure 2 *Scheme of the sensor principle of chemiresistor gas sensors based on graphene.* [adapted from P2]

Comparing the graphene materials investigated as sensor material, most studies are performed with graphene of low quality like rGO. Less works deal with materials of higher quality derived from more efficient preparation methods compared to mechanical exfoliation. The use of free-standing epitaxial grown graphene enabled the detection of NO_2 in the sub-ppm range [98]. But a recovery of the sensor material was only observed after heating to 150 °C. Same observations were made by Yavari *et al.* presenting a chemiresistor based on CVD grown graphene [99]. Unfortunately, the sensor needed a treatment of 200 °C and vacuum to recover. Detection of NO_2 concentrations in the sub-ppt regime at room temperature was shown by Chen *et al.* [100], using a CVD chemiresistor, with additional *in situ* cleaning of the sensing material with UV light illumination. However, whereas most of the graphene applications benefit from a pristine graphene structure, this is not necessarily required in chemical sensors. Target gas molecules may not easily adsorb and desorb at the defect-free graphene surface [102]. Introduction of defects can be a possible solution and has been shown to improve sensitivity compared to pristine graphene [103–105]. The incorporation of hetero atoms within the graphene structure through doping with boron, nitrogen or sulfur showed to enhance the adsorption of various gas molecules [87, 106, 107]. Chung *et al*. [108] reported on the improved detection of NO_2 using ozone treated graphene sheets compared to pristine graphene. Theoretical studies underline these observations and the enhanced sensitivity was attributed to the surface active defect sites like hydroxyl, epoxy and carbonyl groups [109, 110]. These features are already apparent in GO and rGO. Chemically exfoliation of graphene is the easiest way to obtain the material and the resulting aqueous suspensions are rather simple to process. This may be also a reason why rGO is utilized as sensor material in most

studies. Numerous studies showed the highly sensitive detection of various gaseous analytes like NO_2, CO, NH_3, H_2, CH_4, H_2O, formaldehyde, ethanol and ^{i}propanol in the sub-ppm range, applying rGO into a chemiresistor setup [18, 89, 91, 111–117]. However, the low electrical conductance caused by the defects within the sp^2 structure by oxygen containing groups has to be considered. Robinson *et al.* [18] found that sensitivity and noise level are affected by the level of reduction from GO to rGO using hydrazine vapor. An increase of response and recovery time with increasing level of oxidation was observed. They also found that the noise level greatly decreased with increasing film thickness accompanied with an increase of electrical conductance, but also sensitivity decreased. In another study, Prezioso *et al*. [118] showed that good electrical properties are not necessarily needed. A LOD of 20 ppb for NO_2 was observed applying highly oxidized GO in their device. The high sensitivity was attributed to the increased number of oxygen functional groups serving as active adsorption sites. Here, a tradeoff has to be found. Optimization of the defect density is required to balance sensitivity, level of noise, response times and recovery rates of rGO-based sensors.

Nearly all of the devices presented in literature suffer from poor selectivity. Unprocessed graphene materials are sensitive to nearly any kind of surface adsorbate, which alters its electronic structure. Functionalization of the graphene material was shown to be the best way to achieve improved sensor performance and was also a goal of this work. Introduction of defects and hetero atoms [104, 119–121] or functional groups [122], decoration with metal, [123–127] and metal oxide nanoparticles [93, 128–132], and polymer composite materials [133–136] were shown to improve sensitivity to target analytes. The two major possibilities are on the one hand, to enhance the gas adsorption process offering specific binding sites and on the other hand it reduces nonspecific binding and therefore improves selectivity for a certain analyte.

3.2.3 Conclusion

Graphene based gas sensors display superior sensitivity, reversibility and lower detection limits compared to conventional metal oxide chemiresistors. They can be operated at room temperature still showing remarkable high and fast responses upon gas adsorption and therefore the carbon nanomaterial is seen as the sensor material for next generation gas sensors. However, despite all advantages some critical issues have still to be addressed. Main problem is the poor selectivity since a variety of gas molecules absorbed to surface of graphene lead to similar changes in electrical conductance. Here, chemical functionalization and also composite materials can provide a solution. Up to now, it has not been shown that the material can be tailored to superior selectivity for a single analyte. But the altered sensor response in combination with the concept of a sensor array can enable pattern recognition of single gases in complex mixtures. Another issue in terms of commercialization of such sensors is the reproducible preparation of devices, which is rarely addressed in literature. The right choice of graphene preparation, followed by specific modification of the material is mandatory. Graphene obtained by chemical and liquid exfoliation or CVD methods combined with a defined introduction of defects is supposed to be most suitable for this purpose.

3.3 Graphene in Biosensor Application

During the last decade there have been numerous studies on biosensors employing graphene materials. The following chapter summarizes approaches reported on most relevant analytes such as glucose, nucleic acids, proteins, H_2O_2, lipids, pesticides, ions and even whole cells and viruses. For modern biosensor applications, chemically exfoliated graphene is the most frequently used type. It comprises many defects and high polydispersity, yet still has plenty of interesting properties. The ability of GO being dispersible in aqueous solutions enables easy modification with biomolecules via standard immobilization techniques. If the flakes are small, the material shows weak fluorescence, which can be excited over nearly the entire visible range. After a reduction step, the previously highly distorted aromatic system will be recovered, and the resulting material has been shown to exhibit good electrical conductance, as well as promising quenching abilities. The reduced chemically derived graphene (rGO) is also dispersible in water, but does not form stable solutions. It has a high tendency to aggregate due to excellent π-stacking properties. Nevertheless, chemically derived graphene as well as GO can be processed in solution and therefore transferred to any sensor surface by dip coating, drop casting or spin coating. As the material in solution is very inhomogeneous, this is also the case for a sensor layer produced from such a solution. Furthermore, the desired one atom thick layer will not result, but rather, most likely, few-layered graphene will be deposited.

3.3.1 Biosensors for Glucose

Sensors for glucose have been now studied for more than 50 years since Clark and Lyons first proposed the initial concept of enzyme-modified electrodes in 1962 [137]. One reason is that diabetes continues to be an increasing worldwide public health problem. Sensors with good precision and accuracy are already commercially available. Such sensors consume only 100 µL of whole blood for the measurement, and results are displayed within a very short time. However, there are still many tasks and challenges for further research in glucose biosensors, for example, the electrical contact between the redox center of the enzyme and the electrode surface could be greatly improved [138]. Here, the electrical conductance of graphene could be utilized. Another demanding need in the fabrication of enzymatic electrochemical sensors is the immobilization of the biomolecule onto the electrode. In principle one can entrap the enzyme in a thin polymer film or covalently attach it to the electrode surface. For this first strategy, enzyme leaching can become an issue and long-term

stability will be critical to monitor. The second approach is often accompanied by changes in the conformation of the biomolecule and therefore, limitations in the enzyme activity are observed. Furthermore, good electrical communication between the active site of the enzyme and the electrode is mandatory for achieving high sensitivity. The ultimate compromise between the choice of materials and immobilization strategies, which results in the best biosensor for glucose detection, has yet to be established. Thus, research in the field of glucose biosensors, which can achieve high sensitivity, long-term stability, and excellent selectivity is still a hot topic. Carbon nanomaterials, and especially graphene, have become more prevalent in this research due to its good electrical transport properties, high surface to volume ratio, as well as numerous possibilities to attach biomolecules.

In amperometric glucose sensing, there are mainly two prominent detection strategies: First, those that measure the direct electron transfer from the enzyme to the electrode during oxidation of glucose. Second, those techniques, which catalyze the oxidation of the hydrogen peroxide produced by the enzyme in the presence of glucose (Figure 3). Both strategies are purported to enhance the performance by including graphene materials in the sensor design.

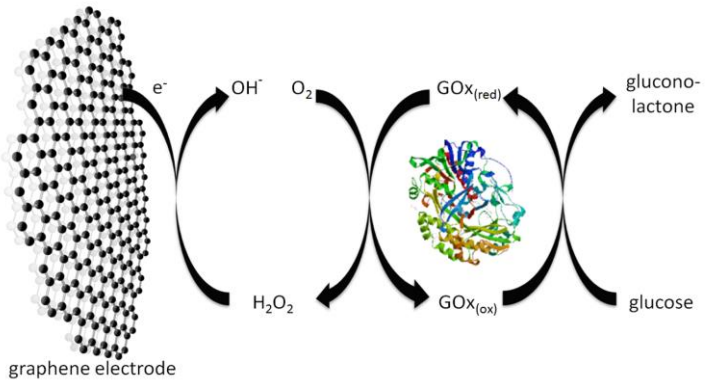

Figure 3 *Scheme of enzymatic detection of glucose.*

In the case of monitoring the direct electron transfer from the enzyme glucose oxidase (GOx) to the electrode, electrodes where the enzyme is entrapped in conducting polymers have been commonly used. However, by replacing the polymer with graphene, a mediator is no longer required. Direct electron transfer has been observed thus far on electrochemically reduced graphene (erGO) on polylysine [139], mixtures of 3-aminopropyltriethoxysilane and graphene [140], a hybrid material of multiwalled carbon nanotubes and erGO [141], mesoporous materials in combination with erGO [142], ionic liquid modified GO [143–145], bimetallic Au/Pd NP decorated erGO [146], and on CdS quantum dot modified graphene [147].

The simplest way to construct an amperometric glucose sensor containing graphene is to immobilize a thin film containing both GOx and the carbon nanomaterial onto an electrode [148–150]. Graphene oxide produced by chemical oxidation of graphite has been used in all three studies. The sensor preparations differ by the fact that in the first case a simultaneous deposition of graphene and enzyme was implemented, while in the second example, GOx was physisorped in a separate step after graphene deposition on the electrode. The sensor characteristics are nearly identical. As one example, Unnikrishnan *et al*. [148] dispersed GO together with GOx in 0.1 M phosphate buffer of pH 7. After sonication for 30 minutes the solution was drop-casted onto a glassy carbon electrode. In a further step the GO was electrochemically reduced by continuous potential cycling between -1.5 to 0 V *vs*. Ag/AgCl for 15 cycles. The authors propose that during the sonication a covalent linkage of the amino groups of the enzyme to the oxygen containing moieties at the edge planes of the GO occur. However, evidence for covalent binding was not provided. From the cyclic voltammogram of such an electrode, a redox peak at -447 mV *vs*. Ag/AgCl can be ascribed to the reduction of the FAD to $FADH_2$, a co-factor of the GOx. A wide linear range for detecting glucose from 0.1 to 27 mM was found, with no interference from AA, UA or dopamine (DA) was observed. The sensor was also successfully used to measure glucose in diluted blood serum. For improvement of the selectivity as well as the stability, an additional layer of Nafion [140] or chitosan [150, 151] was employed (Figure 4).

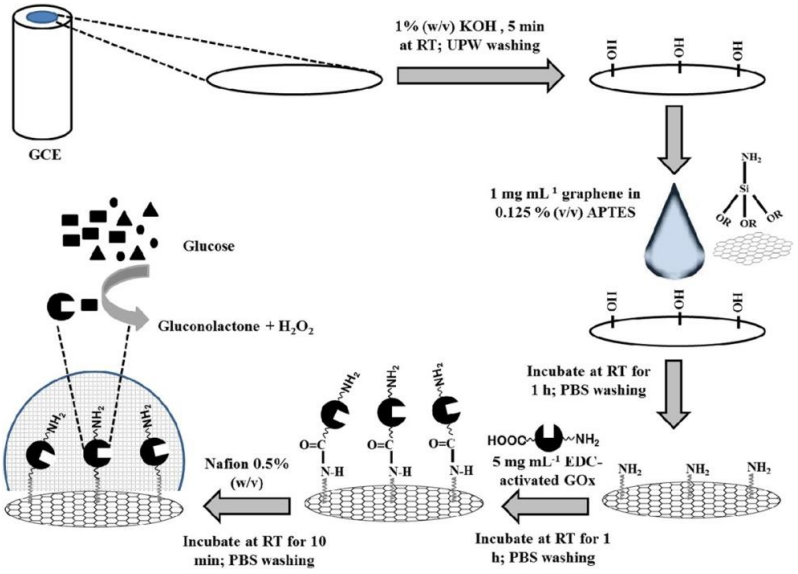

Figure 4. *Scheme of the fabrication of the electrochemical glucose biosensor with APTES modified graphene for enzyme immobilization. (Reprinted from Ref.* [140]*, Copyright (2012), with permission from Elsevier.)*

Mesoporous materials such as ZrO_2 have been used as a support material for amperometric glucose sensors [142]. The high surface area, large pore volume, narrow pore size distribution, as well as the tunable pore size, together with a modest electrical conductance, make this material an attractive host for enzyme immobilization. The sensor was fabricated by electrochemical reduction of GO on a glassy carbon electrode followed by electrodeposition of a thin chitosan film. This polymer layer provides positively charged amino groups, which helps to attach the mesoporous ZrO_2 on top by drop casting. Following the deposition of the ZrO_2 layer, GOx was loaded onto the electrode. Direct electron transfer could be observed when glucose was added. A high Michaelis-Menten constant of 28.01 mM indicated limitations in mass transport, which results in a slow response time in the minutes regime. The sensor was operated at 400 mV *vs*. Ag/AgCl in phosphate buffer of pH 7.4. The detection limit for glucose was reported as 46 µM with a linear range from 0.2 to 1.6 mM. There was no study of interference and no real sample analysis presented. Nevertheless, the high sensitivity of 7.6 $\mu A \cdot mM^{-1} \cdot cm^{-2}$ is remarkable. A comparison to the same sensor scheme without an erGO-layer resulted only in poor redox peaks, therefore one can conclude that the carbon nanomaterial is essential in providing the enhanced direct electron transfer. The simple electrostatic adsorption of the enzyme suffers from long-term stability. Therefore, rGO was modified with ionic liquids possessing positively charged groups [143]. The better adhesion of the biomolecule to the carbon nanomaterial was proposed to be due to the ionic interaction. In case of 1-(3-aminopropyl)-3-methylimidazolium bromide, the sensor covers a linear range from 2 to 16 mM [143]. For the same sensor design with 1-vinyl-3-butylimidazolium bromide as the ionic liquid a linear range from 0.8 to 20 mM was obtained [144] and with 1-butyl-3-methylimidazolium hexafluorophosphate the linear range was reported between 2 and 20 mM [145]. Such modifications using ionic liquids are not outstanding in their performance when compared with other sensors, which use direct electrochemistry for transduction.

Direct electron transfer in amperometric enzyme sensors, with and without the use of graphene, is limited due to the same reasons. The redox center is buried inside the structure of the protein, which hinders the transfer of the electrons to the electrode. Therefore, electron transfer mediators have been widely used. Qiu *et al*. [151] describe such a system which uses graphene. Their sensor is fabricated by dropping ferrocene branched chitosan, GO and GOx onto a glassy carbon electrode, as can be seen in Figure 5. Two effects are observed: First the immobilization of the enzyme is improved due to the electrostatic interaction of the naturally negatively charged enzyme in a positively charged polysaccharide. The native structure of the protein was not destroyed and no leaching was observed. Second, by the use of the redox

mediator ferrocene, the sensitivity could be enhanced to 10 µA·mM^{-1}·cm^{-2}. A Michaelis-Menten constant of 2.1 mM was calculated. The capability of this biosensor was demonstrated in measuring plasma glucose level. The response displayed a linear glucose concentration range from 0.02 to 6.78 mM with a LOD of 7.6 µM. By comparison of the resulting current densities this sensor shows 2.7 times higher signal when GO is used. The working potential of the electrode is lowered to 300 mV *vs*. Ag/AgCl, which increases the selectivity. No interference of AA or UA was found.

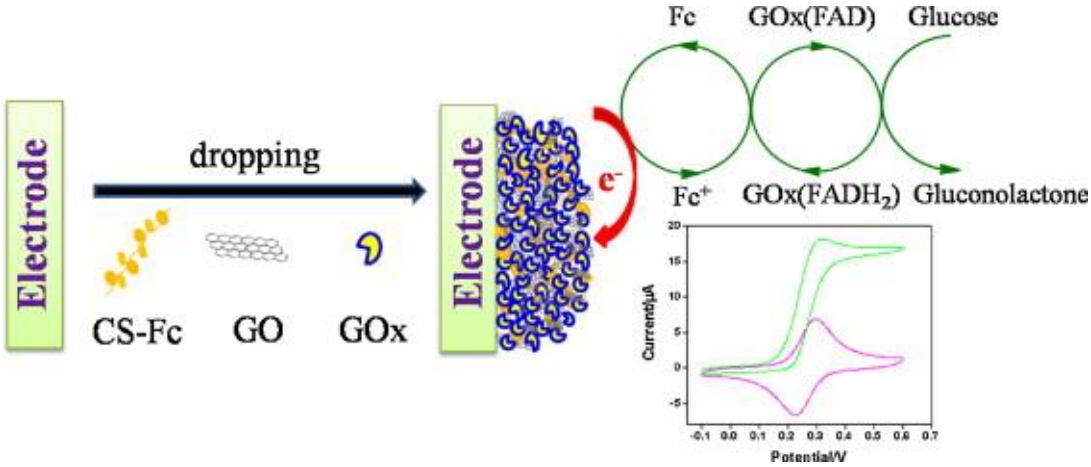

Figure 5. *Sensor design of a glassy carbon electrode modified by ferrocene modified Chitosan (CS-Fc), GO and GOx. The sensor exhibits excellent sensitivity and a low working potential of 300 mV vs. Ag/AgCl. (Reprinted from Ref.* [151]*, Copyright (2011), with permission from Elsevier.)*

A novel platform for the *in situ* chemical immobilization of GOx was developed by Chen *et al*. [152] Citric acid, which was applied to the Au NPs, was used as a capping and reducing agent. The carboxyl groups of the citric acid, along with the amino groups of the GOx, form a peptide bond when immobilization takes place. After drop casting the composite material onto a glassy carbon electrode, glucose could be detected within the range of 0.1 to 10 mM, with an LOD of 35 µM. An enhancement was found when electrochemically reduced GO decorated with bimetallic nanoparticles of 1:1 Au:Pd was used. Extreme high sensitivity of 267 µA mM^{-1} cm^{-2} was reported. The enzyme was simply physically adsorbed on top of the composite material and covered by a thin film of Nafion [146]. A detection limit of 6.9 µM with linearity up to 3.5 mM was found.

Amperometric Glucose Biosensors with Detection of H_2O_2

The glucose level often is indirectly monitored using amperometric biosensors by measuring the current in the oxidation of H_2O_2 produced during the enzymatic reaction of GOx with glucose. In the case of a glassy carbon electrode coated by a thin polymer film of chitosan incorporating rGO and GOx, the oxidation occurs at 780 mV *vs*. Ag/AgCl [153]. To enhance the kinetics and to minimize high over potentials, metal and metal oxide nanoparticles are often introduced. Low working potentials are desired to diminish the risk of interference by other electroactive substances such as ascorbate, ureate, acetaminophen, etc., which are often present in complex matrices. The introduction of additional nanomaterials for catalytic purposes is favorable for large surface area materials such as graphene. Furthermore, a support with high electrical conductance is needed to attach the nanoparticles without agglomeration. For this reason graphene materials are of great interest, as they promote fast electron transfer kinetics and allow simple preparation strategies with respect to decoration by metal nanoparticles.

Composite materials consisting of Pd NPs attached to graphene are very popular in the design of amperometric glucose sensors [154, 155]. Synthesis can be performed in one step by simultaneous reduction of $PdCl_2$ and GO in an 85% hydrazine solution [154]. The resulting nanoparticles are attached to the carbon nanomaterial. With this method agglomeration of the rGO is prevented. The electrode is modified by drop casting the nano-hybrid material. For such electrodes an increase in the LOD to 1.0 µM for the oxidation of hydrogen peroxide at 500 mV *vs*. Ag/AgCl was found. For an identical sensor but without Pd NPs, the detection limit was reported at 2.3 µM. To fabricate an amperometric glucose sensor further immobilization of the enzyme is needed. This was performed by a well-known chemical coupling procedure via glutaraldehyde, which results in a peptide bond between GOx and rGO. Additional blocking is accomplished in the same way by the use of bovine serum albumin (BSA). An alternative strategy is the functionalization of GO with chitosan and reduction of GO with hydrazine in a solution containing $PdCl_2$ [155]. A homogeneous distribution of Pd NPs within the rGO-chitosan is found. This composite material was drop cast onto a glassy carbon electrode. In a last step the GOx was chemically coupled to the electrode via glutaraldehyde chemistry. Such a sensor shows best glucose detection properties at a working potential of 700 mV *vs*. SCE with linearity in current response in the concentration range from 1 to 10 mM. The LOD was reported to be 0.2 µM for glucose. It was found that AA as well as UA interfered with the detection of glucose at such a high

electrode potential. Therefore, a suggestion was made to operate this sensor at -50 mV. Although this change in working potential increased the selectivity, the sensitivity of the system decreased by 93%.

A similar sensor concept was adapted by Claussen *et al.* [156] using Pt NPs to catalyze the oxidation of hydrogen peroxide. In contrast to other reports, they do not use a glassy carbon or a metal electrode; they used graphene on a SiO_2 wafer as the electrode material. The graphene was produced by CVD and consists, on average, of 12 layers. It was functionalized by an oxygen plasma treatment and Pt NPs were electro-deposited on the edges. The GOx was encased in a conductive polymer, poly(3,4-ethylenedioxythiophene). This glucose sensor exhibits a broad linear range from 0.01 to 50 mM, with a detection limit of 0.3 µM. The advantage of this complicated technology to produce such a sensor is to have the ability to create a sensor array by structuring the graphene by plasma treatment.

When platinum is used as a metal coordination polymer (which allows an effective adsorption of GOx), the LOD for glucose decreases to 5 nM [157]. Graphene oxide, modified with poly(*N*-vinyl-2-pyrrolidone) and reduced by hydrazine was suspended together with p-phenylenediamine and H_2PtCl_4 before being drop cast onto the electrode. The electrode potential was adjusted to -300 mV *vs.* SCE and the sensing behavior was not influenced by common interfering substances such as DA, AA or UA. Another approach describes graphene decorated with platinum-gold alloy NANOPARTICLEs, synthesized by simultaneous reduction of Pt- and Au-salts in the presence of GO [158]. As expected, such an electrode is capable of detection of glucose. An LOD of 1 µM is reported. The drawback of this study is the high working potential of 700 mV *vs.* Ag/AgCl, which limits the selectivity of this system.

Composite materials in electro-analytical sensors are most often prepared by simple drop casting of a relatively complex sensor cocktail. There has been little work done in the optimization and characterization of the resulting layer. By this simple technique in sensor fabrication it is very easy to fabricate hybrid materials consisting of different nanomaterials. Gu *et al.* [159] describe a system consisting of a composite layer of rGO with Au NPs (G-AuNP), together with quantum dots (CdSe-CdS), Au NPs and GOx within a Nafion membrane, drop casted onto a gold electrode. The electrocatalytic oxidation scheme is depicted in Figure 6. This sensor exhibits a low working potential of -200 mV *vs.* Ag/AgCl, which could increase the selectivity. One drawback of such systems may be the elaborate synthesis of the nanomaterials required to produce high quality materials in a reproducible

manner. Also such approaches often lack thorough explanations as to why exactly that particular combination of materials works best.

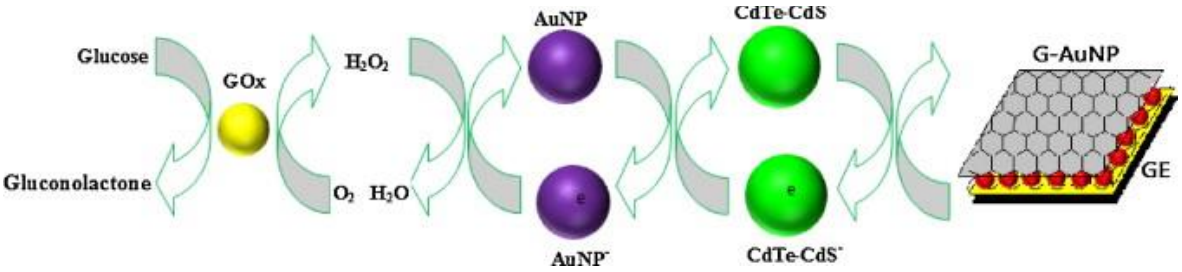

Figure 6. *Electrocatalytic oxidation of glucose in a GOx/AuNP/CdTe-Cd-S/G-AuNP/GE sensor scheme. (Reprinted from Ref.* [159]*, Copyright (2011), with permission from Elsevier.)*

Other nanomaterials that have demonstrated their ability to sense glucose which have been used in combination with graphene (albeit, reported without detailed analytical figures of merit) are ZnO [160], Pt-Au [158] and Au NPs [158]. In the case of ZnO, the hybrid material was encased with graphene, together with the enzyme, in a Nafion film. One purported advantage it that this sensor layer has excellent antibacterial properties. In another work rGO modified with ZnO was used on a glassy carbon electrode for detecting glucose via direct electrochemistry [161]. Glucose oxidase was attached by the electrostatic interaction between the enzyme and the graphene-hybrid material. The linear range of the sensor was reported from 0.02 to 6.24 mM, which in contrast to many other systems is quite narrow. A great enhancement in the sensor properties is reported when using fast Fourier transformation continuous cyclic voltammetry as a detection method in a flow injection system [162]. The sensor was fabricated by the drop casting of a dispersion of graphene and ZnO NPs onto a glassy carbon electrode, which was finally covered by a thin film of Nafion. When integrating the signal from -200 to 600 mV a LOD of 0.02 µM was found for glucose and a linear range up to 20 mM was obtained.

A layer-by-layer fabrication approach using ionic liquid modified reduced graphene oxide (Il-rGO) and sulfonated rGO (S-rGO) results in a hybrid material with a top layer of Il-rGO. As has been described by Gu *et al*. [163], the Il-rGO layer provides a positive surface charge for the electrostatic attraction of GOx and a thin film of Nafion on a glassy carbon electrode. The best sensor response was obtained using an assembly of five alternating layers. The LOD was estimated to be 3.3 µM for glucose. This sensor, operated at a low potential of -200 mV *vs*. Ag/AgCl, was applied to a micro-dialysis probe, which was successfully implanted into the

striatum of a rat. A glucose concentration of 0.38 mM was monitored online. After an injection of insulin into the striatum of the rat, a decrease in the glucose level could be observed for about 25 minutes.

In contrast, by covalent attachment of GOx via glutaraldehyde coupling, a sensor based on ERGO modified with an ionic liquid exhibits a greater linear range (0.005 to 10 mM) with an LOD of 1 µM [164]. This illustrates the fact that it is not always clear which kind of immobilization works best. Although these sensors were both operated under the same conditions and exhibit the same selectivity, the chemically immobilized enzyme sensor [164] exhibits a sensitivity that is three times higher than the sensor where the enzyme was immobilized by ionic interaction [163].

Alwarappan *et al*. [165] report a unique strategy for enhanced glucose biosensing. Here they develop a glassy carbon electrode which is electrochemically modified by polypyrrole that acts as a host material for the immobilization of GOx which is chemically functionalized by graphene. Unfortunately the covalent modification of the enzyme with the graphene was not described in a convincing way. There is no real characterization of the formation of a specific bond between graphene and GOx. The protocol involves simply mixing rGO with the enzyme in phosphate buffer and vortexing for 50 s. Further purification of this mixture from unreacted enzyme as well as excess graphene was also not described. Also the immobilization protocol of the graphene-enzyme-conjugate to the polypyrrole is completely absent. Therefore, one can only say that graphene and GOx was applied to a polypyrrole modified electrode. Nevertheless, this system is reported to detect glucose with linearity in the range of 2 to 40 µM with an LOD of 3 µM.

Most studies of biosensors used for the detection of glucose use chemically derived graphene [141–155, 157, 158, 161, 163–170], with various strategies for the reduction of the GO. Electrochemical reduction has the advantage of convenience; electrode deposition can be performed simultaneously with the reduction step. In contrast, dispersed GO allows easy modification of the carbon nanomaterial with molecules, nanoparticles or biomolecules. To recover the high electrical conductance, the functionalized GO is reduced afterwards. Many studies lack proper characterization of the carbon nanomaterial and the final composite material. Therefore, it is often not clear which parameter contributes most to the enhanced sensor characteristics. To date, there has been little work on the investigation of the influence of the doping of the graphene itself. Wang *et al*. [170] present a study where they use nitrogen-doped graphene in electrochemical biosensing. Nitrogen-doping could be a potential

strategy to regulate the electronic properties in carbon nanomaterials. By treating a chemically derived graphene with nitrogen plasma, it was possible to control the content of nitrogen atoms of the graphene from 0.11 to 1.35%. This was achieved by mixing rGO with chitosan and drop casting this mixture onto a glassy carbon electrode. The electrodes where then exposed to a nitrogen plasma for a specified time. Finally, GOx was physisorbed onto the modified electrodes. A comparison of undoped with N-doped graphene shows that there is an enhancement in the resulting peak current. This sensor could be used either to monitor the direct electron transfer from GOx or to measure the oxidation of hydrogen peroxide. The later technique was performed at 150 mV *vs*. Ag/AgCl to achieve an LOD of 10 µM and a linear range of 0.1 to 1.1 mM for glucose. Uric acid (UA) as well as ascorbic acid (AA) showed no significant interference.

In summary, much research has been made into the use of graphene in enzymatic electrochemical glucose sensing. Regarding hybrid materials, direct electrochemistry involving metallic nanoparticles for the oxidation of hydrogen peroxide was well studied. However, one can conclude that similar trends were found for the monitoring of glucose sensors with and without the use of graphene. It is interesting to note that in most published works the outstanding properties of graphene are discussed to be beneficial for the biosensor design. Alwarappan *et al*. [171] systematically investigated the influence of the graphene material itself on the immobilization of GOx and the resulting electrochemical sensor properties. It is reported that there is almost no difference in the amount of immobilized enzyme as well as in the resulting current density for single layer graphene, few layer graphene and multilayer graphene. This is surprising due to the fact that it is well known that single layer graphene is a semi-metallic conductor, whereas the multi layered material acts as a metallic conductor [172]. Therefore, one can conclude that for glucose biosensing applications, it is less important which kind of graphene material is used. The greater challenge is to find a proper way to immobilize the enzyme or to design a hybrid material, which can really improve the sensing properties in terms of better selectivity and higher sensitivity. To date, hybrid materials with Pt NPs perform best in terms of sensitivity and the indirect detection of glucose by oxidation of hydrogen peroxide is superior to the direct electrochemical detection.

3.3.2 Biosensors for Nucleic Acids

Detection, monitoring and analysis of DNA play an important role in human health aiding in the diagnosis of diseases and genetic mutations, fast detection of biological warfare agents and in the development of improved pharmaceuticals. Thus, the development of DNA detection methods with increased sensitivity and accuracy is highly desirable and is anticipated to play an ever increasing role in the future of medicine.

A typical DNA biosensor system consists of a transducer surface with an immobilized single-stranded DNA (ssDNA) probe. Upon binding with the complementary single stranded nucleic acid sequence, hybridization occurs and the pair is detected. The hybridization event is most typically measured optically, electrochemically or by mass sensitive detection. Historically, the greatest strides in DNA detection using biosensors have been made with the implementation of new or enhanced sensor materials. Such enhancers, or additives, have been critical to the advancement of this field. Various carbon nanostructures (such as carbon nanotubes) have been widely implemented in DNA biosensors. Among them, graphene has recently received particularly strong attention. This section will focus on the developments of graphene-based biosensors, which employ a variety of detection schemes, sensor additives and types of graphene for the detection of oligonucleotides.

Graphene-based DNA biosensors show great promise when applied to diagnosis of genetic diseases and environmental monitoring. The interaction between DNA molecules and graphitic materials has been studied theoretically and experimentally [173–176]. It is understood that the binding between graphene and nucleotides is dominated by the non-electrostatic π-stacking interaction [174, 175, 177–179], which explains how probe DNA is immobilized on graphene. Primarily, fluorescence and electrochemical methods are used as the sensor detection method, with other optical and electrical methods becoming more prevalent. It has been well demonstrated that the hybridization of complementary strands can be monitored with graphene-based sensors.

DNA hybridization can be detected using optical techniques such as fluorescence, chemiluminescence, surface plasmon resonance or interferometry. Fluorescence quenching is the most common and least complicated detection method used for DNA-sensors employing graphene [180–189]. A single strand of nucleic acids has a natural affinity to the aromatic system of graphene via π-stacking of its nucleobases. In this system, fluorescently labeled ssDNA adsorbs onto the surface of the graphene. The interaction between the dye molecule

and the graphene brings them in close proximity, allowing energy transfer to occur, effectively quenching the fluorescence of the fluorophore. Upon hybridization of the ssDNA with its complementary strand, the DNA desorbs from the graphene, and the fluorescence of the system is restored, as depicted in Figure 7. In such a way, so called "turn-on"/"turn-off" sensors can be constructed. Advances in the field of fluorescence DNA-graphene sensors include the implementation of multicolor monitoring for improved specificity [190]. Although fluorescence detection methods have proven to be highly sensitive, these sensors often suffer from low yield due to limited labeling efficiency, contamination issues and require complex purification steps.

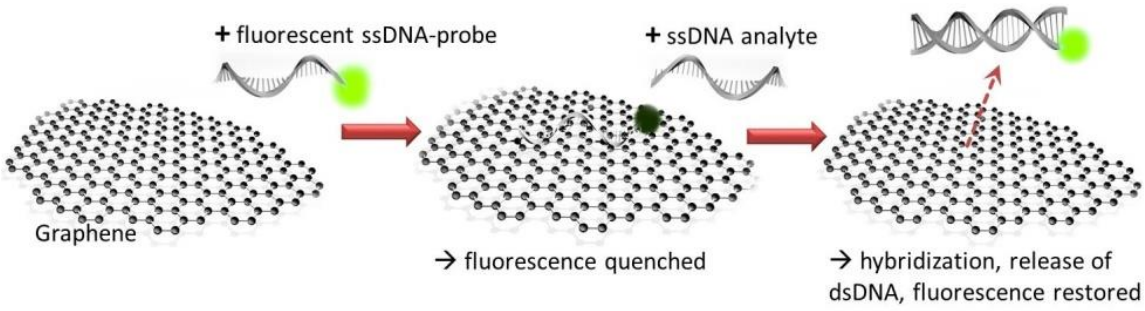

Figure 7. *Mechanism of DNA detection via fluorescence quenching of molecular beacons.*

As an alternative, electrochemical sensing is often employed as a label-free, low cost, selective and sensitive method, which detects the hybridization event and typically requires only a very small volume of material. An additional benefit of using GO in electrochemical sensing methods is that the GO can be electrochemically reduced, resulting in a more environmentally friendly and consistent rGO material. Among all types of electrochemical DNA sensors, those based on the direct oxidation of DNA are the simplest [33, 191]. In such a system, the current signals of all four free bases DNA bases (guanine, adenine, thymine, and cytosine), as well as those of ssDNA and dsDNA can be separated when chemically reduced graphene oxide is used as a mediator [192–194]. In contrast, graphite, CVD-produced graphene and glassy carbon are significantly less sensitive and thus rGO is the material of choice for most graphene-based DNA biosensors [195–198]. The very low LOD reached by using rGO as a component of a DNA biosensor for electrochemical detection methods is attributed to the high electron transfer kinetics of the system. Most attribute this to the high density of edge plane like defect sites and oxygen containing functional groups in rGO, which provide active sites beneficial for accelerating electron transfer between the electrode and species in solution. DNA biosensors based on electrochemical detection techniques also offer

the flexibility of various labels such as enzyme and metal complexes and various organic compounds. Methylene blue is a common label used in DNA biosensors for electrochemical detection. A further significant advantage of such a system is that label-free systems can also be constructed when desired. Examples of such a system are detection based on a change in capacitance or detection of the oxidation of guanine (the most redox-active nitrogenous base in DNA).

Less widely implemented is the detection of DNA by direct electrical methods [199]. The complementary DNA interacts with graphene and an n-doping (electronic doping) effect, based on the graphene-nucleotide interaction, is observed and measurable. Another up and coming technique, which has been applied to DNA biosensors is FETs [200, 201].

The immobilization of the probe DNA plays a key role in determining the final sensitivity of the sensor [202]. In that regard, graphene materials have emerged to efficiently immobilize DNA. With few exceptions [203–205], rGO or GO is used for graphene-based DNA biosensors. However, as previously discussed, due to the lack of characterization of the graphene, which is very often not included in most works involving graphene-based biosensors, it is difficult to properly categorize and compare sensor systems. Most of the recent studies of DNA-graphene-based sensors specifically involve chemically processed, multilayer rGO. This material contains a high density of reactive edges providing functional groups and adsorption sites.

It is evident when the literature is viewed as a whole while sorted by graphene type that rGO-based DNA sensors perform best when tested using electrochemical detection methods. It also appears that GO is perhaps a better choice for fluorescence based detection methods for DNA biosensors. GO acts as a weak acid cation exchange resin due to its carboxylic groups located at the basal plane (edge sites) of the GO [206]. A simple ion exchange, typically with a dye, to form an energy/charge transfer complex for complexation with GO is a common explanation for the mechanism [207, 208]. Additionally, GO is a highly suitable material for interaction with biomolecules as the carboxylic groups render the material soluble in aqueous solutions.

The sensitivity, that is, the ability of the biosensor to detect low DNA concentrations, is essential as is the selectivity and ability to detect a point mutation. With few exceptions, most sensors based on graphene detect in the nM range. It appears that rGO is the preferred type of graphene material, giving detection limits in the range of fM to aM, with graphene oxide also

giving excellent lower limits of detection in the pM to fM range. By comparison, CVD and epitaxial graphene do not provide the low limits of detection offered by rGO or even GO.

In order to meet ever-increasing demands for the detection of trace amounts of DNA, new strategies for enhanced detection and signal amplification are quickly evolving. Many past reports were based on the use of single or duplex DNA signal amplification strategies, although triplex sensing schemes are gaining more attention. The labels used in DNA biosensors are used as a storage reservoir for electrical charge. Multiple labels can be combined, often having different amplification mechanisms, to achieve excellent sensitivity. In such strategies, enzyme schemes are often combined with inorganic nanoparticles such as Au NPs. For example, in the case of one of the lowest reported LODs, Dong *et al*. [197] have developed a triplex amplification strategy, which enabled them to achieve an LOD of 5 aM with the combination of Au NPs, horseradish peroxidase (HRP) and functionalized carbon nanoparticles. This sensor was highly selective to various single-base and three-base mismatched sequences of DNA.

To further increase sensitivity, many DNA-graphene biosensor systems employ the use of nanoparticles such as quantum dots [184, 209], upconverting nanoparticles [210] or metal nanoparticles (most typically silver or gold) [186, 187, 193, 197, 199–201, 211–215], with varying degrees of success for signal enhancement. Au NPs are considered to be biocompatible and highly stable. However, inconsistent signal amplification using metal nanoparticles remains a problem. They are often used in the immobilization layer to increase the quantity of DNA, which is often functionalized with an amine group. The other benefit of Au NPs in such a sensor system is the enhanced signal provided by the plasmon resonance inherent in the properly engineered Au NPs. The adherence of such Au NPs effectively magnifies the hybridized signal, and overall, aims to provide enhanced sensitivity and a lower LOD. On a case-by-case basis, when sensors are developed with or without nanoparticle enhancers, researchers do note an improvement, albeit typically not significant, in the sensor's performance. However, to date, only a few of the top performing sensors employ such sensor additives, but rather contribute the enhanced signal to other material additives or improved detection schemes.

Another area where graphene-based DNA biosensors have recently found moderate success is in the detection of adenosine triphosphate (ATP) [183–185, 188, 210, 216–219], a nucleoside triphosphate used in cells as a coenzyme. Most biosensors in this category use carboxyfluorescein tagged ATP, adsorbed onto GO, which quenches the fluorescence. Upon

hybridization, the dye labeled ATP molecule is released from the GO, and fluorescence is restored. The LODs usually lie in the nM range. Application of some of the advanced techniques mentioned in this section could aid in the further reduction of the LOD for such biosensors.

Recently, graphene-based DNA biosensors have found application for highly sensitive virus detection [184, 189, 194, 220–224] by employing specific recognition DNA elements. SARS [189], Simian [221], and Hepatitis B [184] viruses have been detected in the nM range. Exceptional sensitivity has been obtained in the detection of HIV virus [220, 222–224], with Hu *et al*. [222] reporting an LOD as low as 34 fM. It is worth noting that the authors also tested the same sensor system with [222] and without [223] the addition of Au NPs and found no discernible difference in the achieved LOD.

3.3.3 Biosensors for Proteins

Biosensors for the detection of proteins are found in the literature with growing numbers. These are mostly developed as an immunosensor, that is, a device comprised of an antigen or antibody coupled to a signal transducer, which detects the binding of the complementary species. Miniaturization and production of small compact biosensors with sensitive detection for diagnostic use is one main area of modern biochemical and biomedical research. Indeed, graphene has the potential to play a major role in future diagnostics. To date, the role of graphene materials in biosensors has been primarily to increase of the surface area of the transducer. This sensitive layer is often comprised of a hybrid or composite material, in combination with metal nanoparticles, ionic liquids or membranes made of Nafion or chitosan.

Due to the specific binding of an antibody to its antigen, biosensors based on this interaction are widely used for the specific detection of different targets. The most common way is to immobilize antibodies onto a graphene sensor platform to form enzyme-linked immunosorbent assays (ELISA), which are more sensitive than conventional approaches. Another prominent way is the usage of dye labeled antibodies or specific aptamers. The readout is performed by electrochemical methods such as differential pulse voltammetry, FETs and impedance, or optical methods such as fluorescence or electro-chemiluminescence. In such biosensors, mainly chemically and thermally reduced GO was used for electrochemical detection and GO for optical detection approaches. Optical biosensors employing fluorescence readout schemes seem to be more sensitive by an order of magnitude in comparison with electrochemical detection methods. This section highlights the different sensor strategies by providing examples of the most prominent protein analyte targets, such as cancer biomarkers, thrombin, but also single amino acids and immunoglobulins.

Cancer Biomarkers

A major research field, which pushes the development of smaller and more sensitive immunosensors, is the detection of biomarkers. Their sensitive recognition is essential for early disease diagnosis and offers highly reliable predictions [225, 226]. Therefore, many works investigate and optimize the detection of model markers, especially cancer biomarkers such as alpha-fetoprotein [227–230], prostate-specific antigen (PSA) [231–233], cyclin A2 [234, 235], phosphorylated p53 [236, 237], carcinoembryonic antigen [238, 239], Integrin

avb3 [240], or progastrin releasing peptide [241]. Nearly all of the works combined a sandwich assay with electrochemical readout of the coupled enzymatic reaction.

A very representative electrochemical immunosensor was prepared by Yang *et al.* [242] investigating the detection of PSA, an important tumor marker for clinical diagnosis of prostate cancer. In their work, thermally reduced GO was used in two ways (see Figure 8) to promote the sensitivity to a LOD of 1 pg mL^{-1}. On the one hand, it was applied as an electrode material for the immobilization of a primary antibody via π-π-interactions of a linker molecule. On the other hand, it was used as a support to build up a label consisting of a secondary antibody, HRP and a mediator thionine. The biosensor was prepared by incubating the electrode with PSA solutions of different concentrations, washing, incubating with the label and washing again. The more PSA that was bound, the fewer labels that were attached to the electrode, resulting in a lower amperometric response against fixed H_2O_2 concentrations. This leads to a wide linear sensitivity of 0.002 - 10 ng·mL^{-1}. The large surface-to-volume ratio (leading to a high enzyme loading of the label) and the good electrical conductance of graphene are the main reasons for the improved sensitivity. To test interference and applicability, the immunosensor was tested towards human immunoglobulin G, BSA, vitamin C, glucose, and human serum samples. Satisfactory test results were obtained in comparison with a commercial ELISA system.

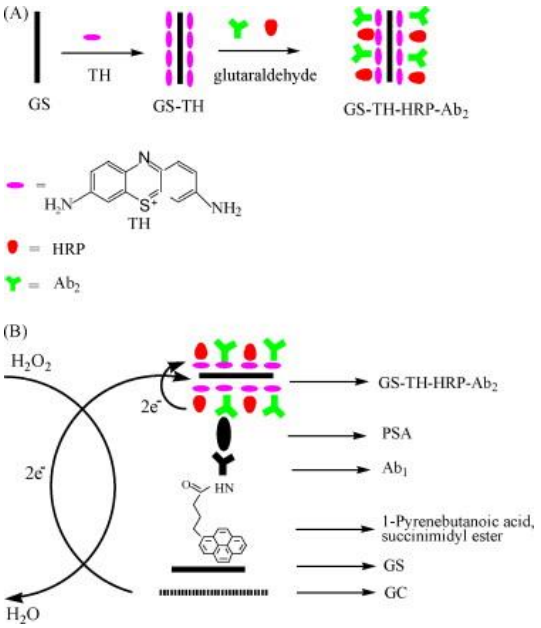

Figure 8. *Schematic representation of preparation (A) and mechanism (B) of the graphene (GS) based immunosensor for PSA. (Reprinted from Ref.* [242], *Copyright (2010), with permission from Elsevier.)*

The main challenge in constructing good labels is to obtain a high loading of enzyme and secondary antibody onto a support material. Therefore, Au NPs, but also several carbon nanomaterials and their composites were demonstrated to be applicable.

Another promising amplification strategy for clinical screening of cancer biomarkers and point-of-care diagnostics was developed by Du *et al.* two years before [243]. Here, the primary alpha-fetoprotein antibody was attached to a screen-printed carbon electrode, which modified with thermally reduced GO and chitosan. The label was comprised of carbon nanospheres loaded with a secondary antibody and HRP. Using two carbon nanomaterials as a support for the antibody coupling also resulted in a quite low LOD of 0.02 $ng \cdot mL^{-1}$ and a linear sensitivity up to 6 $ng \cdot mL^{-1}$. In contrast, measurements without graphene showed a 7-fold decrease in detection signal. With this sensor approach, graphene-based biosensors became competitive with common ELISAs in terms of reproducibility and precision for the investigation of human serum samples.

The detection of biomarkers is also possible via electrical conductance measurements, as was demonstrated by Zhang *et al.* [244] Their biosensor was built-up like a common sandwich-assay as previously mentioned, with rGO as support and HRP bound to a secondary antibody. But instead of detecting only H_2O_2, AA was converted by the enzyme and led to a local pH shift at the graphene surface, resulting in a change of the electrical conductance of the graphene itself. Though PSA could be detected down to an incredible range of 4 $fg \cdot mL^{-1}$ to 0.4 $pg \cdot mL^{-1}$, the sensor was highly unspecific. The electrical conductance of graphene is highly sensitive to any molecule adsorbing onto its surface. Operating such a senor under real conditions could cause some problems due to unspecific binding.

A solution was given here in a recent study of Kim *et al.* [231] by implementing a FET, consisting of an electrically contacted layer of rGO, modified only with a PSA antibody. In addition, they presented an efficient scheme for the formation of homogeneous sensor layers due to the self-assembly of GO on a positively charged support with subsequent chemical reduction. To prevent unspecific binding, the modified rGO as well as the Au electrodes used for contacting were blocked. This enabled the specific binding of only the analyte with the immobilized antibodies and therefore the detection of PSA in real blood samples in the range of 0.1 - 10 $ng \cdot mL^{-1}$.

Thrombin

In addition to the detection of cancer biomarkers, thrombin is an important analyte in molecular biology in terms of regulation of tumor growth, metastasis and angiogenesis [245]. One of the most commonly used strategies for thrombin detection is based on aptamers, which are selected single-stranded oligonucleotides, which bind with thrombin with excellent specificity [246, 247]. The sensor principle is similar to the typical DNA detection scheme using graphene and has been previously explained in Figure 7. The analyte in this case is a peptide, which binds to the fluorescently labeled aptamer. The pair is then released from the graphene, whereby fluorescence is restored. This was shown in the work of Chang *et al.* [248], where by simply using rGO and a FAM-labeled aptamer, they were able to detect thrombin down to an impressive LOD of 31.3 pM. Although the system led to good results in serum samples, the linear range was only in the region of pM. One major criticism was the poor long-term stability of the rGO suspensions. By simply applying the not reduced GO, it is possible to detect thrombin in concentrations ranging from 40 pM to 10 nM [218] or even higher [188, 249, 250].

There are also some approaches to detect thrombin electrochemically [251–254]. For example, an ELISA-like biosensor has been constructed by replacing primary and secondary antibody by the aptamer as was shown by Bai *et al.* [253] With their system, they were able to improve the sensitivity to a LOD of 11 pM and a wide linear range up to 45 nM, which are impressive results for electrochemical detection. Label free biosensors showed comparable and even slightly better results [251, 252, 254]. For these aptasensors, an electrode was modified with rGO, and a thrombin binding aptamer was immobilized on top. If the analyte now binds on the surface of the electrode, an electron transfer barrier for redox probes is formed and leads to a decrease in current with increasing thrombin concentrations. Here, one outstanding work of Wang *et al.* [251] achieved a sensitivity range on the level of fM. Readout via EIS without any redox probe was also possible [252]. The benefit of the graphene in this sensor platform is explained by the greatly enhanced charge transfer of the carbon nanomaterial. Therefore, one main reason for the outstanding sensitivity could be the linkage of the aptamer to the electrode. In the work of Wang *et al.*, this was accomplished via covalent peptide bonding, whereas other studies only coupled the compounds via physical adsorption onto rGO [252] or thiol-gold molecules [254] which resulted in poorer sensitivity.

Amino Acids

Aptamers can also be used for the detection of smaller peptides such as glutathione [255, 256] or even single amino acids such as L-histidine [257], L-tyrosine [258], and especially cysteine (Cys) [249, 255–257, 259–261]. Cys has many vital biological functions and a wide range of physiological and pathophysiological effects [262]. For this category of biosensors, most works gain improved sensitivity by taking advantage of the high quenching efficiency of GO and DNA hybridization. Often dye labeled ssDNA is used, which in the end binds to GO in the absence of Cys or is released in the presence of Cys (Figure 9) and leads to an increase in fluorescence intensity.

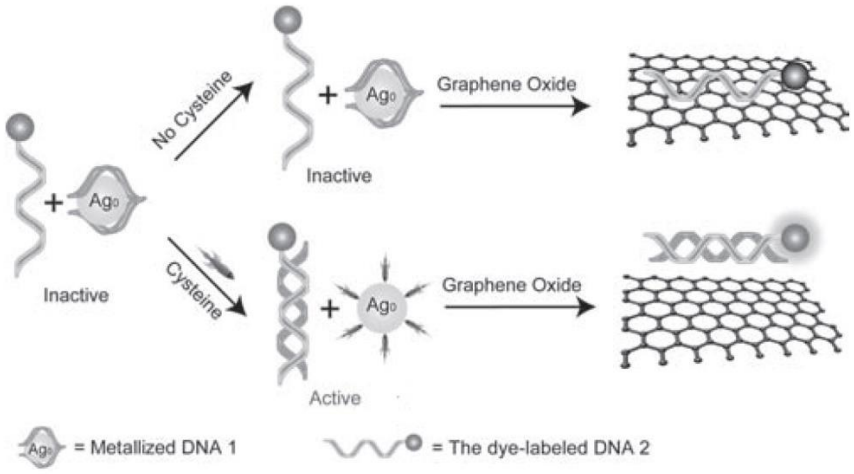

Figure 9. *Schematic illustration of a turn-on fluorescent detection of cystein by using GO as quencher. (Reprinted with permission from Ref.* [261]*, Copyright (2011), WILEY-VCH Verlag GmbH & Co. KGaA, Weinheim.)*

Here, Lin *et al.* [261] used a thiol-activated ssDNA, which is bound to Ag NPs and is complementary to the dye labeled strand. Cys then binds to the Ag surface and releases the previously bound ssDNA, which itself causes the release of the dye labeled DNA from the GO. This leads to detection in the nM range. This was also achieved by Xie *et al.* [260] by using Ag^+ ions and a cytosine-rich DNA probe, which interacts with the ions in absence of Cys. This system was also capable of detecting Ag^+ also in the range of nM. However, all of these approaches are based on metal/thiol interaction and are therefore not specific to different thiols. In real samples one should always consider other biothiols, which could interfere [255]. Measuring biothiols in general is still of great interest, as its level in plasma is a diagnostic tool and is related to diseases such as HIV [263].

Immunoglobulins

The detection of immunoglobulins is often performed in blood serum samples and the preferred sensor concepts on this field are ELISAs with electrochemical readout [264–266]. This concept has been previously described and can be adapted by simply changing the recognition antibody. Additionally, there are other approaches such as the development of specific G-FETs with single graphene flakes (Figure 10) [267–269]. In FET devices, electrical detection is used which exploits the change in electrical conductance that arises when molecules adsorb on the surface of the sensors. Benefits of FETs are label-free and online detection, but also the possibility of miniaturization towards a nanoscale-size complete sensor. There are different strategies for the recognition element on graphene, either applying specific antibodies on Au NPs [269] or aptamers via π-π interaction of linker molecules [268, 269]. All of these schemes realize selective detection in the nM range and are promising for the electrical detection of biomolecules. There are varying feasible explanations for the mechanism as to how analyte binding influences the electrical conductance of the graphene [270, 271], but none of them have been explicitly proven.

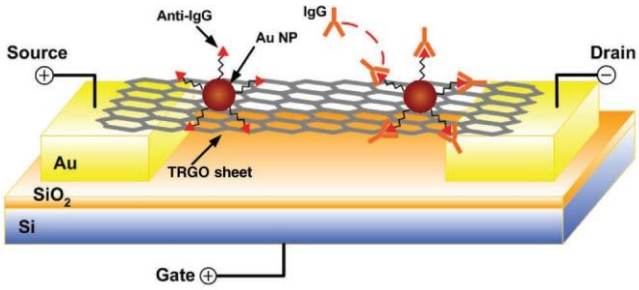

Figure 10. *Schematic of the measurement setup using a G-FET for the detection of IgG. (Reprinted with permission from Ref.* [269]*, Copyright (2010), WILEY-VCH Verlag GmbH & Co. KGaA, Weinheim.)*

Finally, many other biosensor approaches with graphene for different protein analytes have been investigated, including model analytes such as BSA [272], streptavidin [273] or TATA-binding protein [274], but also clinical and biological relevant substances such as platelet-derived growth factors [253, 275], lectins [276], hemin [277] or vasopressin, neurohypophysial hormone [278, 279]. There are also various enzyme assays with fluorescence readout, using graphene and phosphorylase D [280], captase-3 [281], matrix metalloproteinase 2 [265, 282] or lysozyme [283]. In these works, graphene (mostly GO and rGO) was again used as a support material, electrode surface or quencher as described previously. The sensor concepts differ only slightly from those mentioned above.

This section illustrates the versatility in graphene application for protein analytics. By immobilization of specific recognition elements such as enzymes, antibodies or aptamers in combination with graphene, a broad spectrum of selective biosensors with impressive LODs were constructed. Many of the sensor strategies could be adapted for other biomarkers, target protein or other immuno targets.

However, explanations as to why certain combinations of materials result in better sensitivity are lacking and descriptions of particular mechanisms with respect to the graphene are often missing. Major advantages are improved sensitivity, less expensive production and smaller sensor device, which could enable better point-of-care diagnostics and aid in early disease recognition. However, to date, there is no commercial biosensor based on graphene, which could potentially replace the older and more laborious techniques.

3.3.4 Biosensors for other Biologically Relevant Analytes

Aside from carbohydrates, nucleotides and proteins, there are several approaches to detect smaller biomolecules such as lipids and biologically relevant substances such as pesticides, alcohols single cations, anions and also whole cells and viruses.

Cholesterol is an important lipid and its accumulation in blood is related to hypertension, arteriosclerosis, and heart disease [284, 285]. Conventional methods such as spectroscopic, colorimetric, non-enzymatic and other electrochemical approaches suffer from poor specificity and difficulty of analyte standardization [286, 287]. Using a graphene electrodes modified with cholesterol oxidase enables electrochemical detection in the range of µM, whereas an additional decoration with Pt NPs [288] or Au NPs [289, 290] leads to more sensitivity. Further attachment of cholesterol esterase enables the detection of cholesterol esters [288, 291]. But in principle the concept is analogous to the electrochemical enzymatic detection of glucose, as described previously. Metal nanoparticles enhance the conversion of H_2O_2 and their attachment to a graphene modified electrode surface leads to more sensitive recognition. The readout of the H_2O_2 produced could also be realized via ECL with luminol, additionally catalyzed by the iron ions of hemin, which was attached to the graphene [292]. This resulted in an LOD of 0.06 µM, which is two orders of magnitude lower compared to the biosensors mentioned above.

Hydrogen peroxide is an important molecule in biological processes. It occurs as enzymatic byproduct of oxidases or as substrate of peroxidases [293]. Furthermore it is an essential mediator in food, pharmaceutical, or clinical analyses [33]. Therefore, also a lot of sensor approaches, which are using graphene materials are described. The sensor principles are almost the same as have been presented for the glucose sensors, except the usage of other enzymes. Horseradish peroxidase is the most common enzyme to detect hydrogen peroxide [294–307]. The enzyme is adsorbed or immobilized on electrodes surfaces together with GO or rGO. The working potential could be decreased from -400 mV *vs*. SCE [296] by additional incorporation of metallic nanoparticles [294, 298, 299, 305] to -200 mV *vs*. Ag/AgCl, which makes these sensor more selective towards other electro active substances such as AA, UA or DA. The selectivity could also be enhanced by applying perm-selective membranes, which keep away potential interfering substances from the electrode surface. Nafion [302], chitosan [306] or poly-lysine [297] have been used. Remarkable high sensitivity, with a LOD of 10 nM is reported for a system comprising of rGO, HRP, Au NP and thionine [299]. The linear change in the sensor signal ranges from $0.5 \cdot 10^{-3}$ to 1.8 mM. Yet, most sensors reported so far

cannot compete with luminescent probes, which may have the additional benefit that they can be used for the detection of hydrogen peroxide in cellular analysis [308].

The detection of alcohols is easily achievable by also simply changing the enzyme. The enzymatic detection of ethanol with alcohol dehydrogenase (ADH) always involves the sensitive recognition of the cofactor NADH. In conventional electrodes, the over-potential of NADH is greater than 0.6 V (*vs*. Ag/AgCl) [309], which could lead to interference problems in real samples [310]. When graphene is implemented as an electrode material, rGO is typically used, as it enables oxidation of NADH at lower potentials and therefore leads to less cross sensitivity. Many works investigated different sensor electrode additives such as Nafion, [311] chitosan [312] or methylene green [313]. They yield good results, even for common samples, such as wine or beer [312]. Simply casting ADH onto an rGO modified electrode leads to sensitive detection in the range of µM, at a very low potential [314]. Like in other sensor approaches, the question here arises, as to whether complex graphene composites are even necessary at all, since they do not appear to drastically improve the sensitivity. By applying a ruthenium (II) complex to the biosensor, the detection of NADH could be performed again via ECL and was a slightly more sensitive than other approaches [315].

Other biological compounds of interest which have been investigated with graphene-based biosensors are acetic acid, DA [316], UA [316, 317], glucosamine [318], acetylcholine [319], oxygen [302, 320] and clenbuterol [321]. Since all of them use similar strategies that were previously discussed, they will not be explained here again in detail. Again, rGO and GO are used mainly as an electrode, substrate or label material due to their outstanding features. Biosensors with remarkable sensitivity and selectivity were prepared by simple attachment of enzymes, antibodies or aptamers.

In addition to small molecule detection, there are also approaches to detect even whole bacteria or image cells with techniques previously. E.coli bacteria were detected by attaching a specific antigen onto a CVD graphene FET and monitoring the change in electrical conductance when the bacteria are bound to the sensor surface [322]. Although the detection is not completely selective, and the sensing parameters are not suitable for a portable biosensor, this could still find application in assays for drug screening. Sulfate reducing bacteria were detected by a common assay with specific antibodies where GO enhanced the potentiometric stripping analysis (PSA), but also the colorimetric detection [323]. GO sheets were labeled with secondary antibodies, which bind to target bacteria previously attached to the assay. In a further step, GO promotes the reduction of Ag(I) to Ag NPs, which are needed

for a further readout (Figure 11). In another study, they used an electrode covered with rGO covalently modified with aptamers for the specific capture of different cancer cell lines [324]. Only upon cell adhesion, the redox signals of a mediator decreased due to the formation of an inert barrier by the cells.

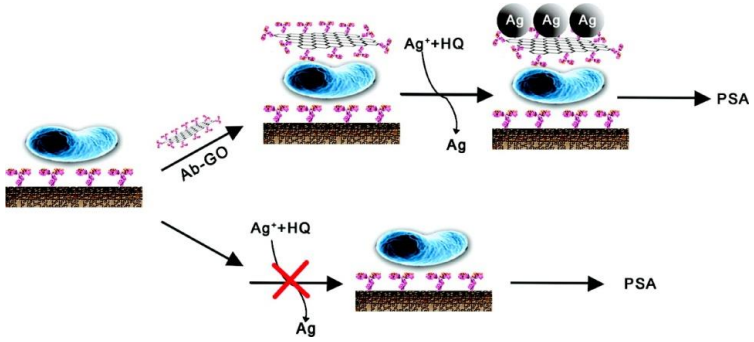

Figure 11. *Schematic representation of a GO based immunoassay combined with silver enhancement for the detection of sulphate-reducing bacteria (SBR). (Reprinted with permission from Ref.* [323]*, Copyright (2010), American Chemical Society.)*

An optical readout was used for the detection of a rotavirus [325]. GO was used here as transparent substrate material, which was further functionalized with antibodies via peptide bonding, but also served as fluorescent dye. A secondary antibody was labeled with Au NPs and through FRET the fluorescence of GO was quenched. With this setup they were able to selectively detect the virus to an LOD of 10^{-5} pfu·mL^{-1}, comparable to common ELISA technology [326].

In a different optical approach, GO was applied as quencher of dye-labeled aptamers, as described previously in the DNA section. Pei *et al*. [272] were able to detect and distinguish between different proteins and also various cell types with the appropriate aptamer receptor. This again demonstrated the broad and easy adaptation of affinity-receptor based applications for which GO can be used. The detection of cancer cells could be one interesting application for this setup and has already been demonstrated in a microfluidic system [327].

3.3.5 Conclusion

The research discussed in this chapter shows that graphene has been extensively studied in biosensors for the detection of glucose, DNA, various proteins, bacteria, and even whole cells. Nevertheless, the advantages of including graphene in a biosensor scheme are not always readily apparently. The lack of a consistent preparation method for large scale-synthesis of well-defined graphene complicates the situation greatly. Most studies are based on rGO which itself is an inhomogeneous material. The oxygen containing groups enable the adaption of well-established immobilization techniques for biomolecules, receptors and linking molecules. Working with this material and the severely lacking material characterization make it difficult to compare results from one sensor concept. This is viewed as a severe hindrance to the success of graphene-based biosensor development.

In order to exploit all of the extraordinary properties of graphene at once it is necessary to produce high quality material on insulating, flexible substrates. The development of ultrasensitive devices is challenging, but the impact of such technology can be great. Novel concepts for surface nanostructuring based on semiconductor technology and for nanopatterning using chemical approaches are needed. Graphene on its own has high sensitivity but without any selectivity at all. One possibility to introduce selectivity is direct chemical modification. Another possibility is to design composite materials together with other nanomaterials.

For all of the optimistic and promising perceptions of graphene, three essential questions for becoming a commercial success in chemo- and biosensors still remain: 1) Is there anything beyond a good paper? 2) Will it be possible to produce more than one device? 3) Can it compete with already existing products? As of now, these questions still are open. Yet, the material cannot compete with existing biosensors, but the constant development and improvement of the preparation and processing techniques can change the situation. One exception seems to be the detection of oligonucleotides using graphene-based biosensors. Electrochemical detection methods provide the best sensitivity when combined with rGO, with typical detection limits in the range of fM to aM. Although GO also yields excellent lower limits of detection in the pM to fM range, CVD and epitaxial graphene do not provide the low limits of detection offered by rGO or even GO. Additionally, the immobilization of DNA onto graphene is relatively easy and understood. With the advancement of sensor additives such as polymers and nanoparticles, and improvements in detection schemes,

graphene can be a leading sensor material in DNA biosensors competitive with other technologies.

The most significant strides will not be made by imitating or improving well-established sensor technologies, but rather by focusing on exploiting the truly unique properties of carbon nanomaterials and in finding new applications and markets. Some of these properties include extremely high surface-to-volume-ratio of graphene, together with its transparency, high electrical conductance, as well as its flexibility, which could lead to new miniaturized biosensors and sensor arrays having high sensitivity, long term stability, multi-detection capabilities and ultrafast response.

[Chapter 3.3 was mainly adapted from P1]

4 Experimental

4.1 Materials and Instrumentations

Unless otherwise stated, all chemicals were of analytical grade and purchased from Merck (www.merck.de, Darmstadt, Germany) or Sigma-Aldrich (www.sigma-aldrich.de, Steinheim, Germany) and used without further purification. Ultra-pure water (0.055 $\mu S \cdot cm^{-1}$) was used in all experiments. All gases and mixtures were purchased from Linde AG (http://www.linde-gas.de, Pullach, Germany).

Characterization with Raman spectroscopy was performed on a Thermo Scientific DXR Raman microscope with a 532 nm excitation laser (10 mW). Optical images were made with a Leica DMRB microscope. Scanning electron microscopy (SEM) was performed with a Zeiss Ultra 55 and on a JOEL JSM-6700F, as well as the energy-dispersive X-ray spectroscopy (EDS), and thermogravimetric analysis coupled to IR spectroscopy (TGA-FTIR) with a Netzsch Iris TG209 connected to a Bruker Equinox 55, all at Infineon Technologies AG Regensburg. Transmission electron microscopy (TEM) was performed using a 120 kV Philips CM12 microscope. Electrochemical characterizations and measurements were performed on a CH Instrument electrochemical analyzer Model 602a, using a three-electrode system consisted of a Pt wire as counter electrode and a saturated calomel electrode (SCE) as reference electrode and graphene electrode as working electrode (chapter 4.4). [partially adapted from P2 and P4]

4.2 Preparation of Different Graphene Materials

Single layer graphene (SG) was obtained through micromechanical exfoliation of graphite flakes (NGS Naturgraphit GmbH, Leinburg, Germany) using an adhesive tape, and transferred onto a Si substrate with a 300 nm thick SiO_2 insulating layer. This kind of graphene flakes is random in shape and size, with a typical size of about 50 μm^2.

Graphene obtained by CVD (CVDG) was purchased on Si/SiO_2 substrates (www.graphenea.com, San Sebastian, Spain). Electron beam lithography and reactive ion etching (O_2/Ar) was used to remove excess graphene, forming rectangular graphene electrodes of about 0.04 mm^2 in size.

Reduced graphene oxide (rGO) was prepared by a slightly modified Hummers method [23] with subsequent reduction [24]. Briefly, 1 g of China flake graphite (K. W. Thielmann & Cie KG, Grolsheim, Germany) was mixed with 0.75 g $NaNO_3$ in 75 mL conc. H_2SO_4 and 4.5 g $KMnO_4$ was added in small portions under vigorous stirring and cooling in an ice bath. The mixture was sonicated for 3 hours and stirred for 3 days at room temperature. After the addition of 75 mL of 5% H_2SO_4 the mixture was heated at 100 °C for 2 hours, followed by an addition of 15 mL of 30% H_2O_2 and constant stirring for 1 hour at room temperature. For purification, the produced GO was washed with the following solutions: four times in 3% H_2SO_4 containing 0.5% H_2O_2; two times in 3% HCl; three times in water. Finally it was dialyzed against 2 L water (14 kDa cut-off) for 10 days, changing the water three times. For the chemical reduction of GO, 7 mL of a GO suspension (0.5 $g \cdot L^{-1}$) were mixed with 31 µL of 32% NH_3. After adding 5 µL of 98% hydrazine hydrate the reaction mixture was refluxed for 1 hour at 100 °C. The resulting black suspension was washed with water and isolated by centrifugation. [partially adapted from P4]

4.3 Modification of Graphene Materials

Functionalization of Reduced Graphene Oxide with Pd and Pt Nanoparticles

Both approaches were adapted from a preparation of graphene-metal nanocomposites by Xu *et al*. [328] and modified slightly. 5 mL of a GO suspension (1 $mg \cdot mL^{-1}$) were mixed with 10 mL ethylene glycol. Afterwards 0.5 mL of a 0.01 M solution of metal precursor (K_2PtCl_4, respectively $PdCl_2$) in water was added and the mixture was first stirred for 30 min at room temperature and then 6 hours at 100 °C. During the heating in both cases the color changed to black indicating that the GO was reduced by ethylene glycol. The resulting suspensions containing the metal-doped carbon nanomaterials (rGO-Pd and rGO-Pt) were centrifuged and washed three times with water. [adapted from P2]

Functionalization of Graphene Oxide with MnO_2

A synthesis for GO-MnO_2 nanocomposites was adapted [329]. 5.1 mg GO and 21 mg $MnCl_2 \cdot 4H_2O$ were dispersed in 5 mL ^{i}propanol and sonicated for 30 min. The reaction mixture was refluxed at 83 °C under vigorous stirring. Afterwards a solution of 12 mg $KMnO_4$ in 0.4 mL water was added and the slurry was refluxed at 83 °C for another 30 min, before it was cooled to room temperature. The composite material was then centrifuged and washed twice with water. The resulting brown product was dried at 60 °C over night. Thermal reduction of GO was performed after the composite was applied to a microelectrode (chapter 4.4.1) heating it to 230°C for 30 s. [adapted from P2]

Functionalization of Reduced Graphene Oxide with TiO_2

For the functionalization of carbon nanomaterials Li *et al*. [330] have reported the modification of single-walled carbon nanotubes by TiO_2. In analogous way rGO was modified with TiO_2 (rGO-TiO_2): 1 mg of TiO_2 with an average particle size of 1 µm was ground thoroughly. Subsequently, the powder was dispersed in 2 mL water, sonicated for 1 hour and 1 mL of an aqueous rGO suspension (0.5 $mg \cdot mL^{-1}$) was added. After another 1 hour sonication a grey suspension was formed where the modified rGO flakes highly tended to aggregate. [adapted from P2]

Functionalization of Graphene Oxide with Octadecylamine

To modify rGO with octadecylamine (ODA), a synthesis of surface functionalized graphene by Wang *et al*. [331] was adapted. 5 mg GO were suspended in 5 mL dichlorobenzene. After adding 50 mg ODA, the reaction mixture was sonicated for 24 hours at 80 °C. To get rid of excess ODA and dichlorobenzene, the reaction mixture was treated with 40 mL ethanol resulting in a black precipitate. The mixture was centrifuged and the resulting solid was washed twice with ethanol and toluene. This washing step was repeated once more and the product was dried at air. Thermal reduction of the product was performed after the composite was applied to a microelectrode (chapter 4.4.1) heating it to 230°C for 30 s. [adapted from P2]

Functionalization of Reduced Graphene Oxide with CuO Nanoparticles

Deposition of CuO nanoparticles was achieved through a wet chemical procedure in a water/^{i}propanol reaction system [332]. Different mass ratios of GO/CuO (1:2, 1:1, 1:0.2, 1:0.02, 1:0) were applied to alter the level of metal oxide doping within the nanocomposite. In the following a typical reaction for e.g. a GO/CuO mass ratio of 1:2 is described: 5 mg of freeze dried GO were dispersed in 5 mL ^{i}propanol and sonicated for 30 min. After the addition of 28 mg $Cu(CH_3COO)_2$ H_2O and further 5 min of sonication, the mixture was heated to reflux at 86 °C under vigorous stirring. The temperature was maintained for 30 min and 0.5 mL water was rapidly introduced into the boiling reaction mixture. The reaction was kept at 86 °C for another 30 min and cooled to room temperature. The product purified by centrifugation, washing with EtOH and water and was dispersed in 5 mL water with 30 min sonication. The resulting suspension was drop casted (1 µL) on the microelectrodes (chapter 4.4.1), dried at room temperature and heated to 230°C to thermally reduce the GO.

Microelectrodes modified with rGO (chapter 4.4.1) were used for the electrochemical deposition of Cu nanoparticles with subsequent oxidation to CuO at 230 °C in air. The deposition of metal nanoparticles on rGO was carried out from a solution of 10 mM $CuSO_4$ in 0.5 M H_2SO_4. A short reduction pulse (10s) at -1.2 V *vs* SCE was applied. The electrode was washed with water and heated to 230 °C for 30 s.

4.4 Fabrication of Graphene Electrodes

4.4.1 Sensor Preparation for Gas Sensing Applications

Suspensions of rGO and modifications were deposited on the microelectrodes via spin coating as not mentioned otherwise. The microelectrodes consist of gold conducting paths Si/SiO_2 substrate comprising an interdigital structure (Figure 12) and were cleaned before usage. The treatment included 5 min sonication in $CHCl_3$, washing with water, 10 s treatment with a mixture of conc. H_2SO_4 and 30% H_2O_2 (3:1) and again washing in water. Afterwards they were kept under ethanol and dried in a stream of nitrogen before usage. For deposition of rGO and composite materials, the respective suspensions were sonicated in a 1:1-mixture of water and ^{i}propanol (0.25 mg·mL^{-1}) for 10 min and 2 µL were spin coated onto the interdigital electrode structure with a Laurell WS-400BZ-6NPP/LITE spin coater (5 s at 500 rpm; 20 s at 3000 rpm). Afterwards the electrodes were heated to approximately 230 °C for 30 s on a hot plate. The electrical resistance between the nearest two gold conducting paths was measured with a UNI-T 109 multimeter and the electrodes have been examined under the microscope to control quality. [partially adapted from P2]

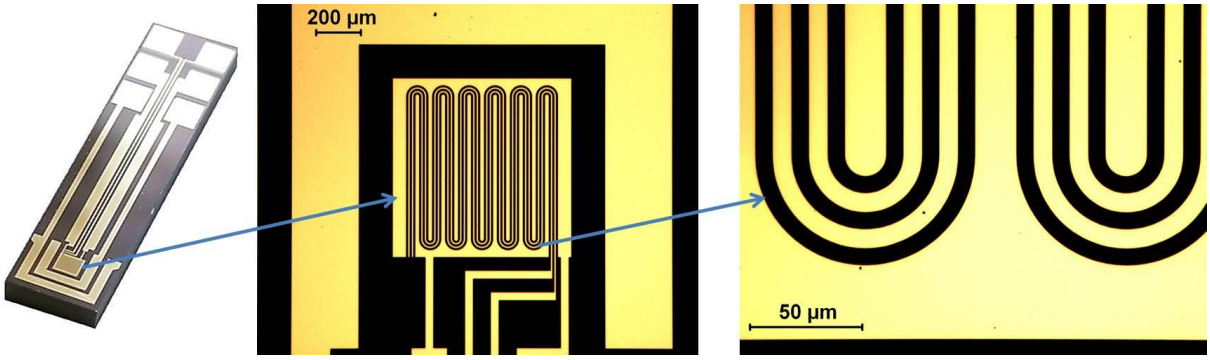

Figure 12 Microelectrodes with interdigital structure consisting of gold conducting paths on Si/SiO_2 wafer substrate.

4.4.2 Preparation of Graphene Electrodes for Electrochemical Comparison

The graphene was partially metallized through evaporation of Ti/Au (5 nm / 60 nm), followed by an acetone/^{i}propanol lift-off process, to provide an electrical contact for SG and CVDG (Figure 13a,b). Electrodes consisting of rGO (Figure 13c) were produced via drop casting of 1 µL of an aqueous rGO suspension (0.25 g·L^{-1}) on microelectrodes with interdigital structure (chapter 4.4.1) and dried at room temperature. A final annealing step of 230 °C for 30 s was applied afterwards. All gold areas in contact with the electrolyte were shielded by dipping the electrode into a solution of 100 µM 1-mercaptooctadecane in ethanol, to form a self-assembled monolayer. The different types of graphene modified electrodes on silicon substrates are depicted in Figure 13. [adapted from P4]

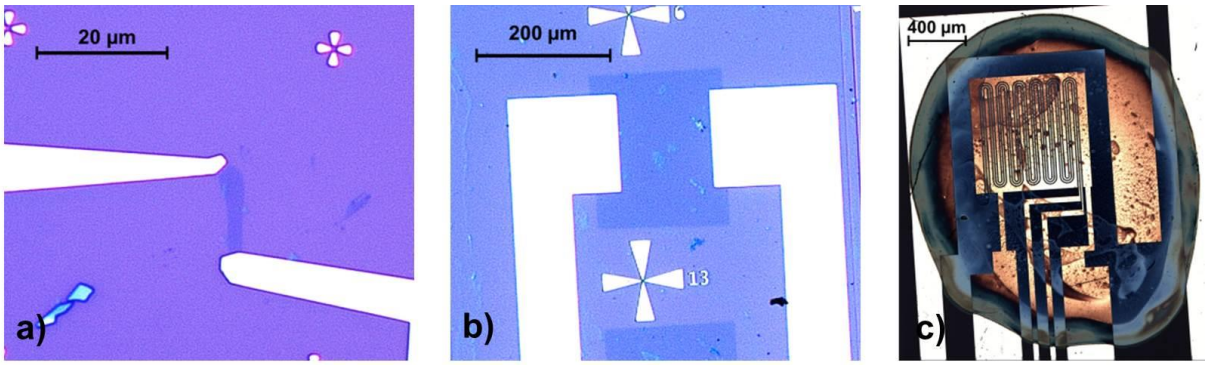

Figure 13 *Microscopic pictures of electrodes prepared with different graphene materials: (a) SG, (b) CVDG and (c) rGO. In (a) and (b) the graphene can be visualized by the microscope due to the interference between reflection paths of the air-SiO_2 and SiO_2-Si interface* [49]. [adapted from P4]

4.5 Gas Measurements

Gas measurements were performed on a homemade gas-mixing device, consisting of mass flow controllers (UFC-8160A and UFC-1660 from Unit Instruments Inc.), a flow cell with two heating elements for temperature control, and a Pt-100 temperature sensor (Figure 14).

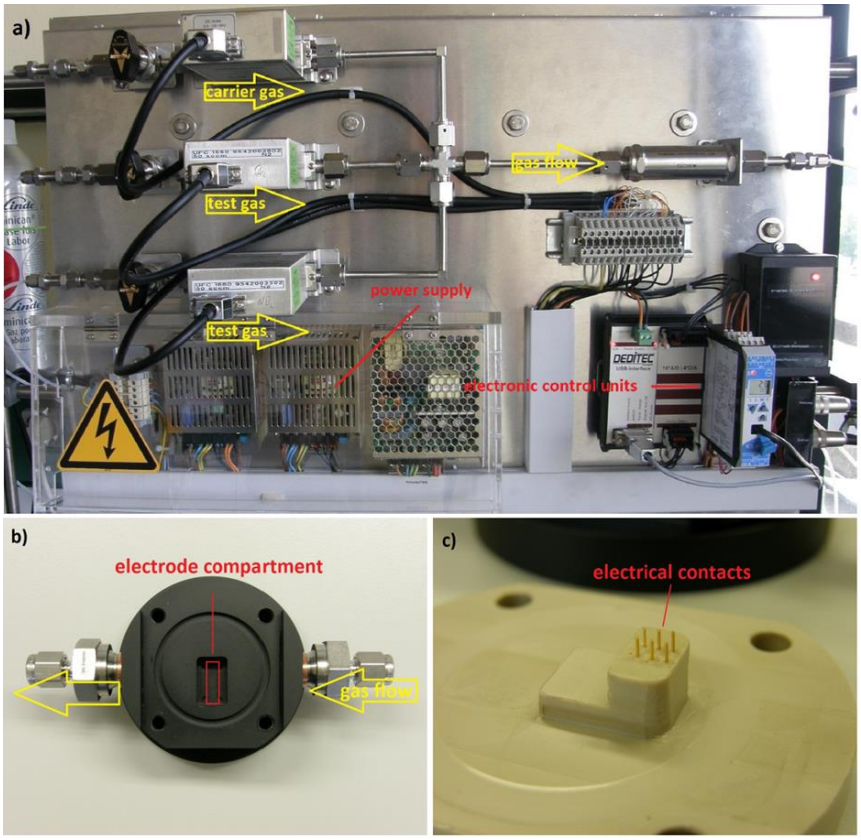

Figure 14 *(a) Gas mixing device, (b) flow cell, (c) corresponding lid with implemented gold pins for contacting of the microelectrode. [adapted from P2]*

Measurement of electrical resistance was accomplished by contacting the two gold conducting paths in the mid-position of the interdigital electrode structure (Figure 12), at constant bias voltage of 50 mV.

Synthetic air (N_2: 80%, O_2: 20%) was used as carrier gas and was mixed with 300 ppm NO_2, 1% H_2 or 1% CH_4. The test gases were all diluted by synthetic air. Furthermore gas adsorption tests were accomplished at constant gas flow at 100 sccm (300 sccm for concentration dependency of NO_2) and at constant temperatures of 85 °C. It was also necessary to heat the electrodes 20 s at 230 °C before each measurement, ensuring that no analyte gas was adsorbed previously by reaching the initial electrical resistance. For measuring the influence of air humidity, the gas flow was piped through the head-space of a flask containing water. [adapted from P2]

Measurements with CO_2 were performed in analogous way, mixing 3000 ppm CO_2 to a constant flow (100 sccm) of synthetic air, in order to achieve concentrations ranging from 150 to 1500 ppm. The flow cell was held at a constant temperature of 25 or 60°C, respectively. Cross sensitivity was tested in the presence of 100 ppm NO_2, 3000 ppm H_2, 3000 ppm CH_4, and 100 ppm CO. Temperature dependency was measured in synthetic air in the range from 25 to 85°C.

Additionally, microelectrodes modified with rGO-CuO (with a GO/CuO ratio of 1:2) were compared to a commercial sensor device. A CDM4161-L00 CO_2 Module from Figaro was applied to the flow cell and sealed. The sensor was run with 4V power supply and the signal output voltage was measured with an UNI-T UT109 multimeter. The output voltage measured in mV is directly proportional to the concentration of CO_2 in ppm. The sensor was calibrated for 2 hours in air before measuring.

4.6 Electrochemical Characterization and Measurements

A custom build carbon disc electrode, comprising a carbon fiber composite (www.conrad.de, Regensburg, Germany) with 2 mm diameter implemented in Teflon or the differently prepared graphene materials (SG, CVDG, and rGO, chapter 4.4.2) assembled on a silicon wafer substrate electrically contacted by gold leads were used as working electrode.

The modified electrodes and the carbon disc electrode were characterized with cyclic voltammetry, chronocoulometry, electrochemical impedance spectroscopy (EIS) and amperometry. For electrochemical experiments, the supporting electrolytes were 0.1 M KCl or 10 mM phosphate buffer with 140 mM NaCl (pH 7.4). Before each measurement Argon was bubbled through the solutions to remove dissolved oxygen. All experiments were performed at room temperature. The amperometric response towards H_2O_2 was investigated in a continuously stirred electrolyte solution (10 mM phosphate buffer, 140 mM NaCl, pH 7.4) by doubling the concentration of peroxide with each addition. The studied analyte concentration covers a range from 25 µM to 25.6 mM. [adapted from P4]

5 Results and Discussion

5.1 Signal Enhancement in Amperometric Peroxide Detection by Using Graphene Materials with Low Number of Defects

In this chapter, graphene materials prepared by mechanical exfoliation (single layer graphene, SG), chemical vapor deposition (chemical vapor deposited graphene, CVDG) and chemical exfoliation (reduced graphene oxide, rGO) were investigated as electrode material for the reductive amperometric detection of H_2O_2 (Figure 15). For the development of electrochemical biosensors based on graphene the choice of preparation technique has to be considered, since it significantly influences further functionalization, transfer and therefore device fabrication.

[Chapter 5.1 was mainly adapted from P4]

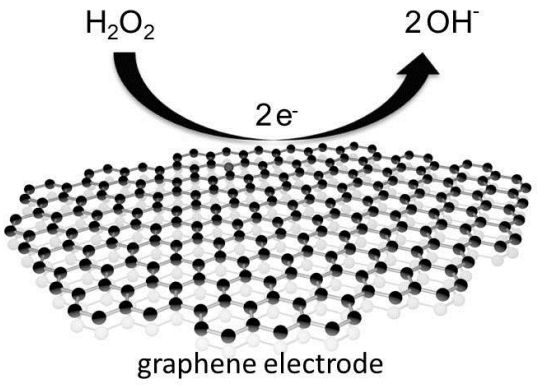

Figure 15 *Scheme of reductive amperometric detection of H_2O_2 utilizing a graphene electrode.*

5.1.1 Characterization of Graphene Materials with Raman Spectroscopy

Raman spectroscopy is established as a versatile characterization method for 2D carbon nanomaterials. Information regarding the number of layers, the amount of defects and impurities can be obtained. Therefore all graphene modified electrodes have been investigated by Raman microscopy. Signals at around 1600 cm^{-1} are usually described as G Peak and originate from the in-phase vibration of the graphene lattice (E_{2g} mode) [74]. The D peak at around 1350 cm^{-1} is caused from structural disorders, which can be found at defects and edges

[333]. Signals above 2400 cm^{-1} can be assigned to secondary peaks or a combination of the peaks mentioned above. As can be seen in Figure 16, no observable D peak, which indicates defects in the aromatic system of the graphene, is evident in the spectrum of SG, which proves the high structural order for this type of graphene. For CVDG a small D peak is observed at 1342 cm^{-1} and especially for rGO the D band at 1352 cm^{-1} becomes dominant and broader, indicating a high level of disorder [334]. A symmetric single 2D peak can be found in the spectra of SG and CVDG at 2676 cm^{-1} and 2684 cm^{-1}, respectively. Further, the significant higher intensity compared to the G band at 1583 cm^{-1} and 1590 cm^{-1} indicate that these materials consist of high quality single layer graphene [74]. In rGO, the noticeable change in shape and intensities of the D, G, and 2D band illustrates the significant presence of multiple layers, lattice disorder and inhomogeneity in this type of graphene. Applying an empirical Tuinstra-Koenig relation [335] which refers to the crystallite size of graphite, the diameter of the sp^2 regions in rGO was calculated to approximately 19 nm.

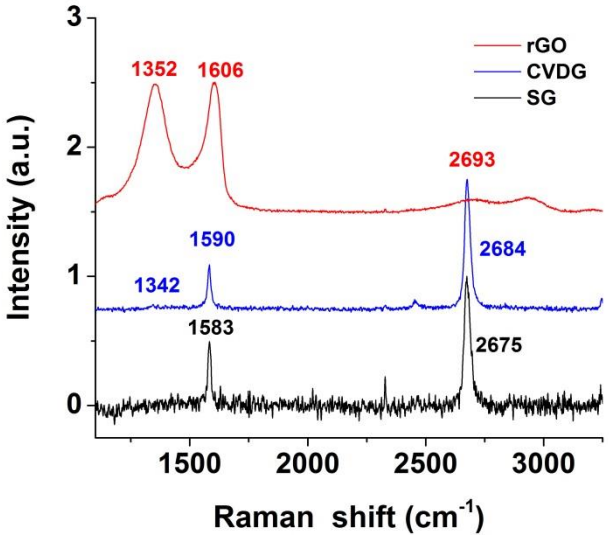

Figure 16 *Raman spectra of SG-, CVDG- and rGO-modified electrodes.*

5.1.2 Electrochemical Characterization of Different Graphene Electrode Materials

The graphene materials were contacted by deposition of gold conducting paths either onto it (for SG and CVDG) or drop casting a suspension of rGO on prestructured microelectrodes. Gold exposed to the electrolyte was shielded by the formation of a self-assembled monolayer of 1-mercaptooctadecane. As the thiol groups are attached to the gold, the hydrophobic long alkyl chains form an electrically passive layer. The successful shielding of the gold contacts exposed to the electrolyte was proven by cyclic voltammetry (Figure 17). A clean microelectrode comprising only gold as electrode surface was used as model substrate. After thiol treatment, oxidation and reduction peaks of a ferro/ferricyanide redox system vanished.

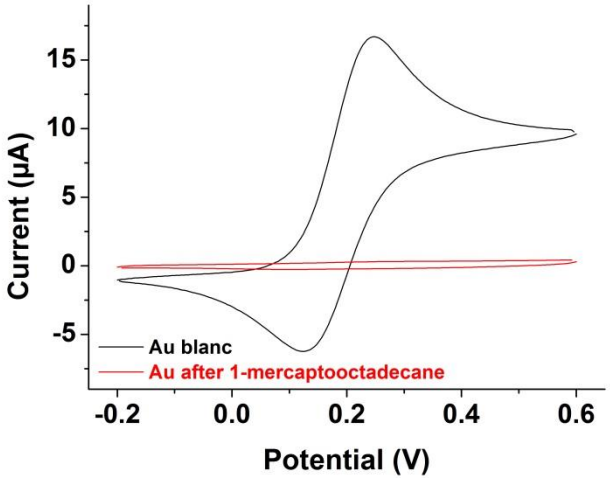

Figure 17 *Cyclic voltammograms of 5 mM $K_4[Fe(CN)_6]$ recorded in 0.1 M KCl (scan rate 0.2 V·s^{-1}) with a bare gold electrode before (black line) and after passivation with 100 µM 1-mercaptooctadecane (red line).*

Due to the different nature of the various types of graphene one cannot prepare electrodes of the same size. But size has huge influence on the sensitivity of the modified electrodes. The geometric area gives only a rough estimation, therefore chronocoulometric measurements in the presence of 0.1 mM $K_3[Fe(CN)_6]$ were performed in order to estimate the total electroactive area of each electrode. The effective surface area of the carbon disc electrode was calculated to be $2.9 \cdot 10^6$ µm^2, $2.6 \cdot 10^6$ µm^2 for rGO, $3.9 \cdot 10^4$ µm^2, for CVDG, and 51 µm^2 for the SG electrode, respectively. These values were further used for the calculation of current densities.

Electrochemical impedance spectroscopy provides information of the interfacial properties of the electrodes. In Figure 18 the Nyquist and Bode plots of the three types of graphene

modified electrodes and the carbon disc electrode in presence of 5 mM $K_4[Fe(CN)_6]$ containing 0.1 M KCl at 0.2 V *vs* SCE are shown. Electrodes modified with SG, CVDG and rGO cannot be fully described by a Randles equivalent circuit, consisting of the electrolyte resistance R_e in series with a parallel combination of double-layer capacitance (C_{dl}), an impedance representing the charge transfer resistance (R_{ct}) and the Warburg element (Z_w) taking diffusion into account. The results from the electrochemical impedance spectroscopy do not take into account that there is a huge difference in the electrode surface area as can be seen from the results of the chronocoulometric measurements. For high frequencies the impedance (Z) for all systems is approaching the electrolyte resistance. For small frequencies the charge-transfer resistance increases for the different electrodes in the order carbon disc, rGO, CVDG to SG. The behavior of the CVDG can be explained by impurities adsorbed on the graphene. These can be a consequence of the transfer process [36]. Here, a polymer layer will deposited on top of the graphene layer; the metallic substrate where the graphene was deposited is etched away so that the polymer modified graphene flake swims on top of the solution. After transfer to the silicon wafer the polymer on top of the graphene is washed away by organic solvents. By this process it is likely that polymer residues can remain. The Nyquist plot in Figure 18a suggests that additional impedance for adsorbates need to be applied to the equivalent circuit. For the rGO system, which consists of multilayers and comprises many defects, it is expected that the impedance spectrum is not in accordance to the simple model described by the Randles equivalent circuit. The SG modified electrode as well as the carbon disc electrode show a diffusion process for the redox species at low frequencies. The higher double-layer capacitance of SG modified electrodes in contrast to the carbon disc electrode as can be seen from the imaginary part in the Nyquist plot (Z") can be attributed to the hydrophobic character of the aromatic system which is repelling the redox species. After normalization of the total impedance Z to the electroactive surface area the charge transfer resistance of carbon disc electrode is approximately $1.2 \cdot 10^6$ times higher than for the SG modified electrode, for CVDG R_{ct} per area is $1.7 \cdot 10^3$ times, for rGO $1.3 \cdot 10^5$ times higher. This shows that all graphene types enhance the electron transfer of the ferro/ferricyanide redox system compared to a plain carbon disc electrode. The differences between the three different types are in accordance to the increase of the number of defects of the two-dimensional carbon nanomaterial. The numbers given here are only rough estimations not taking into account the influence of the border of the CVDG and SG. A detailed investigation of different flake sizes will complete this picture.

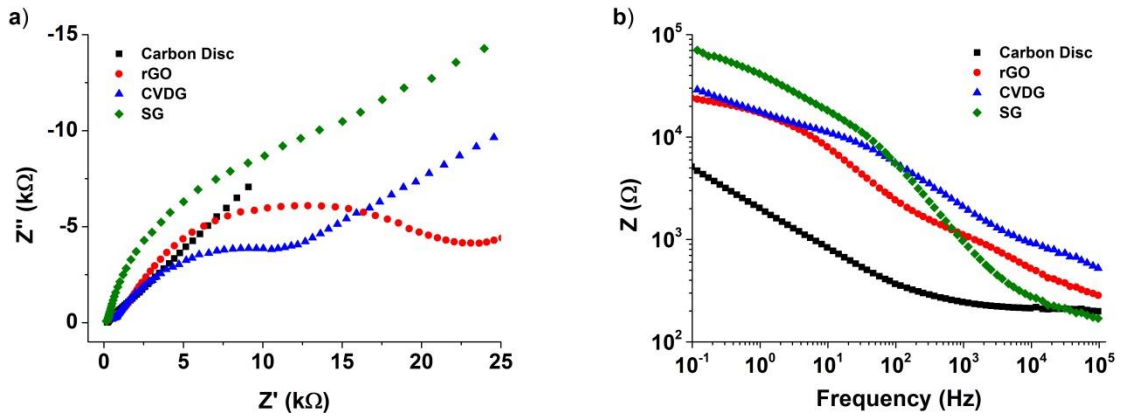

Figure 18 *Nyquist plot (a) and Bode plot (b) derived from electrochemical impedance spectroscopy in 0.1 M KCl and 5 mM $K_4[Fe(CN)_6]$ for carbon disc, rGO, CVDG and SG modified electrodes (at 0.2 V vs SCE with an amplitude of 5 mV).*

5.1.3 Direct Amperometric Detection of H_2O_2

The reduction of H_2O_2 on the different graphene electrodes was studied with cyclic voltammetry (Figure 19) in the presence of 10 mM H_2O_2 in phosphate buffered saline at pH 7.4. Comparison of the cyclic voltammograms before and after applying 10 mM H_2O_2 shows that after the addition of H_2O_2, the cathodic current increased. The increase for electrodes modified with CVDG and SG can be already observed at low potentials of -0.1 V *vs* SCE. This is at lower potentials than for rGO and carbon disc electrode and can be attributed to an electrocatalytic effect of the carbon nanomaterials.

The change in the current density under exactly the same conditions is significantly higher for the graphene materials than for the carbon disc electrode (Figure 20). At a working potential of -0.3 V *vs* SCE the current flow is enhanced about 4 times for rGO, 5 times for SG and 8 times for CVDG. Especially CVDG electrodes provide maximum response, maybe due to the best ratio of pristine graphene lattice to defects and edges.

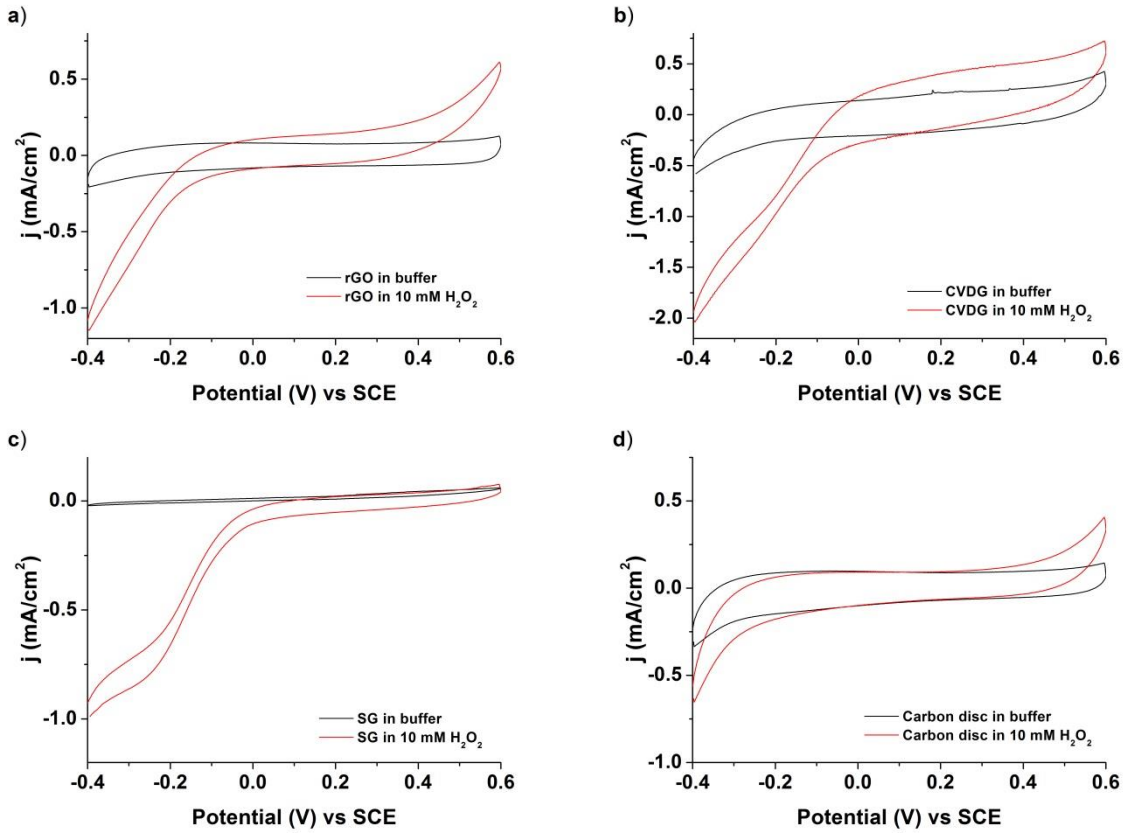

Figure 19 *Steady state current density/voltage cycles of (A) rGO, (B) CVDG, (C) SG, and (D) carbon disc electrode in phosphate buffered saline pH 7.4 and after addition of 10 mM H_2O_2 vs SCE (scan rate 0.1 $V \cdot s^{-1}$).*

In order to get high selectivity in real sample analysis it is desired to determine the analytes at potentials close to 0 V. We found that at very low potentials graphene with low number of defects, here CVDG and SG, show nearly the same enhancement in the signal whereas rGO as very defective material shows a behavior more like the carbon disc electrode (Figure 20). For more negative electrochemical potentials all four types of carbon materials give an individual signal enhancement. From this result one can conclude that for working potentials lower than -0.1 V *vs* SCE it is mandatory to use high quality graphene with low number of defects in order to get any benefit in using a two-dimensional carbon nanomaterial as electrode in amperometric detection of H_2O_2.

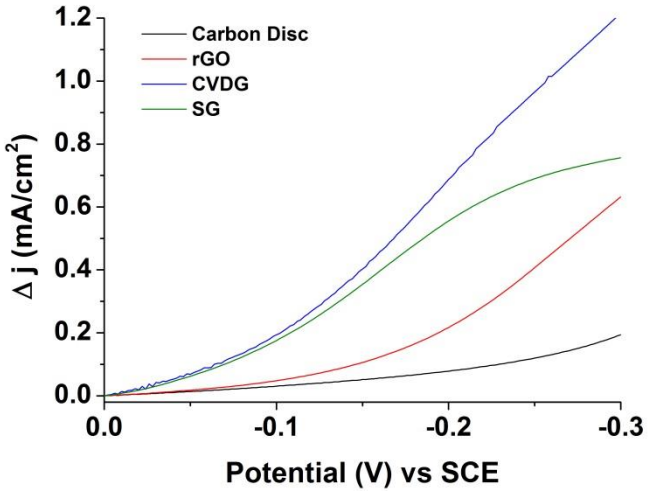

Figure 20 *Change in current density for H_2O_2 reduction during the cyclic voltammetry in phosphate buffered saline pH7.4 with 10 mM H_2O_2 vs SCE (scan rate 0.1 $V \cdot s^{-1}$).*

All three different types of graphene modified electrodes have been tested in an amperometric setup to detect peroxide (Figure 21). A constant potential of -0.3 V *vs* SCE was applied. From Figures 21a,b it can be observed that the reductive current response of all electrodes increase with increasing H_2O_2 concentration. For low concentrations of the analyte one can see that SG does not exhibit notable changes in the current. One reason is that the size of these flakes is very small and therefore the total signal is very small. After normalization of all signals to the total electroactive surface area, the situation changed (Figure 21c): the sensitivity of SG for low amounts of H_2O_2 can be seen. An increase of absolute sensitivity is observed, starting from carbon disc (3.2 $mA \cdot M^{-1} \cdot cm^{-2}$) to rGO (25 $mA \cdot M^{-1} \cdot cm^{-2}$) to CVDG (173 $mA \cdot M^{-1} \cdot cm^{-2}$), and SG modified electrodes (202 $mA \cdot M^{-1} \cdot cm^{-2}$). Again, a lower number of defects lead to a higher sensitivity towards H_2O_2. Nevertheless, the noise level of SG electrodes is higher than the other electrodes which can be attributed to the low absolute current values. Noise at an

amperometric electrode is closely associated with C_{dl} and the quality of attachment to the support. Calculating the LOD from a signal-to-noise ratio of three, values of 9.2 µM for rGO, 15.1 µM for CVDG and 651.5 µM for SG electrodes are obtained.

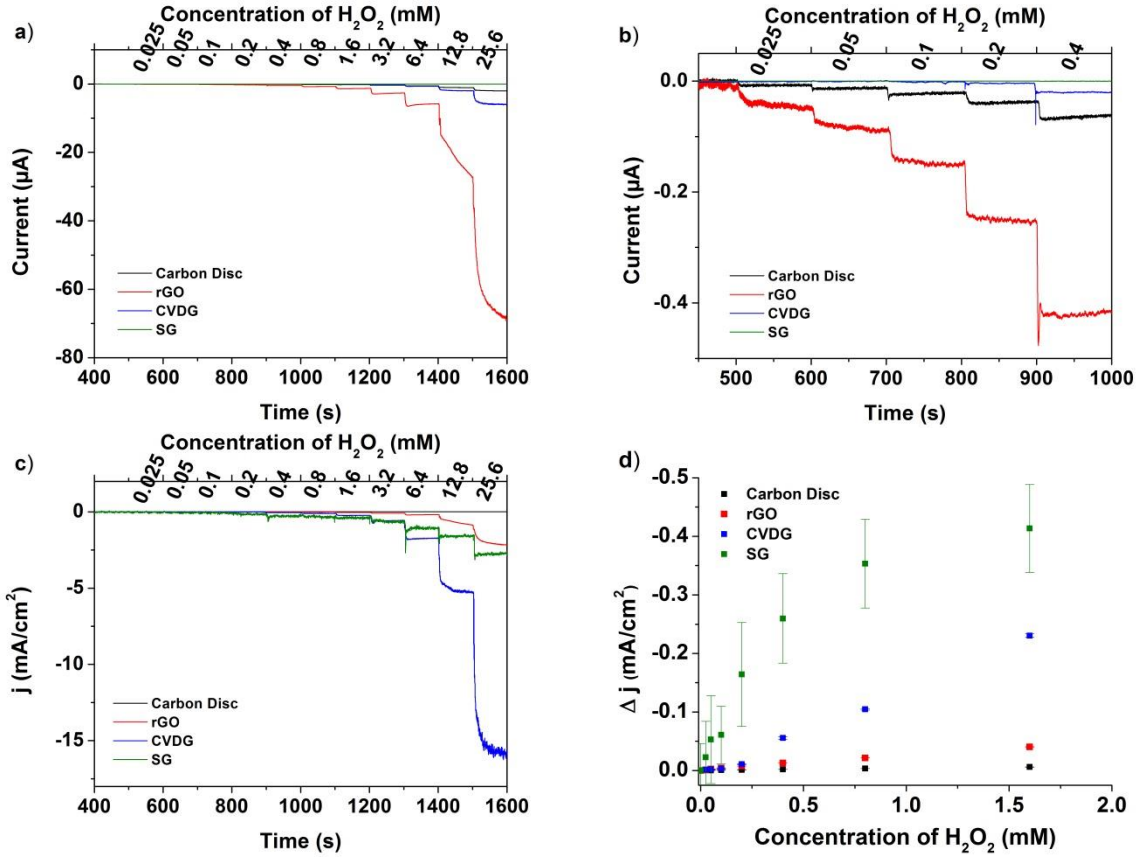

Figure 21 *(a) Amperometric recordings at -0.3 V (vs SCE) for successive addition of 0.025-25.6 mM H_2O_2 into continuously stirred phosphate buffered saline pH 7.4. (b) Response after first addition. (c) Normalized amperometric response referring to the electrodes size.(d) Concentration dependency of the amperometric response.*

These findings indicate the great perspective of graphene in amperometric detection systems. For comparison, the H_2O_2 sensing performance of different graphene based electrode materials from previous reports are displayed in Table 1. All these works are based on chemically derived graphene, which has been further modified with metal or metal oxide nanomaterials to improve sensitivity. One can clearly see that hybrid nanomaterials lead to better sensitivity. From our study one can suggest that there could be further improvement by using graphene of low number of defects. For taking benefit of the electrocatalytic effect of graphene as well as from the signal enhancement it is mandatory to use electrodes consisting of high quality graphene, which means, to use a 2D nanomaterial with as low number of defects and impurities as possible. Up to now it is challenging to provide such a high quality

graphene on an insulating material with electric contacts in reasonable quantities and of adequate size for developing sensor applications operated with a low cost potentiostat. By taking a look to the relative signal changes obtained with the different types of electrodes used in this study one can see that SG performs best, but accompanied by huge error bars due to an enhancement of the noise. This could be overcome by using bigger graphene flakes or by better potentiostats. Good signal enhancement can also be obtained with CVDG. Nevertheless the fabrication of one of such electrodes is a time consuming complex process. This material is already commercially available. But the drawback in using this material for an application is that there is a lack of a technique for a clean and easy transfer of this material onto microelectrodes providing a good electrical contact. This material offers the possibility to be functionalized chemically [336] or by plasma treatment [337]. It is expected that with this technique selectivity can be introduced and functionalized graphene for amperometric detection systems will be designed. The rGO does not result in such great improvement in contrast to the carbon disc electrode, but here processing of the material as well as functionalization is easy. Therefore it offers a pathway to interesting composite materials for electrochemical sensors.

Table 1 Comparison of analytical performance of different graphene and graphene composite materials used for the electrochemical detection of H_2O_2.

Electrode Material	Potential [V]	Sensitivity [$mA \cdot M^{-1} \cdot cm^{-2}$]	LOD [µM]	Reference
PB/Graphene	-0.05 (vs Pt)	196.6	1.9	[338]
CoOxNPs/ERG	0.75 (vs SCE)	148.6	0.2	[45]
MnO_2/GO	-0.3 (vs SCE)	8.2	0.8	[339]
AgNPs/PQ11/ Graphene	-0.4 (vs Ag/AgCl)	56.6	28	[340]
Polydopamine-rGO/Ag	-0.5 (vs Ag/AgCl)	355.8	2.1	[341]
rGO-PMS/AuNPs	-0.75(vs Ag/AgCl)	39.2	0.06	[342]
rGO	-0.3 (vs SCE)	25	9.2	This Work
CVDG	-0.3 (vs SCE)	173	15.1	This Work
SG	-0.3 (vs SCE)	202	651.5	This Work

PB: Prussian Blue; CoOxNPs: Cobalt oxide nanoparticles, ERG: Electrochemically reduced graphene oxide, AgNPs: Silver nanoparticles, PQ11: Poly[(2-ethyldimethylammonioethyl methacrylate ethyl sulfate)-*co*-(1-vinylpyrrolidone)], PMS: Periodic mesopourous silica, AuNPs: Gold nanoparticles, Ag/AgCl: Saturated silver / silver chloride reference electrode

5.1.4 Conclusion

The non-enzymatic detection of H_2O_2 was studied using electrodes based on various types of graphene, without utilizing any functionalization or modification steps. All three graphene materials exhibit sensitivity to the catalytic reduction of H_2O_2 and are able to detect H_2O_2 concentrations in the µM range, showing fast amperometric response upon successive additions of analyte. Moreover, it is clearly demonstrated that mechanically exfoliated graphene as well as graphene prepared by CVD are promising candidates for sensor applications, due to their efficiency in better detection of H_2O_2 with higher sensitivity compared to rGO. However, due to the laborious process needed for production of exfoliated graphene and its irregularity in shape, size and location, this type of graphene is more suitable for theoretical study and proof-of-concept demonstration. In comparison, the CVDG suits commercial purposes and mass production, since it offers uniform continuous films at particular locations and with desired geometries, providing a superior candidate for fabrication of high sensitivity biosensors and sensor arrays. Such carbon nanomaterials can also be used as biosensors by further functionalization with enzymes.

5.2 Reduced Graphene Oxide and Graphene Composite Materials for Improved Gas Sensing at Low Temperature

In this chapter, rGO was investigated as sensitive material for gas sensors in a chemiresitive setup. Reduced graphene oxide was chosen due to features like solution processing, high sensitivity and simple methods for functionalization owed to its defective structure. Covalent attachment of functional groups or doping with metal and metal oxides can change the electronic structure within the material, but may also increase the sensor surface or have a catalytic effect on the gas adsorption.

[Chapter 5.2 was mainly adapted from P2]

5.2.1 Characterization of Reduced Graphene Oxide and Composite Materials

Oxidation of graphite with subsequent reduction leads to a material with inhomogeneous shape and size of graphene sheets. The size of the graphene flakes ranging from 100 nm to about 1 µm as it is indicated by SEM studies (Figure 22a). Characterization with Raman spectroscopy also indicates the inhomogeneity of the material, showing a broad G and D peaks and was discussed previously (chapter 5.1.1).

Regarding the thermogravimetric analysis (TGA) of GO and rGO (Figure 22b) a loss of mass can be observed at temperatures of about 200 °C. In FTIR-TGA this effect can be ascribed to a thermal reduction, where CO and CO_2 is released [343]. Graphene oxide loses about 25% of its mass, while rGO loses around 15% and shows that the reduction by hydrazine is incomplete.

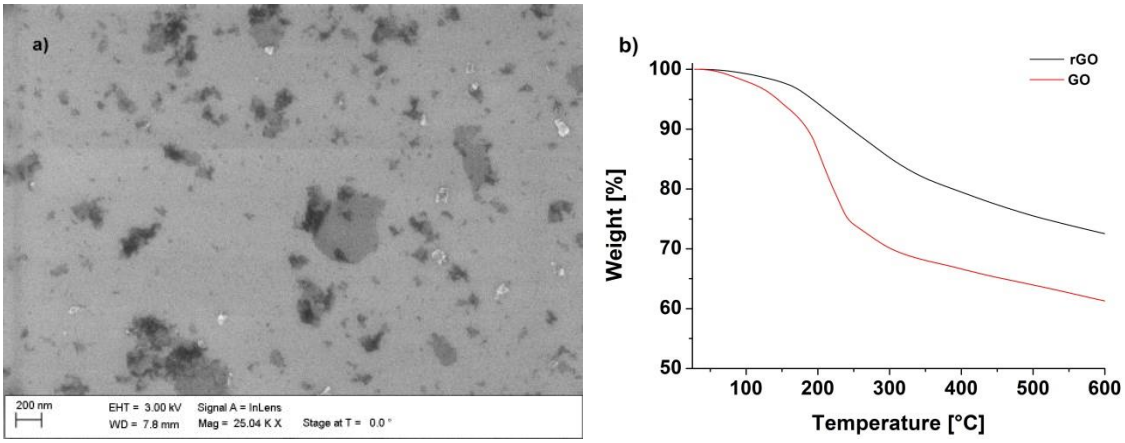

Figure 22 *(a) SEM of rGO on a Si/SiO_2 substrate and (b) thermogravimetric analysis of GO and rGO.*

Functionalization of rGO was performed by wet chemical methods. Generally, all dopants primarily bind/coordinate with the oxygen functionalities of rGO. Whereas ODA reacts with the epoxy groups of GO [331], doping with metals and metal oxides usually includes the interaction of a precursor metal ion with the carboxyl groups of rGO [328, 344]. The successful modification of rGO was revealed by Raman studies. Peaks at 1125 and 1489 cm^{-1} (ODA), at 140, 392, 510 and 644 cm^{-1} (TiO_2), and at 579 and 633 cm^{-1} (MnO_2) were found and can be attributed to the respective modification (Figure 23). Whereas Pt and Pd do not show any prominent Raman modes, the spectra of the graphene-metal composites resemble the spectrum of rGO.

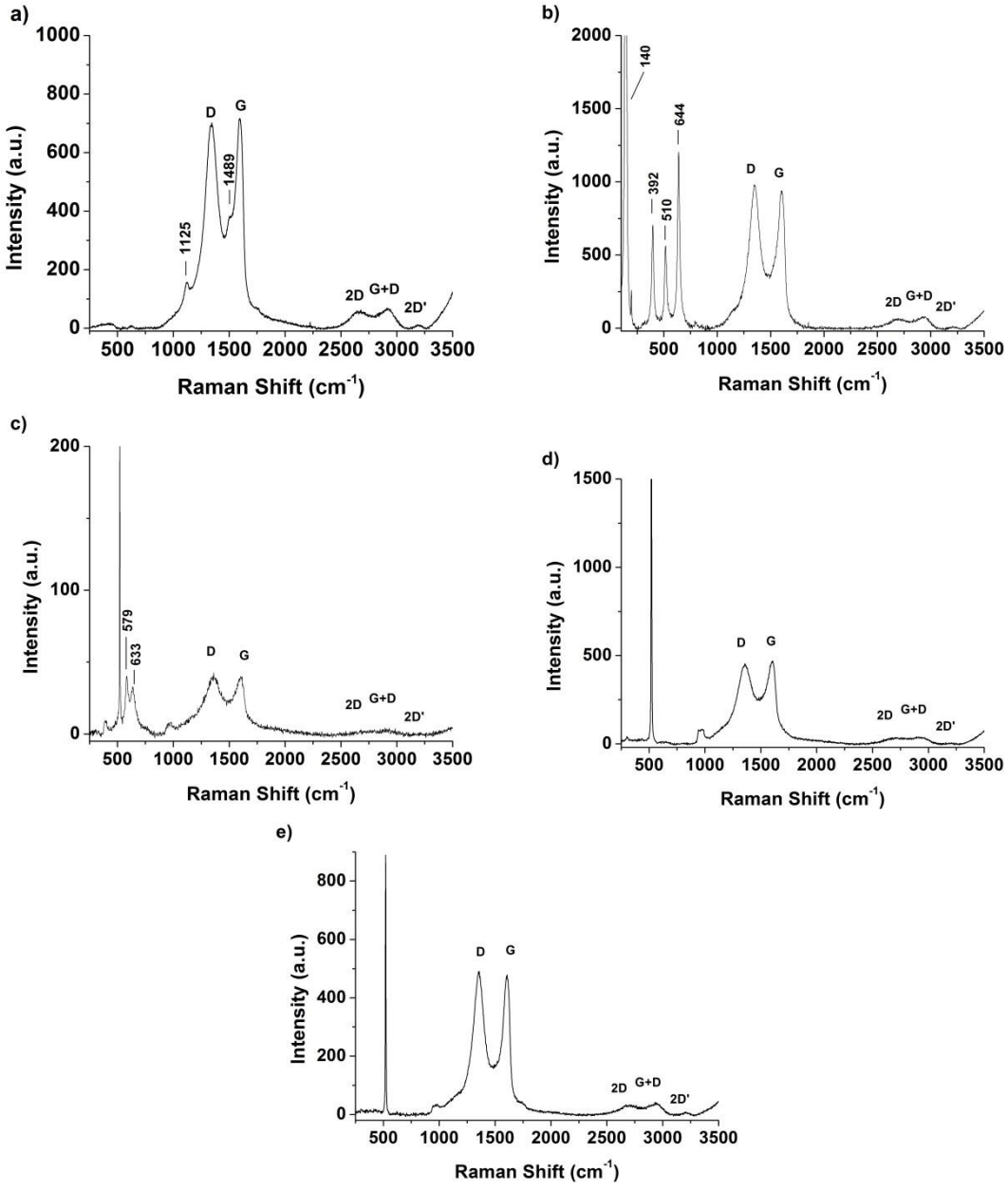

Figure 23 *Raman of rGO modified with (a) ODA, (b) TiO_2, (c) MnO_2, (d) Pd and (e) Pt NPs. Peaks at 520 cm^{-1} and 970 cm^{-1} can be attributed to the Si/SiO_2 substrate.*

Therefore, these composite materials where additionally examined with TEM (Figure 24). A partial coverage of metal nanoparticles (black dots) on distinct regions of rGO was found. The average particle size was below 20 nm for Pd NPs and 10 nm for Pt NPs.

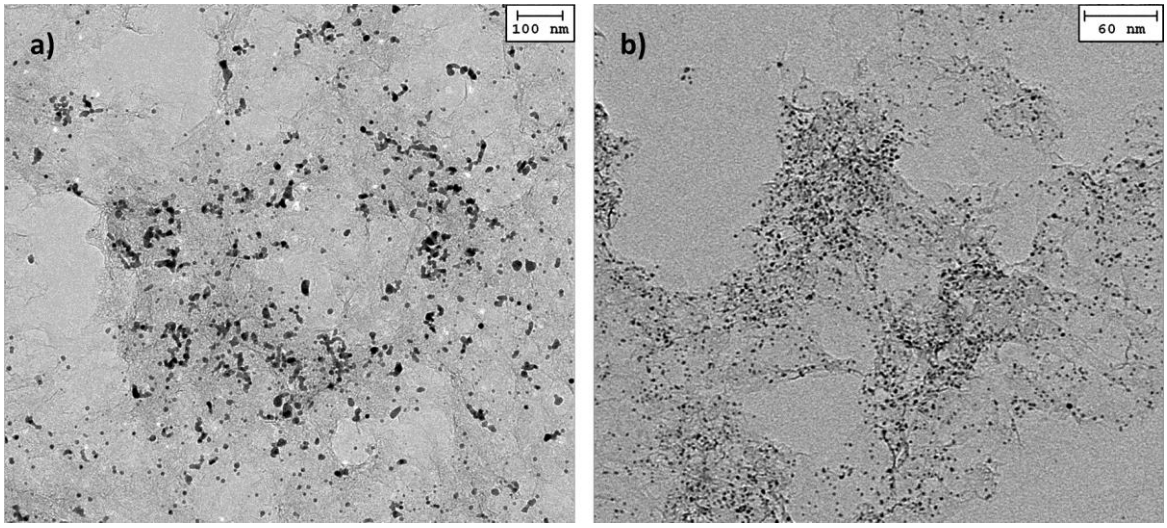

Figure 24 *TEM images of rGO modified with (a) Pd- and (b) Pt NPs.*

The decoration of rGO with metal oxides could be observed in SEM images (Figure 25a,b). Whereas modification with TiO_2 led to a partial coverage of rGO, modification with MnO_2 resulted in a complete coverage of rGO with rod-like nanocrystals of the metal oxide.

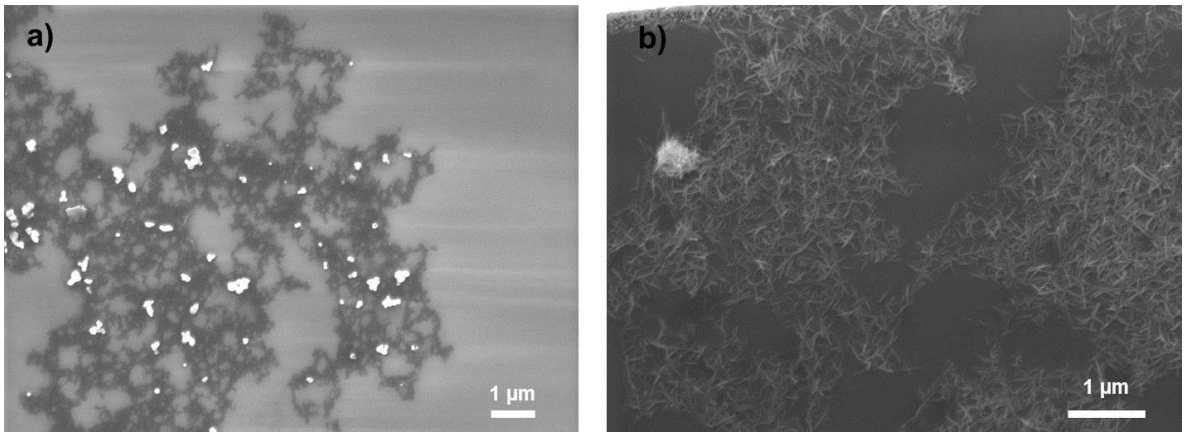

Figure 25 *SEM images of rGO modified with (a) TiO_2, and (b) MnO_2.*

The elemental composition of the different modified materials was confirmed by EDS (Figure 26). Signals at 0.3 keV can be ascribed to the k-alpha line of rGO and additional peaks around 2 keV represent the background signal of the substrate comprising silicon and gold. For every modification the characteristic lines of the appropriate elements could be found and are highlighted within the spectra.

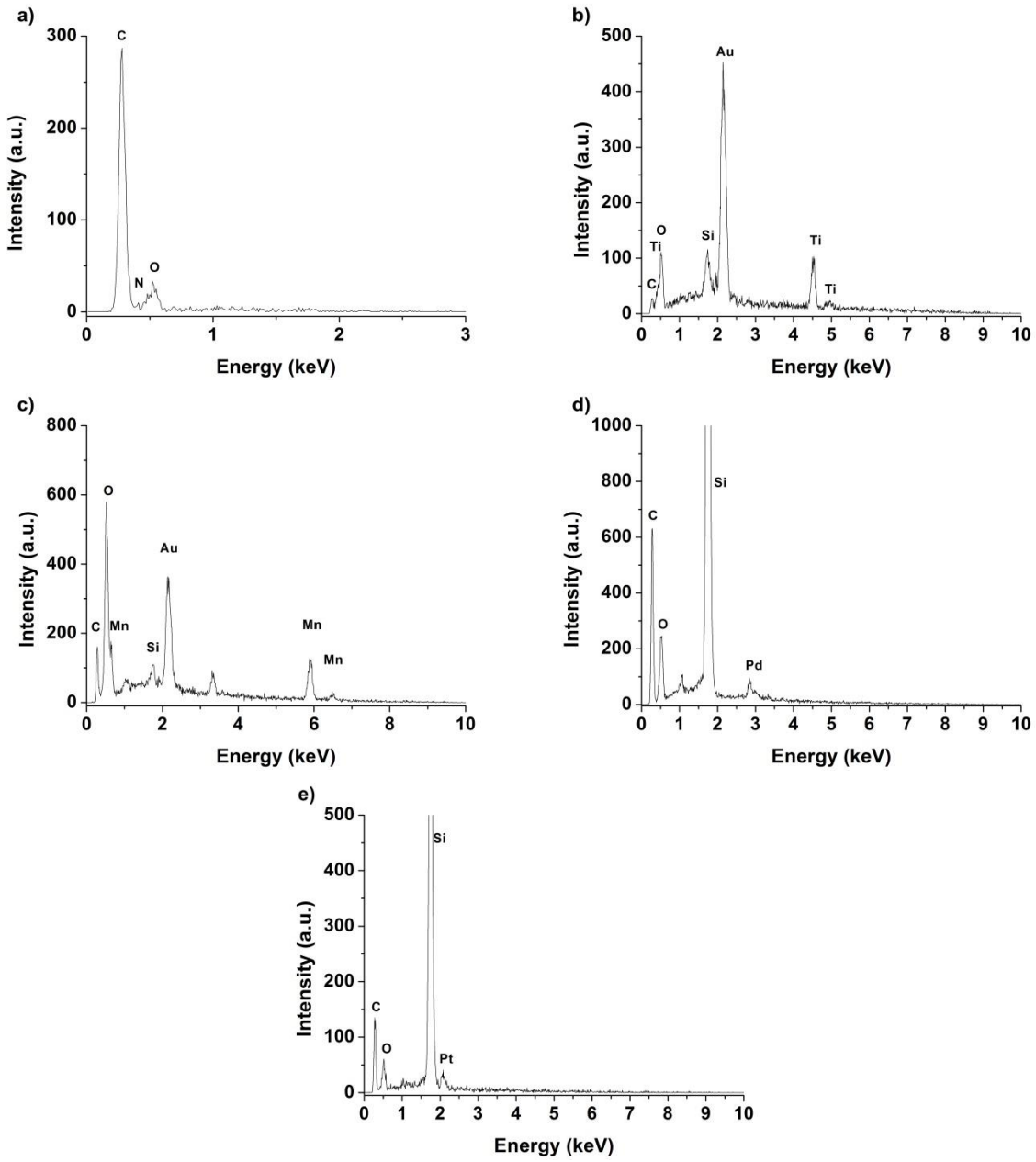

Figure 26 *EDS spectra of rGO modified with (a) ODA, (b) TiO_2, (c) MnO_2, (d) Pd, and (e) Pt. Peaks of Au, Si and partially O can be attributed to the microelectrode substrates.*

5.2.2 Gas Sensor Response

The transfer of graphene materials is still a critical step in sensor preparation using this type of carbon nanomaterial. Aqueous suspensions of rGO can be easily processed and the interdigital electrode structure was covered with a thin layer of rGO via spin coating. Parameters affecting spin coating as the concentration of rGO, the rotation speed and time as well as the usage of certain additives, like ^{i}propanol for improvement of the spreading of the suspension, were optimized to obtain consistent layers with reproducible total electrical resistance. Further, the rGO modified electrodes were heated to 230 °C to guarantee a thermal reduction. During this step, the electrical resistance dropped from about 8.0 MΩ ± 3.8 MΩ to 180 kΩ ± 78 kΩ. The oxidation process of graphite introduces many defects to the sp^2 structure which act like a barrier for the electron flux, resulting in better electrical conductance at higher level of reduction.

To assess the effect of gas adsorption on the conductance of rGO, the electrical resistance of coated microelectrodes was measured for different gases in various concentrations mixed in a constant flow of synthetic air. An operating temperature of 85 °C was chosen to exclude the influence of humidity on the sensor response (Figure 27c). Furthermore, heating to 85°C improved the response time (< 1 min), and an increase in the signal change and the recovery rate was found. Figure 27 displays the change of the relative resistance (R/R_0) in the presence of different gases, such as NO_2, H_2, and CH_4. R_0 is hereby the initial electrical resistance right before the addition of a test gas.

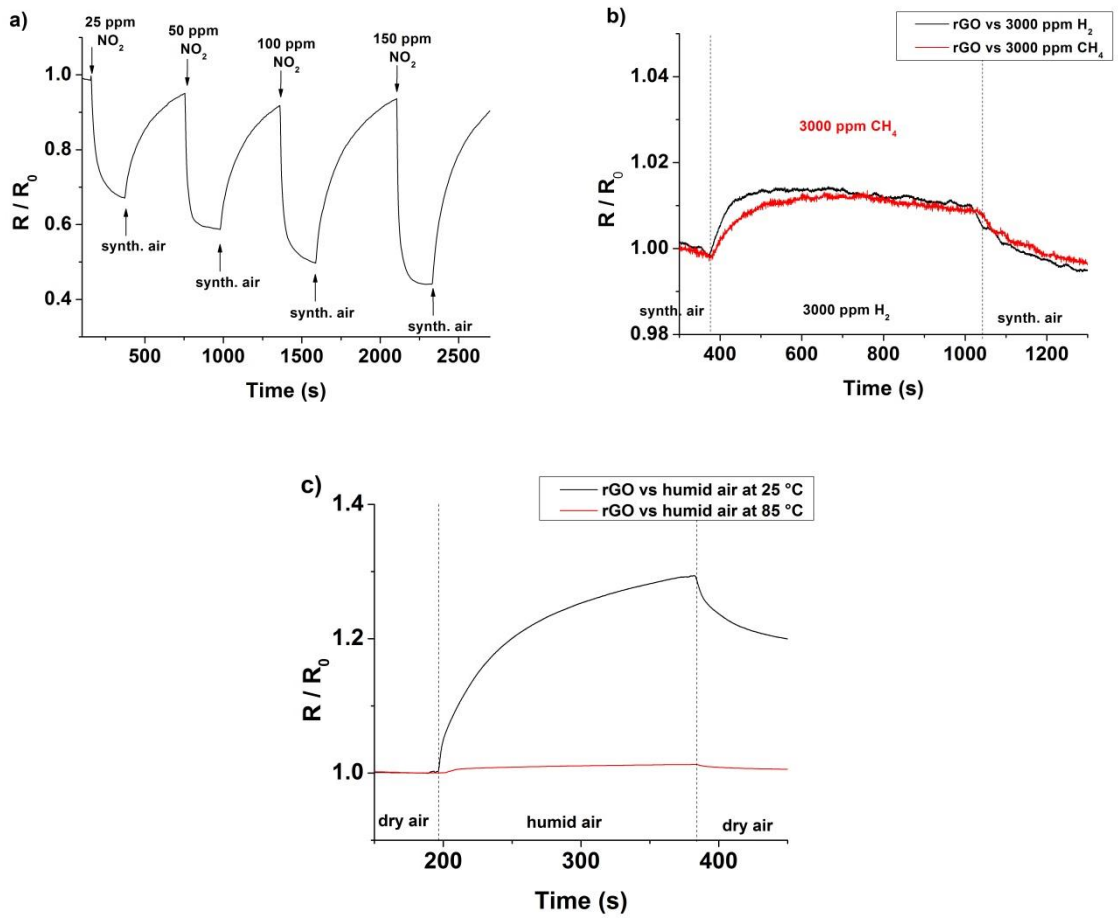

Figure 27 *Change in electrical resistance of rGO layer at 85 °C in the presence of (a) different concentrations of NO_2 and (b) 3000 ppm H_2 or CH_4. (c) Influence of air humidity on conductance of an rGO based sensor at 25and 85 °C.*

Reversibility and concentration dependence of the sensor was evaluated by continually adsorption and desorption of the different gases. The results for NO_2 are shown in Figure 27a, and the changes in electrical conductance for other gases are listed in Table 2. A linear behavior within the applied concentration range (25-150 ppm), a sensitivity of 0.56 ppm^{-1} and a detection limit of 0.3 ppm (S/N = 3) was observed. In contrast to the signal drop for NO_2, the adsorption of H_2 and CH_4 led to an increase in the electrical conductance (Figure 27b). The electron withdrawing effect of the adsorbed NO_2 leads to more positive charge carriers, since rGO is described to show p-type semiconducting behavior [26]. Such gases as H_2 or CH_4 cannot act as electron donor or acceptor. It can be assumed that previously physisorbed molecules from synthetic air (most probably oxygen) at the surface of the graphene are replaced by H_2 or CH_4, leading to an increase in electrical resistance [345].

These results clearly demonstrate that rGO on the one hand is an excellent sensor material for detecting gases. In contrast to metal oxide sensors, which are the most common gas sensors so

far, sensors based on graphene can be operated at low temperatures with fast response times. On the other hand it is demonstrated that graphene based sensors lack on selectivity. Nearly all adsorbates will result in signal changes, therefore they can only be used in detecting analytes in an atmosphere of inert gases [125, 345, 346]. To overcome this drawback graphene was functionalized graphene in different ways and the resulting materials were investigated in their gas sensing behavior. The sensor responses of different functionalized rGO materials towards NO_2, H_2 and CH_4 (Figure 28) are summarized in Table 2. A representative measurement of different concentrations of NO_2 and H_2 with a sensor based on rGO-Pd is shown in Figure 28d.

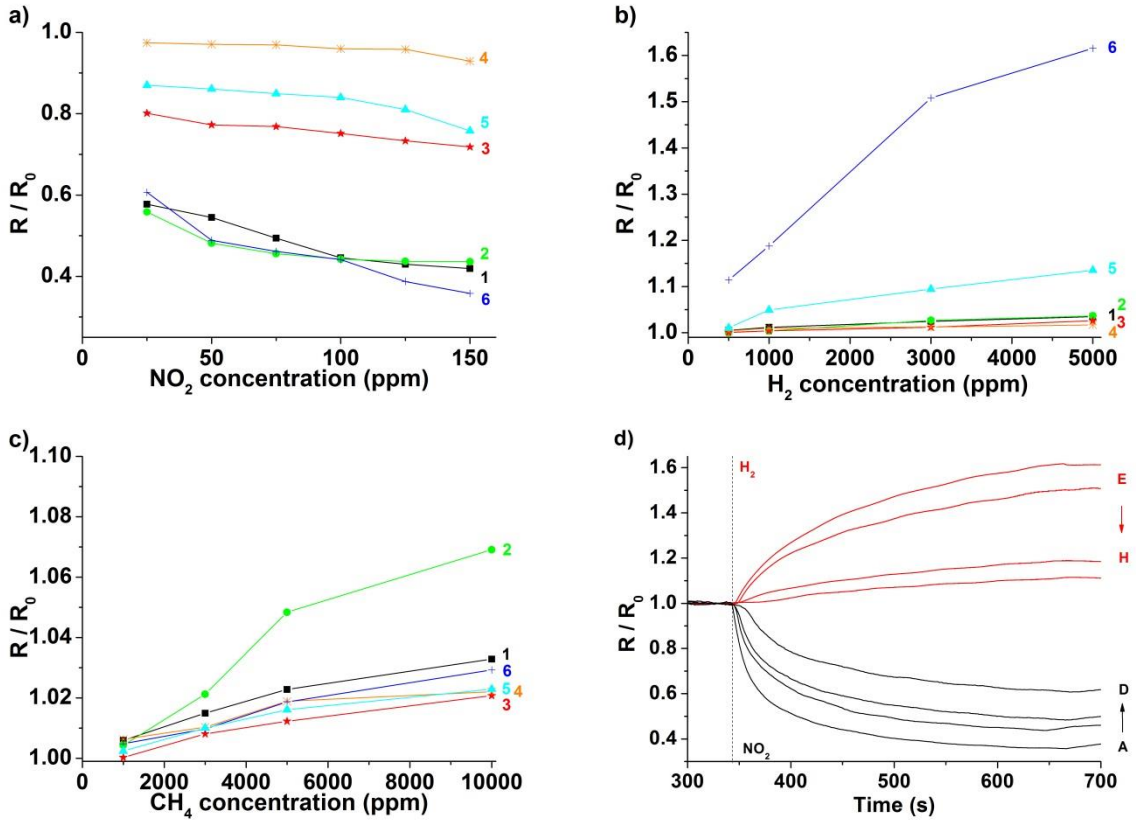

Figure 28 *Concentration dependencies of rGO (1) and graphene composites (2 to 6) for different concentrations of NO_2 (a), H_2 (b) and CH_4 (c). The composites are rGO-ODA (2), rGO-TiO_2 (3), rGO-MnO_2 (4), rGO-Pt (5), and rGO-Pd (6). (d) Change in electrical resistance of rGO-Pd for H_2 (red) and NO_2 (black). The concentration ranges from 25 (A), 50 (B), 100 (C) and 150 (D) ppm for NO_2 and from 500 (E), 1000 (F), 3000 (G) and 5000 (H) ppm for H_2.*

Chemical insertion of ODA led to slightly increased signal changes towards H_2 and CH_4. For NO_2 detection almost no influence of the modification could be found. The composite

material with TiO_2 showed unaffected behavior towards H_2 and CH_4, but a lower response towards NO_2. This indicates that adsorption sites for NO_2 may be blocked. Electrodes coated with rGO which was doped with MnO_2 showed almost no signal change to all of the utilized gases. Therefore, this modification only could deal as a reference signal to compensate small fluctuations in temperature. The most significant change in response was achieved by chemical doping with Pd and Pt NPs. The resulting composite materials showed an increased sensitivity towards H_2 (Figure 28b). Same observations with comparable results have been made with carbon nanotubes decorated with Pt and multilayered graphene nanoribbons doped with Pd. Though, the composite material with rGO is easier to produce and to process. In summary, all composites of rGO are rather simple to prepare and show different behavior in their electrical conductance upon the presence of various gases.

Table 2 Comparison of the response of unmodified rGO and modifications in the presence of different concentrations of NO_2, H_2 and CH_4 at 85 °C.

Gases	Signal [R/R_0]					
	rGO	rGO-ODA	rGO-TiO_2	rGO-MnO_2	rGO-Pd	rGO-Pt
150 ppm NO_2	0,419	0,436	0,718	0,929	0,358	0,758
125 ppm NO_2	0,430	0,437	0,733	0,958	0,387	0,810
100 ppm NO_2	0,445	0,442	0,751	0,959	0,441	0,840
75 ppm NO_2	0,494	0,456	0,768	0,969	0,461	0,849
50 ppm NO_2	0,545	0,481	0,773	0,971	0,489	0,861
25 ppm NO_2	0,578	0,559	0,801	0,974	0,607	0,870
5000 ppm H_2	1,035	1,037	1,026	1,017	1,615	1,135
3000 ppm H_2	1,025	1,027	1,011	1,012	1,508	1,095
1000 ppm H_2	1,012	1,004	1,004	1,010	1,188	1,049
500 ppm H_2	1,005	1,000	1,001	1,004	1,114	1,011
10000 ppm CH_4	1,033	1,069	1,021	1,022	1,029	1,023
5000 ppm CH_4	1,023	1,048	1,012	1,019	1,019	1,016
3000 ppm CH_4	1,015	1,021	1,008	1,010	1,010	1,010
1000 ppm CH_4	1,006	1,004	1,000	1,006	1,005	1,002

5.2.3 Principal Component Analysis for Pattern Recognition of Different Gases

The altered sensitivity of every sensor towards different analyte gases enables pattern recognition using multivariate analysis based on principal component analysis (PCA). With this chemometric technique it is possible to simplify multidimensional datasets without crucial loss of information. Here, the data matrix (Table 2) contains of the normalized sensor response of each sensor material to a certain gas and concentration. This multidimensional matrix can be reduced to two principle components (PC1, PC2). The variance of PC1 (95.75%) and PC2 (2.94%) is above 98% and therefore these components already contain significant information to represent the data in two dimensions (Figure 29). Clear separation between the clusters representing the individual gases with no overlap and a recognizable trend of concentration allows the identification of all analytes with a set of six different electrodes.

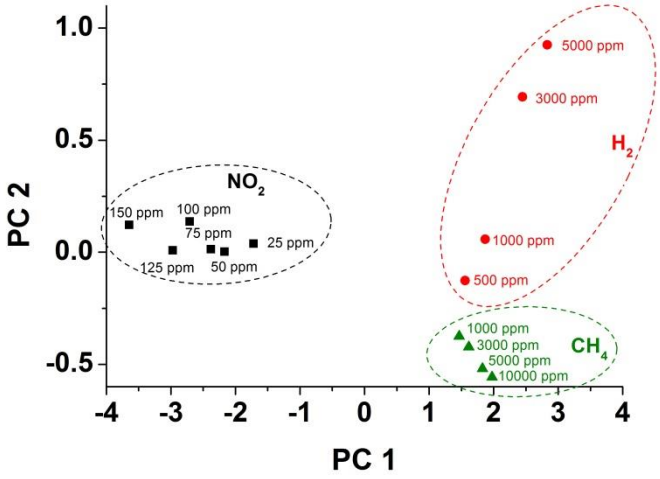

Figure 29 *Pattern analysis based on PCA using six different sensors (modified with rGO, rGO-ODA, rGO-TiO_2, rGO-MnO_2, rGO-Pd, and rGO-Pt) for various concentrations of individual gases (NO_2, H_2, and CH_4).*

Regeneration of the sensor material still is a crucial issue. In this study the regeneration was mostly performed by a short term heat treatment at 230 °C between the measurements to ensure complete desorption of physisorbed impurities. In an application this can be realized by different operation temperatures with short regeneration cycles.

5.2.4 Conclusion

Reduced graphene oxide is an ideal sensor material for chemiresistive gas sensors, due to the simple preparation and functionalization enabling an altered sensitivity. Compared to commercial solid state gas sensors, such sensors have the advantage of being operated at quite low temperatures of 85 °C to exclude the strong influences of humidity. It was demonstrated that spin coating of rGO composites result in reproducible sensor behavior suitable for well-established fabrication technologies. In a chemiresistor setup, unmodified rGO showed high sensitivity towards NO_2 in the ppm level at ambient conditions. The sensor was rather unselective and showed also responses towards H_2 and CH_4. Upon different functionalization, it was possible to achieve different sensor behavior for different gases. This can be used to apply PCA and discriminate each individual gas. It is expected that this approach can be extended to build up sensor arrays for detecting the concentration of many individual gases in a complex matrix at low temperature.

5.3 Graphene Gas Sensor for the Detection of Carbon Dioxide at Room Temperature

In the following chapter, rGO was investigated for its capability to detect CO_2, in order to develop a miniaturized gas sensor which can be operated at room temperature and therefore has low energy consumption. Previous studies shown that single graphene flakes and GO reduced by hydrogen plasma show a decrease of electrical resistance upon CO_2 adsorption [92, 347]. Similar observations have been made in preliminary experiments using rGO as sensitive receptor layer. But one major drawback was the poor regeneration of the sensor after gas adsorption. As seen in Figure 30, the sensor response towards 1000 ppm CO_2 is remarkable, but no regeneration of signal occurs while flushing with synthetic air. This indicates a strong interaction of the analyte with the graphene leading to an irreversible binding at ambient conditions. The analyte could be desorbed by heating the sensor to 400 °C and was reflected by reading the initial value of conductance. Such a regeneration step did not influence the sensor itself. In succeeding measurements of CO_2 the sensor behavior was found as before. Ghosh *et al*. [348] reported earlier that CO_2 can adsorb to the honeycomb structure of the graphene, but also an adsorption at the defective structures was proposed. They calculated a desorption temperature of 384 °C at 1 bar of pressure.

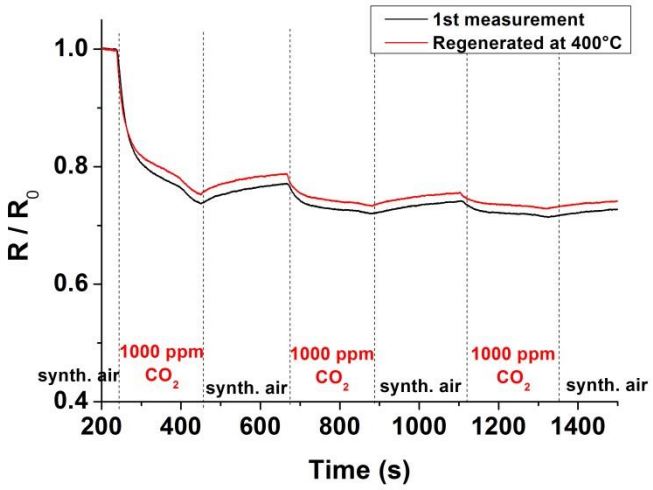

Figure 30 *Change in electrical resistance of a freshly prepared rGO based sensor (solid line) and the same sensor regenerated by heating to 400 °C in between the measurement (dashed line) for CO_2 (1000 ppm, 25 °C).*

An operating temperature or heating cycles of at least 400 °C do not give any advantage over commercial solid state gas sensor based on metal oxides, which are also maintained at

elevated temperatures above 250°C. It consumes too much energy, but also limits their long term stability [17].

In the field of solid state gas sensors based on metal oxides, a tremendous amount of metal oxides have been reported to show enhancement in sensitivity towards various gas analytes by introducing new binding sites or catalytic effects [349–351]. In this context, different rGO metal oxide composite nanomaterials had been synthesized and tested for their ability to detect CO_2 at room temperature. Modifications with different semiconductor nanoparticles, like CuO, SnO_2, Co_3O_4, TiO_2, MnO_2, NiO, and ZnO were screened. Only doping with CuO showed promising first results in terms of high signal change, no drift of signal during gas measurements, stability and especially regeneration of signal and was further investigated in detail. The results are displayed in the following chapter.

5.3.1 Formation and Characterization of CuO Modified Reduced Graphene Oxide

A wet chemical approach for the decoration of graphene by oxide nanoparticles was adapted [332]. A water/^{i}propanol system (1:10, v/v) turned out to result in CuO rod-like crystallites. It is reported that the Cu^{2+} ions, which are formed in ^{i}propanol, interact with the oxygen functionalities of GO and nucleation and growth of CuO nanoparticles occurs directly at the surface and edges of the GO sheets [332]. The addition of a small amount of water at a high temperature of 86 °C leads to large amount of nuclei owing to the hydrolysis reaction of $Cu(CH_3COO)_2$. The concentration of the copper precursor has been adjusted to achieve different levels of metal oxide doping to assess its effect the sensitivity of the material towards CO_2. Subsequent heating to 230 °C at atmosphere, GO was thermally reduced to rGO and the material became conductive.

The formation of CuO nanoparticles at the surface of GO could be observed with different techniques. In SEM pictures, CuO nanoparticles of diameters ranging from 50 to 200 nm have been found, decreasing in size using lower concentrations of copper precursor. Whereas a mass ratio of 1:2 (GO:CuO) led to a complete coverage of the GO by CuO (Figure 31a), using the same ratio of GO and CuO (1:1) resulted in a defined doping of the graphene material (Figure 31a). Hereby, rGO flakes appear as darker areas and the lighter spots reflect the CuO nanoparticles. Lower concentrations of CuO resulted in a composite material which does not show any changes in electrical resistance when applying CO_2.

An alternative route for the functionalization with CuO nanoparticles is the electrochemical reduction of a copper precursor directly at the surface of rGO. This can be an option for later industrial production of such devices and was shown here as a proof of concept. Applying a reduction pulse of at -1.2 V versus SCE in a 10 mM solution of Cu^{2+} leads to a formation of Cu nanoparticles on rGO. Whereas a longer pulse of 10 s result in a complete coverage of rGO (Figure 31e), a shorter pulse led to a partial decoration of nanoparticles with a diameter of around 200 nm (Figure 31f). Subsequent heating of the electrodes to 250°C at atmosphere results in an oxidation of the deposited Cu to the thermodynamic more stable CuO.

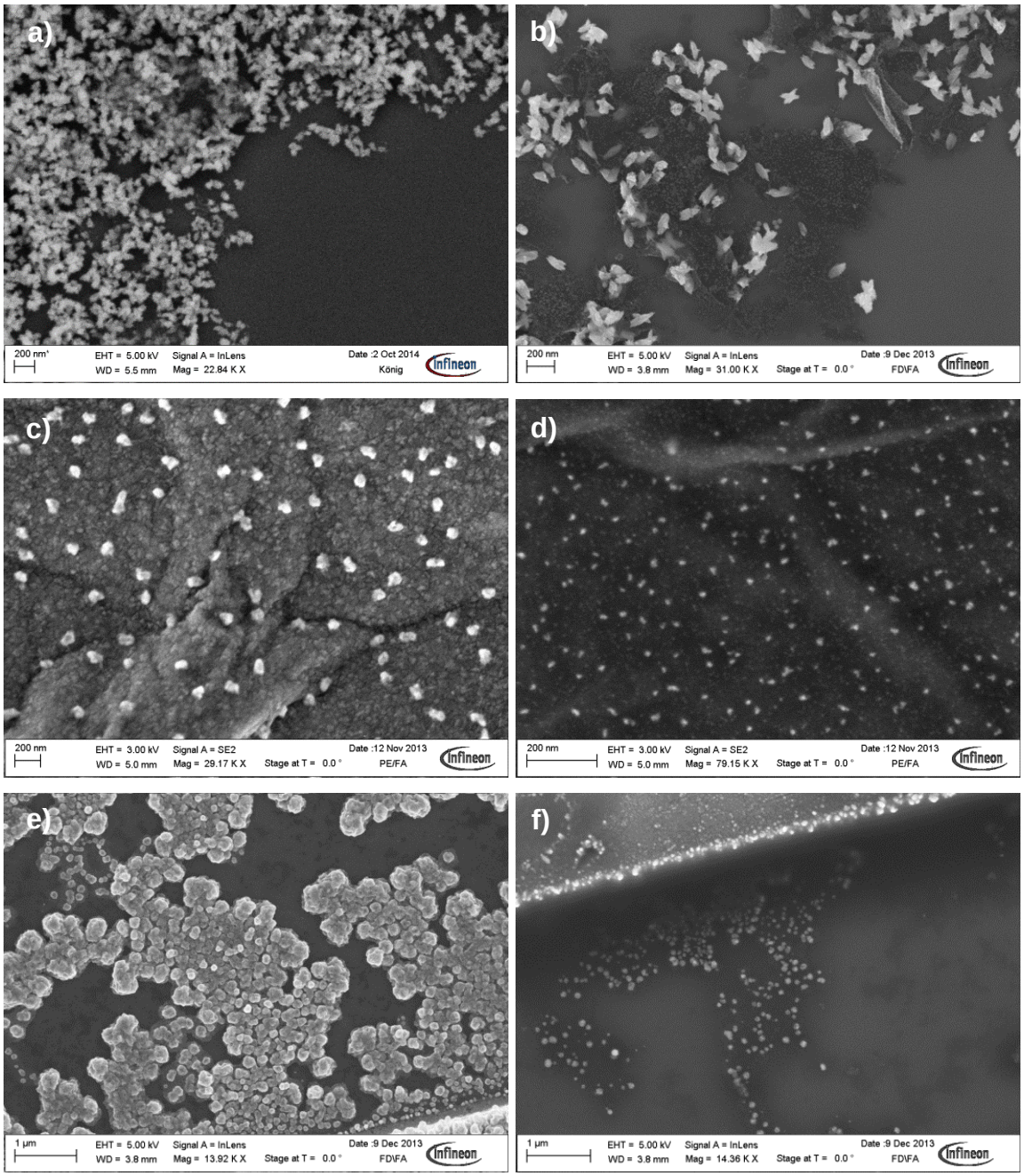

Figure 31 *SEM images of rGO modified with different amounts of CuO nanoparticles. The GO/CuO ratio was (a) 1:2, (b) 1:1, (c) 1:0.2, and (d) 1:0.02. Electrochemical deposited Cu nanoparticles on an rGO modified electrode with a reduction pulse of (e) 10 s and (f) 1 s at -1.2V vs SCE.*

The chemical nature of the copper nanomaterials was revealed by EDS measurements (Figure 32). Peaks around 2 keV can be ascribed to the substrate and the gold electrodes. A synthesis of copper oxide nanoparticles only resulted in a product, showing signals of oxygen and copper. The peak at 0.93 keV represents the L-alpha line of copper and for the rGO-CuO

composite signals at 0.3 keV can be ascribed to the k-alpha line of carbon of rGO. The decreasing intensity of the Cu peak also indicates a different level of doping.

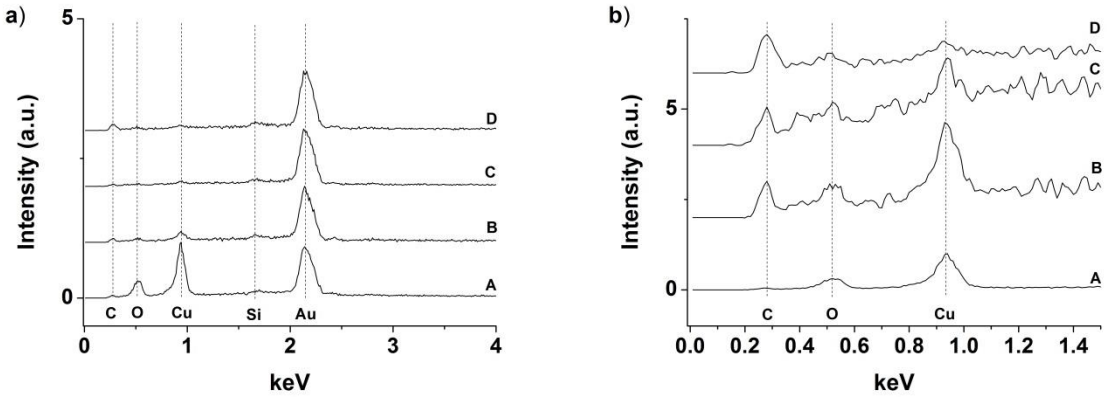

Figure 32 *(a) EDS spectra of rGO-CuO composite materials with a GO/CuO ratio of (A) 0:1 (B) 1:2, (C) 1:1, and (D) 1:0.2. (b) Magnification of the region of carbon, oxygen and copper peaks.*

To complete the picture, the different nanocomposites have been investigated by Raman spectroscopy. The spectra are displayed in Figure 33, peaks at 1353 cm^{-1} and 1606 cm^{-1} can be assigned to the D- and G-peak of rGO. Peaks at 298 cm^{-1}, 346 cm^{-1}, and 630 cm^{-1} can be attributed to A_g and B_g modes of the CuO [332, 352]. From this one can conclude that other copper oxides like Cu_4O_3 or Cu_2O are not present at significant amounts. The characteristic peaks for CuO decreased for lower the levels of metal oxide doping and could not be observed for smallest ratio (1:0.02). A characterization of the electrochemically deposited Cu nanoparticles with subsequent oxidation shows the same characteristic peaks for CuO and rGO mentioned above (Figure 33b).

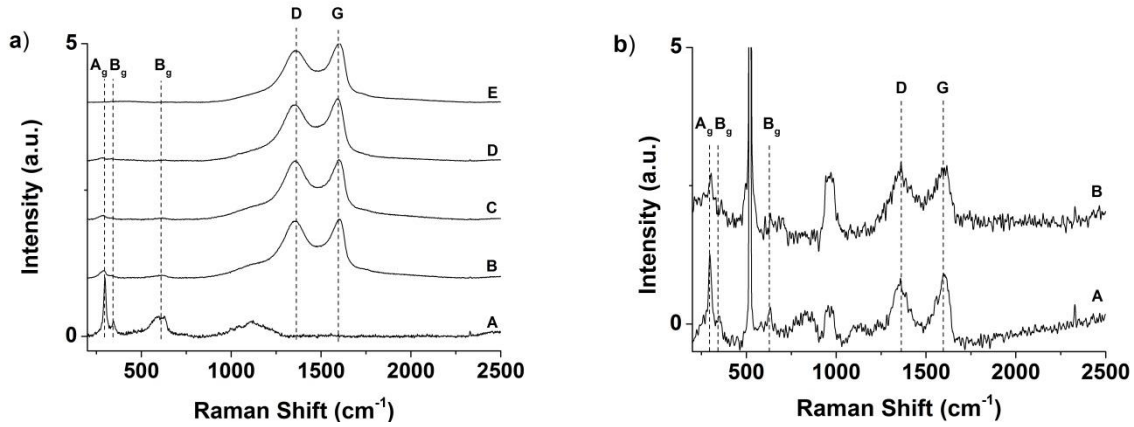

Figure 33 *Raman spectra of (a) of rGO-CuO composite materials with a GO/CuO ratio of (A) 0:1 (B) 1:2, (C) 1:1, (D) 1:0.2, (E) 1:0.02 and (b) electrochemical produced CuO nanoparticles on rGO with a reduction pulse of (A) 10 s and (B) 1 s at -1.2V versus SCE. Additional peaks at 520 and 980 cm^{-1} can be ascribed to the Si/SiO_2 substrate.*

5.3.2 Detection of Carbon Dioxide

Nanocomposites of rGO and CuO turned out to have a huge impact on the sensing behavior of the material towards CO_2. Whereas sensors based on rGO showed nearly no regeneration of signal, combination with the metal oxide nanoparticle led to higher sensitivity and also to an enhanced regeneration, even at room temperature (Figure 34a). The electrical resistance of sensors modified with a GO/CuO ratio of 1:2 dropped by 40% while being exposed to 1000 ppm CO_2. The response time changed from several minutes for rGO to less than 30 seconds for the nanocomposite. The main benefit here is a nearly complete reversibility after flushing 200 seconds with synthetic air. Whereas a complete loading of rGO with metal oxide nanoparticles, leads to an increased sensitivity, a decrease of the level of doping also results in a decreasing sensitivity towards CO_2 (Figure 34b). The electrical resistance dropped only by 7% and 1%, using a GO/CuO ratio of 1:1 and 1:0.2 respectively. A lower ratio of 1:0.02 resulted in a material comparable to rGO, with no signal changes in the presence of 1000 ppm CO_2. This shows the importance of the metal oxide in the gas sensing mechanism. Since sensors with a GO/CuO ratio of 1:2 showed highest sensitivity towards CO_2 and also stability, further experiments were performed with this material referring to it as rGO-CuO.

Sensors with a layer comprising only CuO without involving any rGO show also a change in electrical resistance upon exposure to 1000 ppm CO_2 of about 15% (Figure 34c). Here, a continuous drift of signal and no equilibration in a reasonable time are major drawbacks of this system. One reason might be the mechanical instability of the sensor layer, consisting only of metal particles and the use of rGO is mandatory for a stable sensor response.

Electrochemical preparation of the rGO-CuO composite resulted in a sensor material which electrical resistance dropped by 6% in the presence of 1000 ppm CO_2 with good regeneration characteristics (Figure 34d). Though this approach did not yield in a sensor material with best sensitivity, it reveals an alternative to the wet chemical synthesis and could be used in terms industrial production.

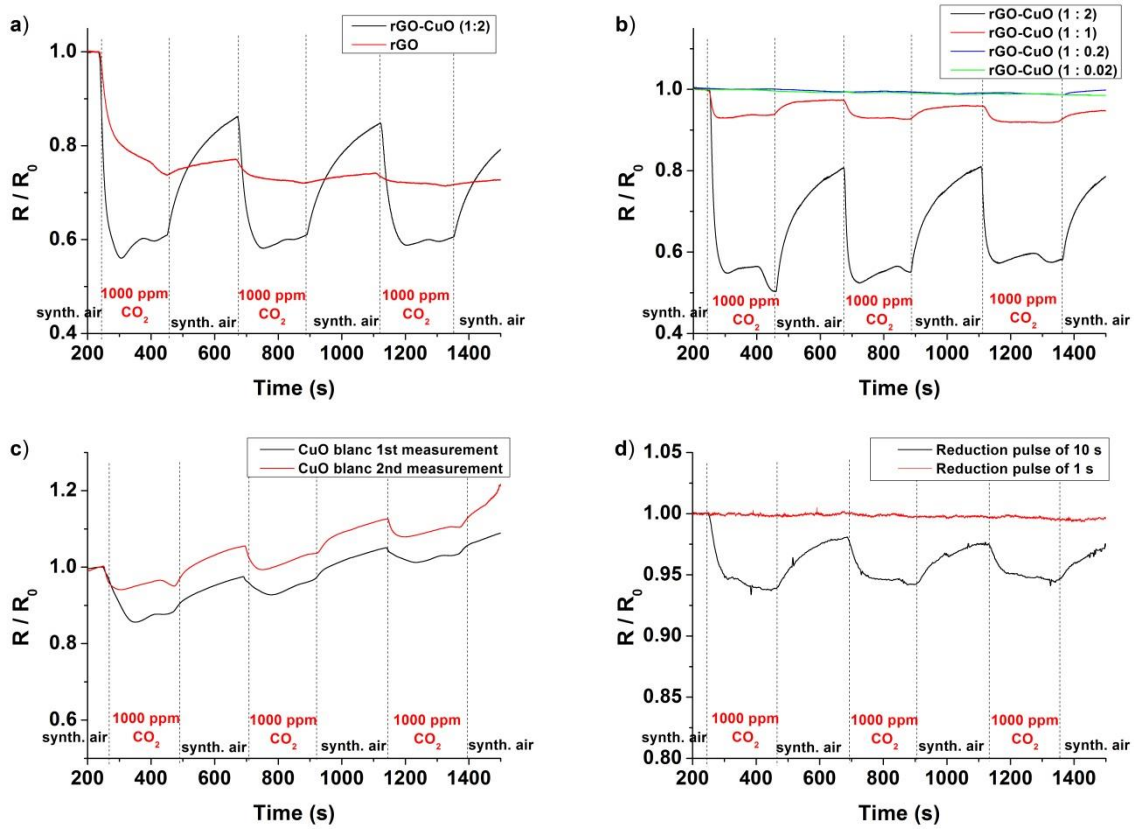

Figure 34 *Relative change in electrical resistance (R/R_0) of sensors based on (a) rGO and composites with CuO using a GO/CuO ratio of 1:2, (b) different levels of CuO doping, (c) CuO without rGO, and (d) electrochemically deposited CuO on rGO with different times of reduction pulse in the presence of 1000 ppm CO_2 at 25 °C.*

The gas sensing mechanism involving metal oxides is usually based on the surface properties of the sensing material [353]. For metal oxide based gas sensors it is described that first, oxygen in the air gets adsorbed and dissociates molecular oxygen ions O^- and O^{2-} [349]. Interaction of CO_2 leads to a change in the electronic depletion layer formed by the oxygen affecting the conductance of the metal oxide. The introduced analyte gas can either react with the oxygen species or a competitive adsorption and replacement of the adsorbed oxygen can take place. It is believed that CO_2 is oxidized to carbonates and releases electrons to the surface material. This would lead to an increase of electrical resistance, because CuO is a p-type semiconductor. Therefore, a mechanism through competitive gas adsorption, where the introduced adsorbent creates more positive charge carriers through charge transfer is more plausible. The interior regions of the metal oxide nanoparticles do not contribute to the sensor response and therefore a high surface area is mandatory. This was achieved by using CuO nanoparticles attached to rGO.

An increase of the temperature from 25 to 85 °C, leads to a drop in signal of rGO-CuO modified electrodes by 91% (Figure 35a), in contrast to a drop of 58% for rGO modified electrodes. The decrease of electrical resistance with increasing temperature is a well-known characteristic feature of semiconductors [25]. The charge transport occurs through variable range hopping between the crystalline graphene structures in rGO which are separated by defects. This mechanism is affected by temperature. The much higher drop of electrical resistance at rGO-CuO indicates that the charge transport of this material is preferable conducted by the metal oxide. A drop by 91% also fits with the temperature dependency of polycrystalline CuO films found earlier [354]. Heating to 60 °C during the measurements had only a slight effect on the sensors response towards 1000 ppm CO_2 (Figure 35a). The overall signal towards the analyte gas stays the same, indicating that the sensing mechanism described above is not affected in this temperature range. The wavelike response curve at 60 °C can be ascribed to the heating cycles of the gas chamber and the high temperature sensitivity of the material.

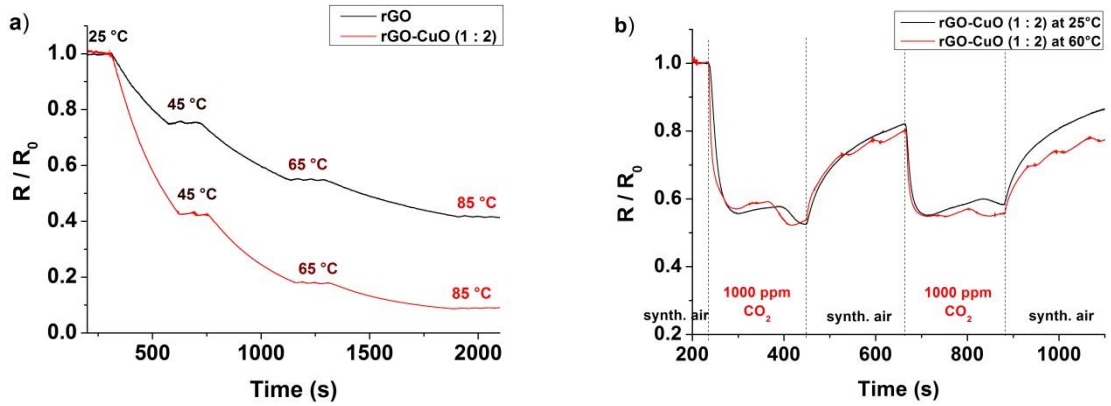

Figure 35 *Influence of temperature on (a) the relative resistance of rGO and rGO-CuO in synthetic air and (b) the response of an rGO-CuO modified electrode towards 1000 ppm CO_2.*

The concentration dependency and reversibility of the sensors was evaluated by continuous adsorption and desorption of different concentrations of CO_2 ranging from 150 to 1500 ppm (Figure 36a). The signal drops faster for higher concentrations leading to a linear detection range from 150 to 1250 ppm. For higher concentrations the sensors showed saturation. Adjusting the thickness of the sensor layer and also the level of metal oxide doping may tune the sensitivity towards favorable directions. Nevertheless, this nearly covers the range of CO_2 concentration typically found indoor which is considered to be of good quality below 800 ppm, average from 800 to 1400 ppm and bad above 1500 ppm CO_2 [355]. The sensors

also show good reversible behavior (Figure 36b), making it suitable for e.g. indoor air quality management in terms of air conditioning.

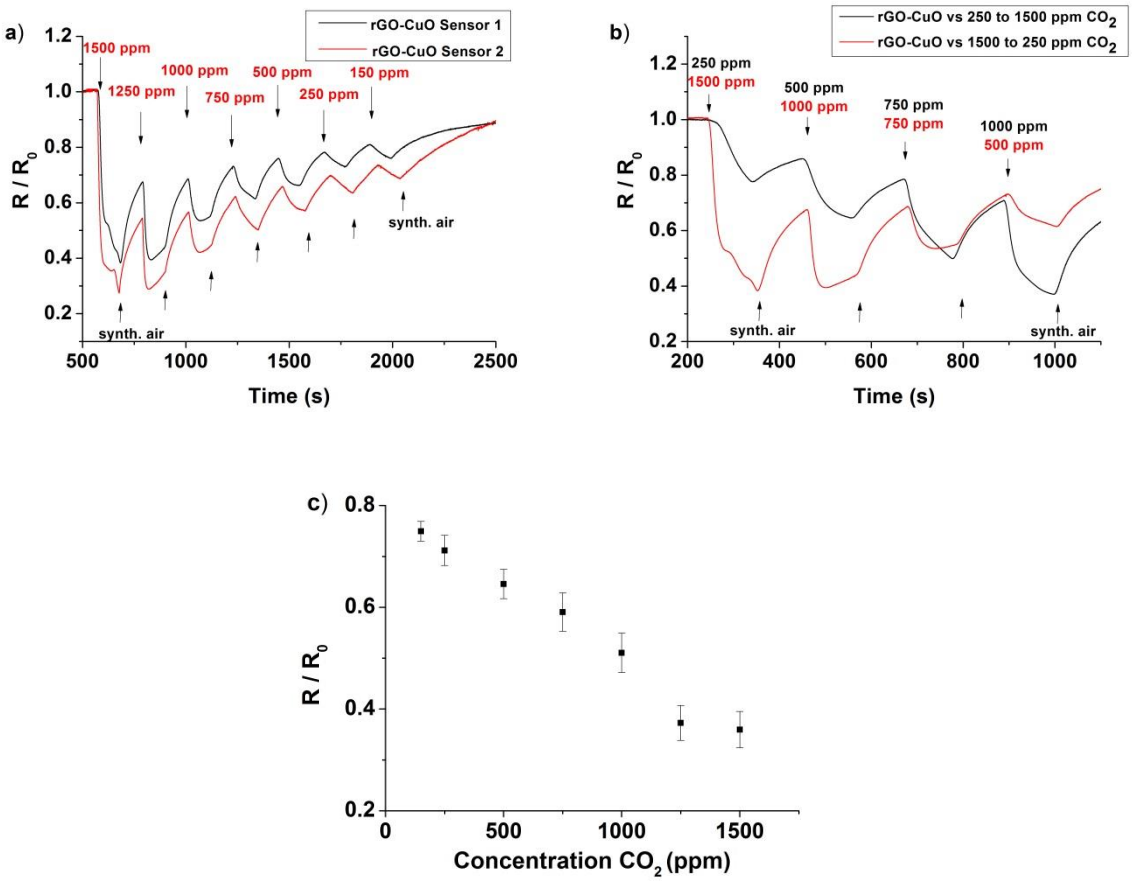

Figure 36 *Changes in relative resistance of (a) different rGO-CuO (1:2) based sensors prepared in the same way in the presence of different concentrations of CO_2 at 25°C, (b) using different concentration profiles. (c) Concentration dependency of an rGO-CuO (1:2) based sensors.*

5.3.3 Cross Sensitivity

Selectivity is a key issue in developing new sensor materials and concepts. Often sensors show cross sensitivity to other gaseous analytes, disallowing the detection of single gases in a gas mixture. A solution could be a sensor array consisting of different modified sensor materials with altered sensitivities. The sensor response of the rGO-CuO composite is characterized by high sensitivity for CO_2, in contrast to rGO. Therefore, these type of sensors were also tested against various analyte gases like NO_2, CH_4, H_2 and CO (Figure 37a). The sensor behavior is very similar to unmodified rGO. Oxidizing gases like NO_2 transfer an electron to the surface layer of CuO and therefore lower the concentration of charge carriers, since CuO as well as rGO show p-type semiconductor behavior. Carbon monoxide can get oxidized at metal oxides, but only at elevated temperatures [349]. The low signals for CO and H_2 are probably due to a competitive adsorption of the introduced gas molecules and previously adsorbed oxygen. In the presence of CH_4 no signal change occurs, assuming that either there is no adsorption to the CuO surface or it no effect on the electrical resistance of the sensor material.

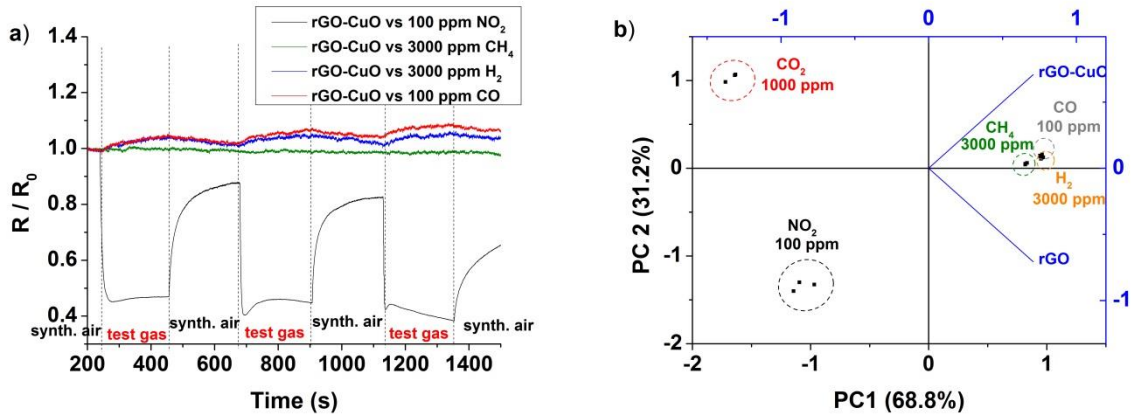

Figure 37 *(a) Response of sensors based on rGO-CuO composite with a GO/CuO ratio of 1:2 in the presence of 100 ppm NO_2, 3000 ppm, CH_4, 3000 ppm H_2, and 100 ppm CO at 25°C. (b) Plot of two principle components (scores plot, black) using a sensor array consisting of unmodified rGO and rGO-CuO electrodes and the contribution to the signal of each sensor (loadings plot, blue).*

Whereas a single sensor based on rGO shows high changes in signal in the presence of NO_2, but cannot detect CO_2, devices based on rGO-CuO are sensitive towards both gases. A combination of both would capable to distinguish between these gases. Applying PCA, as shown in the previous chapter (5.2.3), leads to a clear separation pattern of the applied gases

in the scores plot (Figure 37b). In the loading plot it is shown that the rGO-CuO sensor mainly contributes to the CO_2 detection, the rGO sensor is responsible for the NO_2 signal and both of them contribute to the detection of the other gases in nearly the same amount. The resolution for test gases like CO, CH_4 and H_2 is rather low and other sensors with altered sensitivity are needed for a clear separation of signals.

5.3.4 Comparison to a Commercial Sensor

An optimized sensor consisting of rGO-CuO composite was compared to a commercial sensor device. Therefore, a CDM4161-L00 CO_2 module from Figaro (Figure 38) was measured under the same conditions as used for the other CO_2 tests. The sensor principle is based on potentiometric measurements using a solid electrolyte. It has a detection range of 400 to 4500 ppm CO_2, with ±20% accuracy and a response time of 2 minutes. The integrated electronics process the signal and an amplified voltage is generated proportional to the concentration of CO_2.

Figure 38 *CDM4161 CO_2 Module from Figaro* [356].

Figure 39a shows the result of the comparison of the Figaro sensor and an electrode modified with rGO-CuO composite material. Both show similar characteristics in signal change in the presence of different concentrations of CO_2, except the commercial device is a little bit faster in signal regeneration. The linear detection range of the sensor developed during this work goes down to 250 ppm CO_2 whereas the Figaro sensor is adjusted to concentrations above 400 ppm (Figure 39b). Sensitivities are 2.3 10^{-3} ppm^{-1} and $3.2 \cdot 10^{-4}$ ppm^{-1} for the Figaro sensor and the rGO-CuO device, respectively. Therefore, the commercial sensor is more sensitive by the factor of 20. This is still a remarkable result for the sensor prepared in the frame of this work, considering the signal amplification build within the commercial module. In this state of development, the commercial sensor is surely outperforming the rGO-CuO based sensor, but it holds great promise for the development of miniaturized chemical nanosensors.

Such sensors can be scaled to the micrometer or maybe even nanometer range, because of simplicity of the setup. Resistive type sensors comprise only a sensitive layer contacted by two or more electrodes, if e.g. a four point measurement is required to eliminate the contact resistance. In contrast, a potentiometric setup consists of measurement electrode, electrolyte, reference electrode and a compartment for the reference gas. Further solid electrolyte based gas sensors usually need an elevated temperature to improve the ionic conductivity of the

electrolyte material, while this chemiresistive type gas sensor is optimized to work at room temperature. Heating cycles can be implemented to refresh the sensor layer by desorption of previously bound gas species, if necessary.

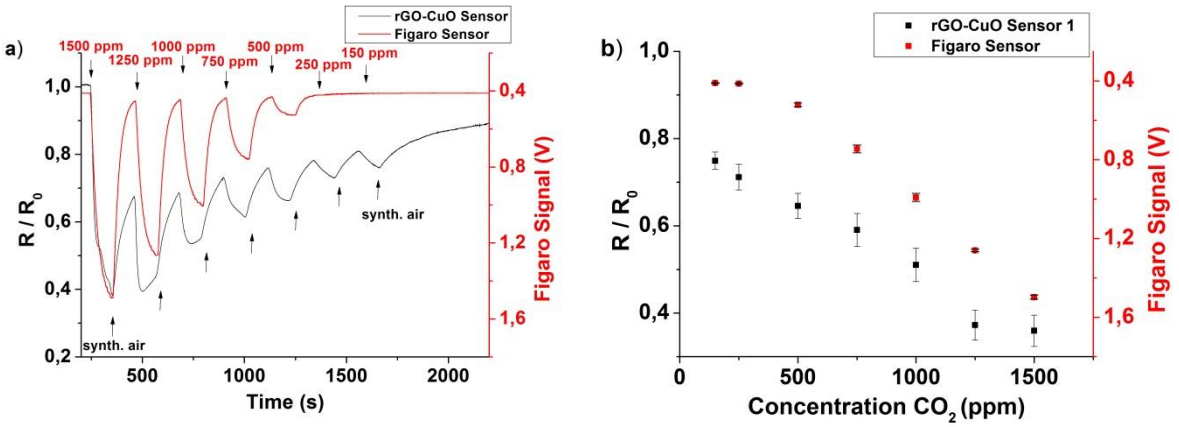

Figure 39 *(a) Response characteristics of the Figaro sensor device and a sensor based on rGO-CuO composite material in the presence of different concentrations of CO_2 at 25°C. (b) Calibration curve of both sensors.*

5.3.5 Conclusion

It was demonstrated that decoration of rGO with CuO nanoparticles leads to an improved sensitivity of the material towards CO_2 in a chemiresistive setup. The sensor material was optimized in terms of level of doping with metal oxide. Complete coverage of rGO with a ratio of GO/CuO ratio of 1:2 turned out to have highest sensitivity ($3.2 \cdot 10^{-4}$ ppm^{-1}) even at room temperature and showed a linear behavior from 150 to 1250 ppm CO_2. The sensor performance was compared to a commercial sensor under identical experimental conditions and showed great potential in this stage of development. The cross sensitivity of such a device was rather low towards H_2, CH_4 and CO, but high towards NO_2. Combination with an unmodified rGO based sensor showed a clear recognition pattern utilizing PCA. An array of these two electrodes is expected capable for a distinct detection of CO_2 and NO_2 at room temperature.

6 Summary

The variability of graphene with its exceptional properties gives rise to improve material chemistry in various fields of applications. The development of graphene is still in the beginning and up to now only a few niche products have reached the market and are highlighted as well as the aim of this work in chapter 1. The goal of this thesis was the investigation of graphene in electrochemical sensor applications. It holds great promise in terms of miniaturization, improving sensitivity and developing new sensor concepts. Many approaches are already described for biosensor applications, often utilizing graphene in an amperometric detection scheme. Therefore, the impact of preparation technique on the detection of the model analyte H_2O_2 was investigated, applying different graphene materials as electrode material. Further, graphene was studied as tunable sensor material in gas sensing applications and how it can be customized for the room temperature detection of CO_2.

Chapter 2 summarizes the author's publications and patents developed in the frame of this work.

The perspectives of graphene in electrochemical sensors were investigated by the means of research performed in this field and are described in chapter 3. The most prominent preparation techniques and the application in biosensor and gas sensor technologies are discussed. Every method provides graphene materials of different characteristics, scalability and further usability. It was shown that defects in the ideal sp^2 carbon lattice decide on the sensor performance, but also on device fabrication and appropriate functionalization. A higher quality of graphene can lead to more sensitivity and reliable device production in electrochemical biosensor technologies. In contrast, a defective structure can enhance the sensitivity and applicability in gas sensing applications, providing additional adsorption sites.

In chapter 4, the experimental work, performed during this work, is described in detail. Chapter 5 comprises the results on graphene and graphene composite materials applied in the electrochemical detection of H_2O_2 and as tunable recognition element in gas sensors. In a first part, graphene materials derived by different preparation techniques were studied as electrode material. The electrochemical behavior of the different materials has been investigated as well as the feasibility in device fabrication was compared. It was shown, that the quality of the graphene has an enormous impact on the reductive amperometric detection of H_2O_2. A

defective structure like in reduced graphene oxide leads to almost no significant improvement in signal enhancement compared to a standard carbon disc electrode. In contrast, fewer defects like in graphene prepared by chemical vapor deposition, resulted in a higher sensitivity, which is 50 times better compared to reduced graphene oxide. This technique was found to be most suitable for the production of highly sensitive electrodes to be further used in amperometric detection and development of biosensors.

Whereas, a material of high quality is desired in electrochemical biosensor applications, defects are beneficial using graphene as transducer in a chemiresistive setup for the detection of gaseous analytes. In the next part of the work, reduced graphene oxide was demonstrated to be an applicable candidate for gas detection at moderate (85 °C) or even room temperature. Analyte gases like NO_2, CH_4 and H_2 were detected due to fast changes in the electrical resistance at of 85 °C. To overcome the poor selectivity, the material was further altered with octadecylamine, metal nanoparticles such as Pd and Pt, and metal oxides such as MnO_2, and TiO_2. This changed the sensor response towards the studied gases and the different response patterns for six different materials allowed a clear discrimination of all test gases by pattern recognition based on principal component analysis.

Based on the feasibility of this concept, a graphene-based sensor for the room temperature detection of CO_2 was developed. Decoration of reduced graphene oxide with CuO nanoparticles led to an improved sensing performance for the target analyte. Different levels of metal oxide doping were applied by wet chemical and electrochemical preparation methods and the resulting composite materials were characterized. It was shown that a complete coverage obtained by wet chemical functionalization leads to highest sensitivity, comparable to a commercial CO_2 sensor, which was also tested in the frame of this work. An array consisting of reduced graphene oxide and the composite with CuO nanoparticles was capable to differentiate CO_2 from NO_2, CO, H_2 and CH_4. This sensor material can lead to the development of miniaturized chemical sensors comprising high and adjustable sensitivity, which can be applied for monitoring air quality and ventilation management. The presented sensor concept based on customized graphene materials can be tailored for the versatile use in appropriate applications.

One of the main challenges remains the reproducible large-scale production of graphene and functionalized graphene combined with reliable transfer techniques in terms of an industrial application. This problem has not been solved completely up to now. But the extensive research going on in this field will lead to a solution in near future and will help graphene to

find its way to be integrated into many electrochemical sensor devices. Further studies should preferably aim for large scale production of the material and devices. The use of high quality graphene with a distinct introduction of defects and a better controlled way of functionalization may be a route to tune the material properties in favorable directions.

7 Zusammenfassung

Graphen birgt großes Potential in den unterschiedlichsten Anwendungsgebieten, aufgrund der bemerkenswerten Eigenschaften, die es in einem Material vereint. Bis jetzt kann es jedoch nur in einigen wenigen kommerziellen Nischenprodukte wiedergefunden werden. Das Ziel dieser Arbeit war es, die Anwendung von Graphen in elektrochemischen Sensoren zu untersuchen. In diesem Zusammenhang kann es dazu beitragen, Bauelemente zu miniaturisieren, die Empfindlichkeiten von Sensoren zu verbessern und neue Messkonzepte zu entwickeln. Viele Studien auf dem Gebiet der Biosensorik befassen sich mit der Anwendung von Graphen und basieren meist auf einem amperometrischen Detektionsprinzip. Hierzu wurden unterschiedlich hergestellte Graphenmaterialien als Elektrodenmaterial zum Nachweis eines Modelanalyten (H_2O_2) eingesetzt und der Einfluss der Materialqualität untersucht. Desweiteren wurde gezeigt, dass sich chemisch hergestelltes Graphen als Sensormaterial zur Detektion von Gasen eignet und wie dessen Ansprech-verhalten zur selektiven Detektion von CO_2 angepasst werden kann.

Kapitel 2 gibt einen Überblick über die Publikationen und Patente des Autors, die im Rahmen dieser Arbeit entstanden sind.

Kapitel 3 beschreibt die Perspektiven von Graphen und dessen Einsatz in elektrochemischen Sensoren anhand der Ergebnisse aktueller Forschung. Zunächst wird auf die bedeutendsten Methoden zu dessen Herstellung eingegangen und deren Anwendbarkeit in Gas- und Biosensortechnologien diskutiert. Dabei liefert jede Herstellungsmethode Graphenematerialien mit unterschiedlichen Eigenschaften und in verschiedenen Dimensionen und Mengen, was die weitere Verarbeitung stark beeinflusst. Es zeigte sich, dass Defekte in der sp^2 Struktur der Kohlenstoffschichten maßgeblich die Leistungsfähigkeit der Sensoren, als auch deren Herstellung und entsprechende Funktionalisierung beeinflussen. Graphen von hoher Qualität zeigt erhöhte Sensitivität und zuverlässigere Produktion in elektrochemischen Biosensoren. Im Gegensatz dazu profitieren Anwendungen in der Gassensorik von Defekten im Material, da diese zusätzliche Bindungstellen für Analyten aufweisen.

In Kapitel 4 werden die experimentellen Einzelheiten dieser Arbeit beschrieben. Die dabei entstandenen Ergebnisse zu Graphen und Kompositmaterialien, angewandt zur elektrochemischen Detektion von H_2O_2 und als variables Sensorelement zur Detektion von Gasen,

sind in Kapitel 5 dargestellt. Im ersten Teil wurden die elektrochemischen Eigenschaften von Graphenelektroden, welche auf unterschiedliche Weise hergestellt wurden, verglichen. Es wurde gezeigt, dass die Qualität des Graphens einen erheblichen Einfluss auf die reduktive amperometrische Erfassung von H_2O_2 hat. Eine defektreiche Struktur, wie in reduziertem Graphenoxid, zeigte dabei nur geringfügige Signalverstärkung verglichen mit einer herkömmlichen Kohlenstoffelektrode. Graphen, welches durch chemische Gasphasen-abscheidung hergestellt wurde und eine geringere Anzahl an Defekten aufweist, zeigte im Gegensatz dazu eine um den Faktor 50 höhere Sensitivität als reduziertes Graphenoxid. Daher eignet sich gerade diese Methode der Graphensynthese zur Herstellung von hochsensitiven Elektroden und Entwicklung amperometrischer Biosensoren.

In elektrochemischen Biosensoren ist eine hohe Materialqualität wünschenswert. Bei der Detektion von Gasen können sich jedoch Defekte im Material vorteilhaft auswirken. Im nächsten Teil der Arbeit wurde reduziertes Graphenoxid als signalgebendes Element in chemischen Leitfähigkeitssensoren eingesetzt. Diese Sensoren konnten bei niedrigen Temperaturen von 85 °C oder sogar Raumtemperatur betrieben werden. Eine schnelle Änderung des elektrischen Widerstandes, bedingt durch die Adsorption von Gasmolekülen, ermöglichte eine Erfassung von NO_2, CH_4 und H_2, jedoch mit schlechter Selektivität. Um diese zu verbessern, wurde das Material mit Octadecylamin, Metallnanopartikeln (Pd, Pt) sowie Metalloxiden (TiO_2, MnO_2) modifiziert und ein verändertes Ansprechverhalten gegenüber der getesteten Gase festgestellt. Das Erkennungsmuster von sechs verschiedenen Sensormaterialien kombiniert mit einer Datenverarbeitung mittels Hauptkomponentenanalyse ermöglichte schließlich eine klare Unterscheidung der Gase.

Basierend auf diesem Konzept, wurde im nächsten Teil der Arbeit ein Sensor zur Detektion von CO_2 bei Raumtemperatur entwickelt. Das Ansprechverhalten von reduziertem Graphenoxid konnte durch Abscheidung von CuO Nanopartikeln erheblich verbessert werden. Reduziertes Graphenoxid wurde mittels nasschemischer und elektrochemischer Methoden in unterschiedlichen Verhältnissen mit dem Metalloxid beladen und die entsprechenden Kompositmaterialien charakterisiert. Eine vollständige Bedeckung mit Metalloxidpartikeln führte dabei zur höchsten Sensitivität gegenüber CO_2. Im Rahmen dieses Projekts wurde ein solcher Sensor mit einem kommerziell erhältlichen CO_2-Messgerät verglichen und lieferte durchaus gleichwertige Resultate. Zusätzlich wurde gezeigt, dass ein Verbund aus zwei Sensoren, basierend auf reduziertem Graphenoxid und dem Kompositmaterial mit CuO Nanopartikeln, CO_2 gegenüber NO_2, CO, H_2 und CH_4 selektiv

unterscheiden kann. Das Kompositmaterial kann zur Entwicklung von miniaturisierten chemischen Sensoren mit hoher und einstellbarer Sensitivität beitragen und könnte in der Überwachung von Luftqualität und automatischer Belüftungssteuerung Anwendung finden. Das hier vorgestellte Sensorkonzept, bestehend aus individuell modifizierten Graphen-materialien, bietet ein vielseitiges Spektrum an Einsatzmöglichkeiten.

Die reproduzierbare Herstellung von Graphen und funktionalisierten Materialien im Zusammenspiel mit geeigneten Transfertechniken ist bis heute der limitierende Faktor, um es letztendlich für industrielle Anwendungen verfügbar zu machen. Dieses Problem ist noch nicht vollständig gelöst. Jedoch lässt der Fortschritt auf diesem Gebiet auf Lösungsansätze in naher Zukunft hoffen. Graphen wird damit voraussichtlich den Weg in viele elektrochemische Sensoren finden. Weiterführende Studien sollten sich daher vor allem mit der groß angelegten Produktion von Materialen und Sensoren befassen. Eine Möglichkeit ist hierbei die Verwendung von Graphenmaterialien von definierter Qualität, in die auf kontrollierter Weise Defekte und entsprechende Funktionalisierungen eingebracht werden.

8 References

1. Novoselov KS, Geim AK, Morozov SV, Jiang D, Zhang Y, Dubonos SV, Grigorieva IV, Firsov AA (2004) Electric Field Effect in Atomically Thin Carbon Films. Science 306:666–669
2. (2013) Graphene in the heart of Europe. Nat Nanotechnol 8:221–221
3. Liu F, Ming P, Li J (2007) Ab initio calculation of ideal strength and phonon instability of graphene under tension. Phys Rev B 76:064120
4. Geim AK (2009) Graphene: Status and Prospects. Science 324:1530–1534
5. Nair RR, Blake P, Grigorenko AN, Novoselov KS, Booth TJ, Stauber T, Peres NMR, Geim AK (2008) Fine structure constant defines visual transparency of graphene. Science 320:1308
6. Chae HK, Siberio-Pérez DY, Kim J, Go Y, Eddaoudi M, Matzger AJ, O'Keeffe M, Yaghi OM (2004) A route to high surface area, porosity and inclusion of large molecules in crystals. Nature 427:523–527
7. http://store.vorbeck.com/collections/all, 13.06.2015.
8. http://www.head.com/tennis/technologies/?region=eu&id=706, 13.06.2015.
9. http://www.vittoria.com/news/the-revolutionary-g-material/, 13.06.2015.
10. http://www.catlike.es/global/en/innovation/helmets-technologies/graphene/, 13.06.2015.
11. Li Y, Chopra N (2014) Progress in Large-Scale Production of Graphene. Part 2: Vapor Methods. JOM 67:44–52
12. https://www.zapandgocharger.com/pre-order.html, 12.06.2015.
13. Yuan W, Shi G (2013) Graphene-based gas sensors. J Mater Chem A 1:10078–10091
14. Samet JM (2007) Traffic, Air Pollution, and Health. Inhal Toxicol 19:1021–1027
15. Moseley PT (1997) Solid state gas sensors. Meas Sci Technol 8:223
16. Korotcenkov G (2007) Metal oxides for solid-state gas sensors: What determines our choice? Mater Sci Eng B 139:1–23
17. Tricoli A, Righettoni M, Teleki A (2010) Semiconductor Gas Sensors: Dry Synthesis and Application. Angew Chem Int Ed 49:7632–7659
18. Robinson JT, Perkins FK, Snow ES, Wei Z, Sheehan PE (2008) Reduced graphene oxide molecular sensors. Nano Lett 8:3137–3140

19. Leenaerts O, Partoens B, Peeters FM (2008) Adsorption of H2O, NH3, CO, NO2, and NO on graphene: A first-principles study. Phys Rev B 77:125416
20. Schedin F, Geim AK, Morozov SV, Hill EW, Blake P, Katsnelson MI, Novoselov KS (2007) Detection of individual gas molecules adsorbed on graphene. Nat Mater 6:652–655
21. Stoller MD, Park S, Zhu Y, An J, Ruoff RS (2008) Graphene-Based Ultracapacitors. Nano Lett 8:3498–3502
22. Rao CNR, Sood AK, Subrahmanyam KS, Govindaraj A (2009) Graphene: The New Two-Dimensional Nanomaterial. Angew Chem Int Ed 48:7752–7777
23. Hummers WS, Offeman RE (1958) Preparation of Graphitic Oxide. J Am Chem Soc 80:1339–1339
24. Li D, Müller MB, Gilje S, Kaner RB, Wallace GG (2008) Processable aqueous dispersions of graphene nanosheets. Nat Nanotechnol 3:101–105
25. Gómez-Navarro C, Weitz RT, Bittner AM, Scolari M, Mews A, Burghard M, Kern K (2007) Electronic transport properties of individual chemically reduced graphene oxide sheets. Nano Lett 7:3499–3503
26. Gilje S, Han S, Wang M, Wang KL, Kaner RB (2007) A chemical route to graphene for device applications. Nano Lett 7:3394–3398
27. Zhang Y-H, Chen Y-B, Zhou K-G, Liu C-H, Zeng J, Zhang H-L, Peng Y (2009) Improving gas sensing properties of graphene by introducing dopants and defects: a first-principles study. Nanotechnology 20:185504
28. Eda G, Fanchini G, Chhowalla M (2008) Large-area ultrathin films of reduced graphene oxide as a transparent and flexible electronic material. Nat Nanotechnol 3:270–274
29. Xu Y, Shi G (2011) Assembly of chemically modified graphene: methods and applications. J Mater Chem 21:3311–3323
30. Persily AK (1997) Evaluating building IAQ and ventilation with indoor carbon dioxide. Trans-Am Soc Heat Refrig AIR Cond Eng 103:193–204
31. Scheff PA, Paulius VK, Huang SW, Conroy LM (2000) Indoor Air Quality in a Middle School, Part I: Use of CO2 as a Tracer for Effective Ventilation. Appl Occup Environ Hyg 15:824–834
32. Pérez-López B, Merkoçi A (2012) Carbon nanotubes and graphene in analytical sciences. Microchim Acta 179:1–16

33. Zhou M, Zhai Y, Dong S (2009) Electrochemical Sensing and Biosensing Platform Based on Chemically Reduced Graphene Oxide. Anal Chem 81:5603–5613
34. Kochmann S, Hirsch T, Wolfbeis OS (2012) Graphenes in chemical sensors and biosensors. TrAC Trends Anal Chem 39:87–113
35. Marcano DC, Kosynkin DV, Berlin JM, Sinitskii A, Sun Z, Slesarev A, Alemany LB, Lu W, Tour JM (2010) Improved Synthesis of Graphene Oxide. ACS Nano 4:4806–4814
36. Kim KS, Zhao Y, Jang H, Lee SY, Kim JM, Kim KS, Ahn J-H, Kim P, Choi J-Y, Hong BH (2009) Large-scale pattern growth of graphene films for stretchable transparent electrodes. Nature 457:706–710
37. Shang NG, Papakonstantinou P, McMullan M, Chu M, Stamboulis A, Potenza A, Dhesi SS, Marchetto H (2008) Catalyst-Free Efficient Growth, Orientation and Biosensing Properties of Multilayer Graphene Nanoflake Films with Sharp Edge Planes. Adv Funct Mater 18:3506–3514
38. Novoselov KS, Fal′ko VI, Colombo L, Gellert PR, Schwab MG, Kim K (2012) A roadmap for graphene. Nature 490:192–200
39. Park S, Ruoff RS (2009) Chemical methods for the production of graphenes. Nat Nanotechnol 4:217–224
40. Tang L, Wang Y, Li Y, Feng H, Lu J, Li J (2009) Preparation, Structure, and Electrochemical Properties of Reduced Graphene Sheet Films. Adv Funct Mater 19:2782–2789
41. Ambrosi A, Chua CK, Bonanni A, Pumera M (2014) Electrochemistry of Graphene and Related Materials. Chem Rev 114:7150–7188
42. Lu L-M, Qiu X-L, Zhang X-B, Shen G-L, Tan W, Yu R-Q (2013) Supramolecular assembly of enzyme on functionalized graphene for electrochemical biosensing. Biosens Bioelectron 45:102–107
43. Chen S, Yuan R, Chai Y, Hu F (2012) Electrochemical sensing of hydrogen peroxide using metal nanoparticles: a review. Microchim Acta 180:15–32
44. Cui X, Wu S, Li Y, Wan G (Gary) (2014) Sensing hydrogen peroxide using a glassy carbon electrode modified with in-situ electrodeposited platinum-gold bimetallic nanoclusters on a graphene surface. Microchim Acta 182:265–272
45. Li S-J, Du J-M, Zhang J-P, Zhang M-J, Chen J (2014) A glassy carbon electrode modified with a film composed of cobalt oxide nanoparticles and graphene for electrochemical sensing of H2O2. Microchim Acta 181:631–638

46. Chen X, Wu G, Cai Z, Oyama M, Chen X (2013) Advances in enzyme-free electrochemical sensors for hydrogen peroxide, glucose, and uric acid. Microchim Acta 181:689–705
47. Yuping Lin XC (2015) Non-enzymatic sensing of hydrogen peroxide using a glassy carbon electrode modified with a nanocomposite made from carbon nanotubes and molybdenum disulfide. Microchim Acta. doi: 10.1007/s00604-015-1517-5
48. Kang J, Shin D, Bae S, Hong BH (2012) Graphene transfer: key for applications. Nanoscale 4:5527–5537
49. Roddaro S, Pingue P, Piazza V, Pellegrini V, Beltram F (2007) The Optical Visibility of Graphene: Interference Colors of Ultrathin Graphite on SiO2. Nano Lett 7:2707–2710
50. Morozov SV, Novoselov KS, Katsnelson MI, Schedin F, Elias DC, Jaszczak JA, Geim AK (2008) Giant Intrinsic Carrier Mobilities in Graphene and Its Bilayer. Phys Rev Lett 100:016602
51. Emtsev KV, Bostwick A, Horn K, et al (2009) Towards wafer-size graphene layers by atmospheric pressure graphitization of silicon carbide. Nat Mater 8:203–207
52. Moon JS, Curtis D, Hu M, et al (2009) Epitaxial-Graphene RF Field-Effect Transistors on Si-Face 6H-SiC Substrates. IEEE Electron Device Lett 30:650–652
53. Lin Y-M, Dimitrakopoulos C, Jenkins KA, Farmer DB, Chiu H-Y, Grill A, Avouris P (2010) 100-GHz transistors from wafer-scale epitaxial graphene. Science 327:662
54. Li X, Cai W, Colombo L, Ruoff RS (2009) Evolution of Graphene Growth on Ni and Cu by Carbon Isotope Labeling. Nano Lett 9:4268–4272
55. Ago H, Ogawa Y, Tsuji M, Mizuno S, Hibino H (2012) Catalytic Growth of Graphene: Toward Large-Area Single-Crystalline Graphene. J Phys Chem Lett 3:2228–2236
56. Mattevi C, Kim H, Chhowalla M (2011) A review of chemical vapour deposition of graphene on copper. J Mater Chem 21:3324–3334
57. Bae S, Kim H, Lee Y, et al (2010) Roll-to-roll production of 30-inch graphene films for transparent electrodes. Nat Nanotechnol 5:574–578
58. Ryu J, Kim Y, Won D, et al (2014) Fast Synthesis of High-Performance Graphene Films by Hydrogen-Free Rapid Thermal Chemical Vapor Deposition. ACS Nano 8:950–956
59. Stankovich S, Dikin DA, Piner RD, Kohlhaas KA, Kleinhammes A, Jia Y, Wu Y, Nguyen ST, Ruoff RS (2007) Synthesis of graphene-based nanosheets via chemical reduction of exfoliated graphite oxide. Carbon 45:1558–1565

60. Gao X, Jang J, Nagase S (2010) Hydrazine and Thermal Reduction of Graphene Oxide: Reaction Mechanisms, Product Structures, and Reaction Design. J Phys Chem C 114:832–842
61. Shao Y, Wang J, Engelhard M, Wang C, Lin Y (2010) Facile and controllable electrochemical reduction of graphene oxide and its applications. J Mater Chem 20:743–748
62. Dreyer DR, Park S, Bielawski CW, Ruoff RS (2009) The chemistry of graphene oxide. Chem Soc Rev 39:228–240
63. Pham VH, Cuong TV, Hur SH, Shin EW, Kim JS, Chung JS, Kim EJ (2010) Fast and simple fabrication of a large transparent chemically-converted graphene film by spray-coating. Carbon 48:1945–1951
64. Zheng Q, Ip WH, Lin X, Yousefi N, Yeung KK, Li Z, Kim J-K (2011) Transparent Conductive Films Consisting of Ultralarge Graphene Sheets Produced by Langmuir–Blodgett Assembly. ACS Nano 5:6039–6051
65. Torrisi F, Hasan T, Wu W, et al (2012) Inkjet-Printed Graphene Electronics. ACS Nano 6:2992–3006
66. Ciesielski A, Samorì P (2013) Graphene via sonication assisted liquid-phase exfoliation. Chem Soc Rev 43:381–398
67. Hernandez Y, Nicolosi V, Lotya M, et al (2008) High-yield production of graphene by liquid-phase exfoliation of graphite. Nat Nanotechnol 3:563–568
68. Schlierf A, Yang H, Gebremedhn E, et al (2013) Nanoscale insight into the exfoliation mechanism of graphene with organic dyes: effect of charge, dipole and molecular structure. Nanoscale 5:4205–4216
69. Lotya M, King PJ, Khan U, De S, Coleman JN (2010) High-Concentration, Surfactant-Stabilized Graphene Dispersions. ACS Nano 4:3155–3162
70. Paton KR, Varrla E, Backes C, et al (2014) Scalable production of large quantities of defect-free few-layer graphene by shear exfoliation in liquids. Nat Mater 13:624–630
71. Narita A, Feng X, Müllen K (2015) Bottom-Up Synthesis of Chemically Precise Graphene Nanoribbons. Chem Rec 15:295–309
72. Cai J, Ruffieux P, Jaafar R, et al (2010) Atomically precise bottom-up fabrication of graphene nanoribbons. Nature 466:470–473
73. Dreyer DR, Ruoff RS, Bielawski CW (2010) From Conception to Realization: An Historial Account of Graphene and Some Perspectives for Its Future. Angew Chem Int Ed 49:9336–9344

74. Ferrari AC, Meyer JC, Scardaci V, et al (2006) Raman Spectrum of Graphene and Graphene Layers. Phys Rev Lett 97:187401
75. Tille T (2012) Requirements for Gas Sensors in Automotive Air Quality Applications. In: Fleischer M, Lehmann M (eds) Solid State Gas Sens. - Ind. Appl. Springer Berlin Heidelberg, pp 13–33
76. Galatsis K, Wlodarski W, Kalantar-Zadeh K, Trinchi A (2002) Investigation of gas sensors for cabin air quality monitoring. In: 2002 Conf. Optoelectron. Microelectron. Mater. Devices. pp 229–232
77. Blaschke M, Tille T, Robertson P, Mair S, Weimar U, Ulmer H (2006) MEMS Gas-Sensor Array for Monitoring the Perceived Car-Cabin Air Quality. IEEE Sens J 6:1298–1308
78. Ampuero S, Bosset JO (2003) The electronic nose applied to dairy products: a review. Sens Actuators B Chem 94:1–12
79. Becher C, Kaul P, Mitrovics J, Warmer J (2010) The detection of evaporating hazardous material released from moving sources using a gas sensor network. Sens Actuators B Chem 146:513–520
80. Wang J (2007) Electrochemical Sensing of Explosives. Electroanalysis 19:415–423
81. Fine GF, Cavanagh LM, Afonja A, Binions R (2010) Metal Oxide Semi-Conductor Gas Sensors in Environmental Monitoring. Sensors 10:5469–5502
82. Capone S, Forleo A, Francioso L, Rella R, Siciliano P, Spadavecchia J, Presicce DS, Taurino AM (2003) Solid state gas sensors: state of the art and future activities. J Optoelectron Adv Mater 5:1335–1348
83. Mao S, Lu G, Chen J (2014) Nanocarbon-based gas sensors: progress and challenges. J Mater Chem A 2:5573–5579
84. Hill EW, Vijayaragahvan A, Novoselov K (2011) Graphene Sensors. IEEE Sens J 11:3161–3170
85. Zhang T, Mubeen S, Myung NV, Deshusses MA (2008) Recent progress in carbon nanotube-based gas sensors. Nanotechnology 19:332001
86. Llobet E (2013) Gas sensors using carbon nanomaterials: A review. Sens Actuators B Chem 179:32–45
87. Dai J, Yuan J, Giannozzi P (2009) Gas adsorption on graphene doped with B, N, Al, and S: A theoretical study. Appl Phys Lett 95:232105

88. Huang B, Li Z, Liu Z, Zhou G, Hao S, Wu J, Gu B-L, Duan W (2008) Adsorption of Gas Molecules on Graphene Nanoribbons and Its Implication for Nanoscale Molecule Sensor. J Phys Chem C 112:13442–13446
89. Lu G, Ocola LE, Chen J (2009) Gas detection using low-temperature reduced graphene oxide sheets. Appl Phys Lett 94:083111
90. Hu N, Yang Z, Wang Y, Zhang L, Wang Y, Huang X, Wei H, Wei L, Zhang Y (2014) Ultrafast and sensitive room temperature NH3 gas sensors based on chemically reduced graphene oxide. Nanotechnology 25:025502
91. Lu G, Ocola LE, Chen J (2009) Reduced graphene oxide for room-temperature gas sensors. Nanotechnology 20:445502
92. Muhammad Hafiz S, Ritikos R, Whitcher TJ, et al (2014) A practical carbon dioxide gas sensor using room-temperature hydrogen plasma reduced graphene oxide. Sens Actuators B Chem 193:692–700
93. Zhang H, Feng J, Fei T, Liu S, Zhang T (2014) SnO2 nanoparticles-reduced graphene oxide nanocomposites for NO2 sensing at low operating temperature. Sens Actuators B Chem 190:472–478
94. Wang Z, Xiao Y, Cui X, Cheng P, Wang B, Gao Y, Li X, Yang T, Zhang T, Lu G (2014) Humidity-Sensing Properties of Urchinlike CuO Nanostructures Modified by Reduced Graphene Oxide. ACS Appl Mater Interfaces 6:3888–3895
95. Ghosh R, Midya A, Santra S, Ray SK, Guha PK (2014) Humidity Sensing by Chemically Reduced Graphene Oxide. In: Jain VK, Verma A (eds) Phys. Semicond. Devices. Springer International Publishing, pp 699–701
96. Tran QT, Hoa HTM, Yoo D-H, Cuong TV, Hur SH, Chung JS, Kim EJ, Kohl PA (2014) Reduced graphene oxide as an over-coating layer on silver nanostructures for detecting NH3 gas at room temperature. Sens Actuators B Chem 194:45–50
97. Su P-G, Shieh H-C (2014) Flexible NO2 sensors fabricated by layer-by-layer covalent anchoring and in situ reduction of graphene oxide. Sens Actuators B Chem 190:865–872
98. Iezhokin I, Offermans P, Brongersma SH, Giesbers AJM, Flipse CFJ (2013) High sensitive quasi freestanding epitaxial graphene gas sensor on 6H-SiC. Appl Phys Lett 103:053514
99. Yavari F, Castillo E, Gullapalli H, Ajayan PM, Koratkar N (2012) High sensitivity detection of NO2 and NH3 in air using chemical vapor deposition grown graphene. Appl Phys Lett 100:203120

100. Chen G, Paronyan TM, Harutyunyan AR (2012) Sub-ppt gas detection with pristine graphene. Appl Phys Lett 101:053119
101. Kumar S, Kaushik S, Pratap R, Raghavan S (2015) Graphene on Paper: A Simple, Low-Cost Chemical Sensing Platform. ACS Appl Mater Interfaces 7:2189–2194
102. Dan Y, Lu Y, Kybert NJ, Luo Z, Johnson ATC (2009) Intrinsic Response of Graphene Vapor Sensors. Nano Lett 9:1472–1475
103. Wei X-L, Chen Y-P, Liu W-L, Zhong J-X (2012) Enhanced gas sensor based on nitrogen-vacancy graphene nanoribbons. Phys Lett A 376:559–562
104. Niu F, Liu J-M, Tao L-M, Wang W, Song W-G (2013) Nitrogen and silica co-doped graphene nanosheets for NO2 gas sensing. J Mater Chem A 1:6130–6133
105. Cagliani A, Mackenzie DMA, Tschammer LK, Pizzocchero F, Almdal K, Bøggild P (2014) Large-area nanopatterned graphene for ultrasensitive gas sensing. Nano Res 7:743–754
106. Zhang H, Luo X, Lin X, Lu X, Leng Y, Song H (2013) Density functional theory calculations on the adsorption of formaldehyde and other harmful gases on pure, Ti-doped, or N-doped graphene sheets. Appl Surf Sci 283:559–565
107. Tavakol H, Mollaei-Renani A (2014) DFT, AIM, and NBO study of the interaction of simple and sulfur-doped graphenes with molecular halogens, CH3OH, CH3SH, H2O, and H2S. Struct Chem 25:1659–1667
108. Chung MG, Kim DH, Lee HM, Kim T, Choi JH, Seo D kyun, Yoo J-B, Hong S-H, Kang TJ, Kim YH (2012) Highly sensitive NO2 gas sensor based on ozone treated graphene. Sens Actuators B Chem 166–167:172–176
109. Peng Y, Li J (2013) Ammonia adsorption on graphene and graphene oxide: a first-principles study. Front Environ Sci Eng 7:403–411
110. Tang S, Cao Z (2011) Adsorption of nitrogen oxides on graphene and graphene oxides: Insights from density functional calculations. J Chem Phys 134:044710
111. Fowler JD, Allen MJ, Tung VC, Yang Y, Kaner RB, Weiller BH (2009) Practical Chemical Sensors from Chemically Derived Graphene. ACS Nano 3:301–306
112. Lee H-K, Lee J, Choi N-J, Moon SE, Lee H, Yang WS (2011) Efficient Reducing Method of Graphene Oxide for Gas Sensor Applications. Procedia Eng 25:892–895
113. Lipatov A, Varezhnikov A, Wilson P, Sysoev V, Kolmakov A, Sinitskii A (2013) Highly selective gas sensor arrays based on thermally reduced graphene oxide. Nanoscale 5:5426–5434

114. Lu G, Park S, Yu K, Ruoff RS, Ocola LE, Rosenmann D, Chen J (2011) Toward Practical Gas Sensing with Highly Reduced Graphene Oxide: A New Signal Processing Method To Circumvent Run-to-Run and Device-to-Device Variations. ACS Nano 5:1154–1164
115. Varghese SS, Lonkar S, Singh KK, Swaminathan S, Abdala A (2015) Recent advances in graphene based gas sensors. Sens Actuators B Chem 218:160–183
116. Li X, Xie D, Dai R, Xu J, Jiang Y (2014) Formadelyde-sensing properties of reduced graphene oxide by layer-by-layer self-assemble method. Int. Conf. Electron Devices Solid-State Circuits EDSSC. 1–2
117. Zhou Y, Jiang Y, Xie T, Tai H, Xie G (2014) A novel sensing mechanism for resistive gas sensors based on layered reduced graphene oxide thin films at room temperature. Sens Actuators B Chem 203:135–142
118. Prezioso S, Perrozzi F, Giancaterini L, Cantalini C, Treossi E, Palermo V, Nardone M, Santucci S, Ottaviano L (2013) Graphene Oxide as a Practical Solution to High Sensitivity Gas Sensing. J Phys Chem C 117:10683–10690
119. Ma C, Shao X, Cao D (2014) Nitrogen-doped graphene as an excellent candidate for selective gas sensing. Sci China Chem 57:911–917
120. Hussain T, Panigrahi P, Ahuja R (2014) Enriching physisorption of H2S and NH3 gases on a graphane sheet by doping with Li adatoms. Phys Chem Chem Phys 16:8100–8105
121. Niu F, Tao L-M, Deng Y-C, Wang Q-H, Song W-G (2014) Phosphorus doped graphene nanosheets for room temperature NH3 sensing. New J Chem 38:2269–2272
122. Cui S, Pu H, Mattson EC, Wen Z, Chang J, Hou Y, Hirschmugl CJ, Chen J (2014) Ultrasensitive Chemical Sensing through Facile Tuning Defects and Functional Groups in Reduced Graphene Oxide. Anal Chem 86:7516–7522
123. Pak Y, Kim S-M, Jeong H, et al (2014) Palladium-Decorated Hydrogen-Gas Sensors Using Periodically Aligned Graphene Nanoribbons. ACS Appl Mater Interfaces 6:13293–13298
124. Cui S, Mao S, Wen Z, Chang J, Zhang Y, Chen J (2013) Controllable synthesis of silver nanoparticle-decorated reduced graphene oxide hybrids for ammonia detection. Analyst 138:2877–2882
125. Li W, Geng X, Guo Y, et al (2011) Reduced Graphene Oxide Electrically Contacted Graphene Sensor for Highly Sensitive Nitric Oxide Detection. ACS Nano 5:6955–6961

126. Gutés A, Hsia B, Sussman A, Mickelson W, Zettl A, Carraro C, Maboudian R (2012) Graphene decoration with metal nanoparticles: Towards easy integration for sensing applications. Nanoscale 4:438–440
127. Huang L, Wang Z, Zhang J, Pu J, Lin Y, Xu S, Shen L, Chen Q, Shi W (2014) Fully Printed, Rapid-Response Sensors Based on Chemically Modified Graphene for Detecting NO2 at Room Temperature. ACS Appl Mater Interfaces 6:7426–7433
128. Liu S, Yu B, Zhang H, Fei T, Zhang T (2014) Enhancing NO2 gas sensing performances at room temperature based on reduced graphene oxide-ZnO nanoparticles hybrids. Sens Actuators B Chem 202:272–278
129. Mao S, Cui S, Lu G, Yu K, Wen Z, Chen J (2012) Tuning gas-sensing properties of reduced graphene oxide using tin oxide nanocrystals. J Mater Chem 22:11009–11013
130. Uddin ASMI, Chung G-S (2014) Synthesis of highly dispersed ZnO nanoparticles on graphene surface and their acetylene sensing properties. Sens Actuators B Chem 205:338–344
131. Meng H, Yang W, Ding K, Feng L, Guan Y (2014) Cu2O nanorods modified by reduced graphene oxide for NH3 sensing at room temperature. J Mater Chem A 3:1174–1181
132. Su P-G, Peng S-L (2015) Fabrication and NO2 gas-sensing properties of reduced graphene oxide/WO3 nanocomposite films. Talanta 132:398–405
133. Zhang L, Li C, Liu A, Shi G (2012) Electrosynthesis of graphene oxide/polypyrene composite films and their applications for sensing organic vapors. J Mater Chem 22:8438–8443
134. Yang Y, Yang X, Yang W, Li S, Xu J, Jiang Y (2014) Porous conducting polymer and reduced graphene oxide nanocomposites for room temperature gas detection. RSC Adv 4:42546–42553
135. Wang Y, Zhang L, Hu N, Wang Y, Zhang Y, Zhou Z, Liu Y, Shen S, Peng C (2014) Ammonia gas sensors based on chemically reduced graphene oxide sheets self-assembled on Au electrodes. Nanoscale Res Lett 9:251
136. Xie T, Xie G, Zhou Y, Huang J, Wu M, Jiang Y, Tai H (2014) Thin film transistors gas sensors based on reduced graphene oxide poly(3-hexylthiophene) bilayer film for nitrogen dioxide detection. Chem Phys Lett 614:275–281
137. Clark LC, Lyons C (1962) Electrode systems for continuous monitoring in cardiovascular surgery. Ann N Y Acad Sci 102:29–45

138. Wang J (2001) Glucose Biosensors: 40 Years of Advances and Challenges. Electroanalysis 13:983–988
139. Hua L, Wu X, Wang R (2012) Glucose sensor based on an electrochemical reduced graphene oxide-poly(L-lysine) composite film modified GC electrode. Analyst 137:5716–5719
140. Zheng D, Vashist SK, Al-Rubeaan K, Luong JHT, Sheu F-S (2012) Mediatorless amperometric glucose biosensing using 3-aminopropyltriethoxysilane-functionalized graphene. Talanta 99:22–28
141. Mani V, Devadas B, Chen S-M (2013) Direct electrochemistry of glucose oxidase at electrochemically reduced graphene oxide-multiwalled carbon nanotubes hybrid material modified electrode for glucose biosensor. Biosens Bioelectron 41:309–315
142. Cai C-J, Xu M-W, Bao S-J, Lei C, Jia D-Z (2012) A facile route for constructing a graphene-chitosan-ZrO2 composite for direct electron transfer and glucose sensing. RSC Adv 2:8172–8178
143. Jiang Y, Zhang Q, Li F, Niu L, Jiang Y, Zhang Q, Li F, Niu L (2012) Glucose oxidase and graphene bionanocomposite bridged by ionic liquid unit for glucose biosensing application. Sens Actuators B Chem 161:728–733
144. Zhang Q, Wu S, Zhang L, Lu J, Verproot F, Liu Y, Xing Z, Li J, Song X-M (2011) Fabrication of polymeric ionic liquid/graphene nanocomposite for glucose oxidase immobilization and direct electrochemistry. Biosens Bioelectron 26:2632–2637
145. Yang MH, Choi BG, Park H, Hong WH, Lee SY, Park TJ (2010) Development of a Glucose Biosensor Using Advanced Electrode Modified by Nanohybrid Composing Chemically Modified Graphene and Ionic Liquid. Electroanalysis 22:1223–1228
146. Yang J, Deng S, Lei J, Ju H, Gunasekaran S (2011) Electrochemical synthesis of reduced graphene sheet–AuPd alloy nanoparticle composites for enzymatic biosensing. Biosens Bioelectron 29:159–166
147. Wang K, Liu Q, Guan Q-M, Wu J, Li H-N, Yan J-J (2011) Enhanced direct electrochemistry of glucose oxidase and biosensing for glucose via synergy effect of graphene and CdS nanocrystals. Biosens Bioelectron 26:2252–2257
148. Unnikrishnan B, Palanisamy S, Chen S-M (2013) A simple electrochemical approach to fabricate a glucose biosensor based on graphene–glucose oxidase biocomposite. Biosens Bioelectron 39:70–75

149. Wu P, Shao Q, Hu Y, Jin J, Yin Y, Zhang H, Cai C (2010) Direct electrochemistry of glucose oxidase assembled on graphene and application to glucose detection. Electrochimica Acta 55:8606–8614
150. Kang X, Wang J, Wu H, Aksay IA, Liu J, Lin Y (2009) Glucose Oxidase–graphene–chitosan modified electrode for direct electrochemistry and glucose sensing. Biosens Bioelectron 25:901–905
151. Qiu J-D, Huang J, Liang R-P (2011) Nanocomposite film based on graphene oxide for high performance flexible glucose biosensor. Sens Actuators B Chem 160:287–294
152. Chen Y, Li Y, Sun D, Tian D, Zhang J, Zhu J-J (2011) Fabrication of gold nanoparticles on bilayer graphene for glucose electrochemical biosensing. J Mater Chem 21:7604–7611
153. Liu S, Tian J, Wang L, Luo Y, Lu W, Sun X (2011) Self-assembled graphene platelet–glucose oxidase nanostructures for glucose biosensing. Biosens Bioelectron 26:4491–4496
154. Tavares AJ, Noor MO, Vannoy CH, Algar WR, Krull UJ (2012) On-Chip Transduction of Nucleic Acid Hybridization Using Spatial Profiles of Immobilized Quantum Dots and Fluorescence Resonance Energy Transfer. Anal Chem 84:312–319
155. Zeng Q, Cheng J-S, Liu X-F, Bai H-T, Jiang J-H (2011) Palladium nanoparticle/chitosan-grafted graphene nanocomposites for construction of a glucose biosensor. Biosens Bioelectron 26:3456–3463
156. Claussen JC, Kumar A, Jaroch DB, Khawaja MH, Hibbard AB, Porterfield DM, Fisher TS (2012) Nanostructuring Platinum Nanoparticles on Multilayered Graphene Petal Nanosheets for Electrochemical Biosensing. Adv Funct Mater 22:3399–3405
157. Guo Y, Han Y, Shuang S, Dong C (2012) Rational synthesis of graphene–metal coordination polymer composite nanosheet as enhanced materials for electrochemical biosensing. J Mater Chem 22:13166–13173
158. Baby TT, Aravind SSJ, Arockiadoss T, Rakhi RB, Ramaprabhu S (2010) Metal decorated graphene nanosheets as immobilization matrix for amperometric glucose biosensor. Sens Actuators B Chem 145:71–77
159. Zhiguo G, Shuping Y, Zaijun L, Xiulan S, Guangli W, Yinjun F, Junkang L (2011) An ultrasensitive electrochemical biosensor for glucose using CdTe-CdS core–shell quantum dot as ultrafast electron transfer relay between graphene-gold nanocomposite and gold nanoparticle. Electrochimica Acta 56:9162–9167

160. Kavitha T, Gopalan AI, Lee K-P, Park S-Y (2012) Glucose sensing, photocatalytic and antibacterial properties of graphene–ZnO nanoparticle hybrids. Carbon 50:2994–3000
161. Palanisamy S, Vilian AE, Chen S-M (2012) Direct electrochemistry of glucose oxidase at reduced graphene oxide/zinc oxide composite modified electrode for glucose sensor. Int J Electrochem Sci 7:2153–2163
162. Norouzi P, Ganjali H, Larijani B, Ganjali MR, Faridbod F, Zamani HA (2011) A glucose biosensor based on nanographene and ZnO nanoparticles using FFT continuous cyclic voltammetry. Int J Electrochem Sci 6:5189–5195
163. Gu H, Yu Y, Liu X, Ni B, Zhou T, Shi G (2012) Layer-by-layer self-assembly of functionalized graphene nanoplates for glucose sensing in vivo integrated with on-line microdialysis system. Biosens Bioelectron 32:118–126
164. Ping J, Wang Y, Fan K, Wu J, Ying Y (2011) Direct electrochemical reduction of graphene oxide on ionic liquid doped screen-printed electrode and its electrochemical biosensing application. Biosens Bioelectron 28:204–209
165. Alwarappan S, Liu C, Kumar A, Li C-Z (2010) Enzyme-doped graphene nanosheets for enhanced glucose biosensing. J Phys Chem C 114:12920–12924
166. Shi J, Zhang H, Snyder A, Wang M, Xie J, Porterfield DM, Stanciu LA (2012) An aqueous media based approach for the preparation of a biosensor platform composed of graphene oxide and Pt-black. Biosens Bioelectron 38:314–320
167. Wu H, Wang J, Kang X, Wang C, Wang D, Liu J, Aksay IA, Lin Y (2009) Glucose biosensor based on immobilization of glucose oxidase in platinum nanoparticles/graphene/chitosan nanocomposite film. Talanta 80:403–406
168. Shan C, Yang H, Han D, Zhang Q, Ivaska A, Niu L (2010) Graphene/AuNPs/chitosan nanocomposites film for glucose biosensing. Biosens Bioelectron 25:1070–1074
169. Zhang Y, Liu S, Wang L, Qin X, Tian J, Lu W, Chang G, Sun X (2012) One-pot green synthesis of Ag nanoparticles-graphene nanocomposites and their applications in SERS, H 2 O 2, and glucose sensing. Rsc Adv 2:538–545
170. Wang Y, Shao Y, Matson DW, Li J, Lin Y (2010) Nitrogen-doped graphene and its application in electrochemical biosensing. ACS Nano 4:1790–1798
171. Alwarappan S, Boyapalle S, Kumar A, Li C-Z, Mohapatra S (2012) Comparative study of single-, few-, and multilayered graphene toward enzyme conjugation and electrochemical response. J Phys Chem C 116:6556–6559
172. Rao CNR, Sood AK, Subrahmanyam KS, Govindaraj A (2009) Graphen, das neue zweidimensionale Nanomaterial. Angew Chem 121:7890–7916

173. Lu C-H, Yang H-H, Zhu C-L, Chen X, Chen G-N (2009) A graphene platform for sensing biomolecules. Angew Chem Int Ed Engl 48:4785–4787
174. Manohar S, Mantz AR, Bancroft KE, Hui C-Y, Jagota A, Vezenov DV (2008) Peeling single-stranded DNA from graphite surface to determine oligonucleotide binding energy by force spectroscopy. Nano Lett 8:4365–4372
175. Varghese N, Mogera U, Govindaraj A, Das A, Maiti PK, Sood AK, Rao CNR (2009) Binding of DNA nucleobases and nucleosides with graphene. ChemPhysChem 10:206–210
176. Liu Z, Robinson JT, Sun X, Dai H (2008) PEGylated nanographene oxide for delivery of water-insoluble cancer drugs. J Am Chem Soc 130:10876–10877
177. Antony J, Grimme S (2008) Structures and interaction energies of stacked graphene–nucleobase complexes. Phys Chem Chem Phys 10:2722–2729
178. Gowtham S, Scheicher RH, Ahuja R, Pandey R, Karna SP (2007) Physisorption of nucleobases on graphene: Density-functional calculations. Phys Rev B 76:033401
179. Ortmann F, Schmidt WG, Bechstedt F (2005) Attracted by long-range electron correlation: adenine on graphite. Phys Rev Lett 95:186101
180. Zhu W, Zhao Z, Li Z, Jiang J, Shen G, Yu R (2012) A graphene oxide platform for the assay of DNA 3′-phosphatases and their inhibitors based on hairpin primer and polymerase elongation. J Mater Chem B 1:361–367
181. Yang L, Liu C, Ren W, Li Z (2012) Graphene surface-anchored fluorescence sensor for sensitive detection of microRNA coupled with enzyme-free signal amplification of hybridization chain reaction. ACS Appl Mater Interfaces 4:6450–6453
182. Zhou D-M, Xi Q, Liang M-F, Chen C-H, Tang L-J, Jiang J-H (2013) Graphene oxide-hairpin probe nanocomposite as a homogeneous assay platform for DNA base excision repair screening. Biosens Bioelectron 41:359–365
183. Tan X, Chen T, Xiong X, Mao Y, Zhu G, Yasun E, Li C, Zhu Z, Tan W (2012) Semiquantification of ATP in live cells using nonspecific desorption of DNA from graphene oxide as the internal reference. Anal Chem 84:8622–8627
184. Zhang C, Xu J, Zhang S, Ji X, He Z (2012) One-Pot Synthesized DNA–CdTe Quantum Dots Applied in a Biosensor for the Detection of Sequence-Specific Oligonucleotides. Chem- Eur J 18:8296–8300
185. Xing X-J, Liu X-G, Luo Q-Y, Tang H-W, Pang D-W (2012) Graphene oxide based fluorescent aptasensor for adenosine deaminase detection using adenosine as the substrate. Biosens Bioelectron 37:61–67

186. Tao Y, Lin Y, Huang Z, Ren J, Qu X (2012) DNA-templated silver nanoclusters–graphene oxide nanohybrid materials: a platform for label-free and sensitive fluorescence turn-on detection of multiple nucleic acid targets. Analyst 137:2588–2592
187. Mei Q, Zhang Z (2012) Photoluminescent graphene oxide ink to print sensors onto microporous membranes for versatile visualization bioassays. Angew Chem Int Ed 51:5602–5606
188. Liu X, Aizen R, Freeman R, Yehezkeli O, Willner I (2012) Multiplexed aptasensors and amplified DNA sensors using functionalized graphene oxide: application for logic gate operations. ACS Nano 6:3553–3563
189. Jang H, Kim Y-K, Kwon H-M, Yeo W-S, Kim D-E, Min D-H (2010) A Graphene-Based Platform for the Assay of Duplex-DNA Unwinding by Helicase. Angew Chem 122:5839–5843
190. He S, Song B, Li D, Zhu C, Qi W, Wen Y, Wang L, Song S, Fang H, Fan C (2010) A graphene nanoprobe for rapid, sensitive, and multicolor fluorescent DNA analysis. Adv Funct Mater 20:453–459
191. Drummond TG, Hill MG, Barton JK (2003) Electrochemical DNA sensors. Nat Biotechnol 21:1192–1199
192. Ba X, Luo L, Ding Y, Zhang Z, Chu Y, Wang B, Ouyang X (2012) Poly (alizarin red)/graphene modified glassy carbon electrode for simultaneous determination of purine and pyrimidine. Anal Chim Acta 752:94–100
193. Du M, Yang T, Jiao K (2010) Immobilization-free direct electrochemical detection for DNA specific sequences based on electrochemically converted gold nanoparticles/graphene composite film. J Mater Chem 20:9253–9260
194. Merchant CA, Healy K, Wanunu M, Ray V, Peterman N, Bartel J, Fischbein MD, Venta K, Luo Z, Johnson AC (2010) DNA translocation through graphene nanopores. Nano Lett 10:2915–2921
195. Yang T, Guan Q, Guo X, Meng L, Du M, Jiao K (2013) Direct and Freely Switchable Detection of Target Genes Engineered by Reduced Graphene Oxide-Poly(m-Aminobenzenesulfonic Acid) Nanocomposite via Synchronous Pulse Electrosynthesis. Anal Chem 85:1358–1366
196. Sun W, Qi X, Zhang Y, Yang H, Gao H, Chen Y, Sun Z (2012) Electrochemical DNA biosensor for the detection of Listeria monocytogenes with dendritic nanogold and electrochemical reduced graphene modified carbon ionic liquid electrode. Electrochimica Acta 85:145–151

197. Dong H, Zhu Z, Ju H, Yan F (2012) Triplex signal amplification for electrochemical DNA biosensing by coupling probe-gold nanoparticles–graphene modified electrode with enzyme functionalized carbon sphere as tracer. Biosens Bioelectron 33:228–232
198. Du M, Yang T, Li X, Jiao K (2012) Fabrication of DNA/graphene/polyaniline nanocomplex for label-free voltammetric detection of DNA hybridization. Talanta 88:439–444
199. Dong X, Shi Y, Huang W, Chen P, Li L-J (2010) Electrical Detection of DNA Hybridization with Single-Base Specificity Using Transistors Based on CVD-Grown Graphene Sheets. Adv Mater 22:1649–1653
200. Du Y, Guo S, Dong S, Wang E (2011) An integrated sensing system for detection of DNA using new parallel-motif DNA triplex system and graphene–mesoporous silica–gold nanoparticle hybrids. Biomaterials 32:8584–8592
201. Dong X, Huang W, Chen P (2010) In Situ Synthesis of Reduced Graphene Oxide and Gold Nanocomposites for Nanoelectronics and Biosensing. Nanoscale Res Lett 6:60
202. Tang Z, Wu H, Cort JR, Buchko GW, Zhang Y, Shao Y, Aksay IA, Liu J, Lin Y (2010) Constraint of DNA on functionalized graphene improves its biostability and specificity. Small 6:1205–1209
203. Dubuisson E, Yang Z, Loh KP (2011) Optimizing label-free DNA electrical detection on graphene platform. Anal Chem 83:2452–2460
204. Bonanni A, Pumera M (2011) Graphene platform for hairpin-DNA-based impedimetric genosensing. ACS Nano 5:2356–2361
205. Bo Y, Yang H, Hu Y, Yao T, Huang S (2011) A novel electrochemical DNA biosensor based on graphene and polyaniline nanowires. Electrochimica Acta 56:2676–2681
206. Dikin DA, Stankovich S, Zimney EJ, Piner RD, Dommett GHB, Evmenenko G, Nguyen ST, Ruoff RS (2007) Preparation and characterization of graphene oxide paper. Nature 448:457–460
207. Liang Y, Wu D, Feng X, Müllen K (2009) Dispersion of graphene sheets in organic solvent supported by ionic interactions. Adv Mater 21:1679–1683
208. Xu Y, Bai H, Lu G, Li C, Shi G (2008) Flexible graphene films via the filtration of water-soluble noncovalent functionalized graphene sheets. J Am Chem Soc 130:5856–5857
209. Dong H, Gao W, Yan F, Ji H, Ju H (2010) Fluorescence resonance energy transfer between quantum dots and graphene oxide for sensing biomolecules. Anal Chem 82:5511–5517

210. Liu C, Wang Z, Jia H, Li Z (2011) Efficient fluorescence resonance energy transfer between upconversion nanophosphors and graphene oxide: a highly sensitive biosensing platform. Chem Commun 47:4661–4663
211. Liu F, Piao Y, Choi KS, Seo TS (2012) Fabrication of free-standing graphene composite films as electrochemical biosensors. Carbon 50:123–133
212. Lin L, Liu Y, Tang L, Li J (2011) Electrochemical DNA sensor by the assembly of graphene and DNA-conjugated gold nanoparticles with silver enhancement strategy. Analyst 136:4732–4737
213. Zhang Y, Jiang W (2012) Decorating graphene sheets with gold nanoparticles for the detection of sequence-specific DNA. Electrochimica Acta 71:239–245
214. Niu S, Sun J, Nan C, Lin J (2013) Sensitive DNA biosensor improved by 1,10-phenanthroline cobalt complex as indicator based on the electrode modified by gold nanoparticles and graphene. Sens Actuators B Chem 176:58–63
215. Yin H, Zhou Y, Zhang H, Meng X, Ai S (2012) Electrochemical determination of microRNA-21 based on graphene, LNA integrated molecular beacon, AuNPs and biotin multifunctional bio bar codes and enzymatic assay system. Biosens Bioelectron 33:247–253
216. Zhu W, Zhao Z, Li Z, Jiang J, Shen G, Yu R (2012) A ligation-triggered highly sensitive fluorescent assay of adenosine triphosphate based on graphene oxide. Analyst 137:5506–5509
217. Wang L, Xu M, Han L, Zhou M, Zhu C, Dong S (2012) Graphene Enhanced Electron Transfer at Aptamer Modified Electrode and Its Application in Biosensing. Anal Chem 84:7301–7307
218. Wang L, Zhu J, Han L, Jin L, Zhu C, Wang E, Dong S (2012) Graphene-Based Aptamer Logic Gates and Their Application to Multiplex Detection. ACS Nano 6:6659–6666
219. Huang P-JJ, Kempaiah R, Liu J (2011) Synergistic pH effect for reversible shuttling aptamer-based biosensors between graphene oxide and target molecules. J Mater Chem 21:8991–8993
220. Luo M, Chen X, Zhou G, Xiang X, Chen L, Ji X, He Z (2012) Chemiluminescence biosensors for DNA detection using graphene oxide and a horseradish peroxidase-mimicking DNAzyme. Chem Commun 48:1126–1128

221. Wu C, Zhou Y, Miao X, Ling L (2011) A novel fluorescent biosensor for sequence-specific recognition of double-stranded DNA with the platform of graphene oxide. Analyst 136:2106–2110
222. Hu Y, Hua S, Li F, Jiang Y, Bai X, Li D, Niu L (2011) Green-synthesized gold nanoparticles decorated graphene sheets for label-free electrochemical impedance DNA hybridization biosensing. Biosens Bioelectron 26:4355–4361
223. Hu Y, Li F, Bai X, Li D, Hua S, Wang K, Niu L (2011) Label-free electrochemical impedance sensing of DNA hybridization based on functionalized graphene sheets. Chem Commun 47:1743–1745
224. Gong Q, Yang H, Dong Y, Zhang W (2015) A sensitive impedimetric DNA biosensor for the determination of the HIV gene based on electrochemically reduced graphene oxide. Anal Methods 7:2554–2562
225. Kitano H (2002) Systems biology: a brief overview. Science 295:1662–1664
226. Srinivas PR, Kramer BS, Srivastava S (2001) Trends in biomarker research for cancer detection. Lancet Oncol 2:698–704
227. Zeng L, Li Q, Tang D, Chen G, Wei M (2012) Metal platinum-wrapped mesoporous carbon for sensitive electrochemical immunosensing based on cyclodextrin functionalized graphene nanosheets. Electrochimica Acta 68:158–165
228. Guo Z, Hao T, Duan J, Wang S, Wei D (2012) Electrochemiluminescence immunosensor based on graphene–CdS quantum dots–agarose composite for the ultrasensitive detection of alpha fetoprotein. Talanta 89:27–32
229. Tang J, Tang D, Su B, Li Q, Qiu B, Chen G (2011) Silver nanowire–graphene hybrid nanocomposites as label for sensitive electrochemical immunoassay of alpha-fetoprotein. Electrochimica Acta 56:8168–8175
230. Huang K-J, Niu D-J, Sun J-Y, Zhu J-J (2011) An electrochemical amperometric immunobiosensor for label-free detection of α-fetoprotein based on amine-functionalized graphene and gold nanoparticles modified carbon ionic liquid electrode. J Electroanal Chem 656:72–77
231. Kim D-J, Sohn IY, Jung J-H, Yoon OJ, Lee N-E, Park J-S (2013) Reduced graphene oxide field-effect transistor for label-free femtomolar protein detection. Biosens Bioelectron 41:621–626
232. Han J, Zhuo Y, Chai Y, Yuan R, Zhang W, Zhu Q (2012) Simultaneous electrochemical detection of multiple tumor markers based on dual catalysis

amplification of multi-functionalized onion-like mesoporous graphene sheets. Anal Chim Acta 746:70–76

233. Xu S, Liu Y, Wang T, Li J (2011) Positive Potential Operation of a Cathodic Electrogenerated Chemiluminescence Immunosensor Based on Luminol and Graphene for Cancer Biomarker Detection. Anal Chem 83:3817–3823
234. Feng L, Wu L, Wang J, Ren J, Miyoshi D, Sugimoto N, Qu X (2012) Detection of a Prognostic Indicator in Early-Stage Cancer Using Functionalized Graphene-Based Peptide Sensors. Adv Mater 24:125–131
235. Wang X, Wang C, Qu K, Song Y, Ren J, Miyoshi D, Sugimoto N, Qu X (2010) Ultrasensitive and Selective Detection of a Prognostic Indicator in Early-Stage Cancer Using Graphene Oxide and Carbon Nanotubes. Adv Funct Mater 20:3967–3971
236. Xie Y, Chen A, Du D, Lin Y (2011) Graphene-based immunosensor for electrochemical quantification of phosphorylated p53 (S15). Anal Chim Acta 699:44–48
237. Du D, Wang L, Shao Y, Wang J, Engelhard MH, Lin Y (2011) Functionalized Graphene Oxide as a Nanocarrier in a Multienzyme Labeling Amplification Strategy for Ultrasensitive Electrochemical Immunoassay of Phosphorylated p53 (S392). Anal Chem 83:746–752
238. Tu W, Wang W, Lei J, Deng S, Ju H (2012) Chemiluminescence excited photoelectrochemistry using graphene–quantum dots nanocomposite for biosensing. Chem Commun 48:6535–6537
239. Li Y, Yang W-K, Fan M-Q, Liu A (2011) A Sensitive Label-free Amperometric CEA Immunosensor Based on Graphene-Nafion Nanocomposite Film as an Enhanced Sensing Platform. Anal Sci 27:727–727
240. Wang Z, Huang P, Bhirde A, Jin A, Ma Y, Niu G, Neamati N, Chen X (2012) A nanoscale graphene oxide–peptide biosensor for real-time specific biomarker detection on the cell surface. Chem Commun 48:9768–9770
241. Zhuo Y, Chai Y-Q, Yuan R, Mao L, Yuan Y-L, Han J (2011) Glucose oxidase and ferrocene labels immobilized at Au/TiO2 nanocomposites with high load amount and activity for sensitive immunoelectrochemical measurement of ProGRP biomarker. Biosens Bioelectron 26:3838–3844
242. Yang M, Javadi A, Li H, Gong S (2010) Ultrasensitive immunosensor for the detection of cancer biomarker based on graphene sheet. Biosens Bioelectron 26:560–565

243. Du D, Zou Z, Shin Y, Wang J, Wu H, Engelhard MH, Liu J, Aksay IA, Lin Y (2010) Sensitive Immunosensor for Cancer Biomarker Based on Dual Signal Amplification Strategy of Graphene Sheets and Multienzyme Functionalized Carbon Nanospheres. Anal Chem 82:2989–2995
244. Zhang B, Cui T (2011) An ultrasensitive and low-cost graphene sensor based on layer-by-layer nano self-assembly. Appl Phys Lett 98:073116
245. Nierodzik ML, Karpatkin S (2006) Thrombin induces tumor growth, metastasis, and angiogenesis: Evidence for a thrombin-regulated dormant tumor phenotype. Cancer Cell 10:355–362
246. Xiao Y, Piorek BD, Plaxco KW, Heeger AJ (2005) A Reagentless Signal-On Architecture for Electronic, Aptamer-Based Sensors via Target-Induced Strand Displacement. J Am Chem Soc 127:17990–17991
247. Zhao Q, Lu X, Yuan C-G, Li X-F, Le XC (2009) Aptamer-Linked Assay for Thrombin Using Gold Nanoparticle Amplification and Inductively Coupled Plasma−Mass Spectrometry Detection. Anal Chem 81:7484–7489
248. Chang H, Tang L, Wang Y, Jiang J, Li J (2010) Graphene Fluorescence Resonance Energy Transfer Aptasensor for the Thrombin Detection. Anal Chem 82:2341–2346
249. Zhang M, Yin B-C, Tan W, Ye B-C (2011) A versatile graphene-based fluorescence "on/off" switch for multiplex detection of various targets. Biosens Bioelectron 26:3260–3265
250. Zhang M, Yin B-C, Wang X-F, Ye B-C (2011) Interaction of peptides with graphene oxide and its application for real-time monitoring of protease activity. Chem Commun 47:2399–2401
251. Wang Y, Xiao Y, Ma X, Li N, Yang X (2011) Label-free and sensitive thrombin sensing on a molecularly grafted aptamer on graphene. Chem Commun 48:738–740
252. Bonanni A, Loo AH, Pumera M (2012) Graphene for impedimetric biosensing. TrAC Trends Anal Chem 37:12–21
253. Bai L, Yuan R, Chai Y, Zhuo Y, Yuan Y, Wang Y (2012) Simultaneous electrochemical detection of multiple analytes based on dual signal amplification of single-walled carbon nanotubes and multi-labeled graphene sheets. Biomaterials 33:1090–1096
254. Sun T, Wang L, Li N, Gan X (2011) Label-free electrochemical aptasensor for thrombin detection based on the nafion@graphene as platform. Bioprocess Biosyst Eng 34:1081–1085

255. Gao Y, Li Y, Zou X, Huang H, Su X (2012) Highly sensitive and selective detection of biothiols using graphene oxide-based “molecular beacon”-like fluorescent probe. Anal Chim Acta 731:68–74
256. Mei Q, Zhang Z (2012) Photoluminescent Graphene Oxide Ink to Print Sensors onto Microporous Membranes for Versatile Visualization Bioassays. Angew Chem Int Ed 51:5602–5606
257. Liang J, Chen Z, Guo L, Li L (2011) Electrochemical sensing of L-histidine based on structure-switching DNAzymes and gold nanoparticle–graphene nanosheet composites. Chem Commun 47:5476–5478
258. Wei J, Qiu J, Li L, Ren L, Zhang X, Chaudhuri J, Wang S (2012) A reduced graphene oxide based electrochemical biosensor for tyrosine detection. Nanotechnology 23:335707
259. Shi Y, Wu J, Sun Y, Zhang Y, Wen Z, Dai H, Wang H, Li Z (2012) A graphene oxide based biosensor for microcystins detection by fluorescence resonance energy transfer. Biosens Bioelectron 38:31–36
260. Xie WY, Huang WT, Li NB, Luo HQ (2011) Design of a dual-output fluorescent DNA logic gate and detection of silver ions and cysteine based on graphene oxide. Chem Commun 48:82–84
261. Lin Y, Tao Y, Pu F, Ren J, Qu X (2011) Combination of Graphene Oxide and Thiol-Activated DNA Metallization for Sensitive Fluorescence Turn-On Detection of Cysteine and Their Use for Logic Gate Operations. Adv Funct Mater 21:4565–4572
262. Song Y, Chen Y, Feng L, Ren J, Qu X (2011) Selective and quantitative cancer cell detection using target-directed functionalized graphene and its synergetic peroxidase-like activity. Chem Commun 47:4436–4438
263. Staal FJT, Ela SW, Roederer M, Anderson MT, Herzenberg LA (1992) Glutathione deficiency and human immunodeficiency virus infection. The Lancet 339:909–912
264. Liu B, Tang D, Tang J, Su B, Li Q, Chen G (2011) A graphene-based Au(111) platform for electrochemical biosensing based catalytic recycling of products on gold nanoflowers. Analyst 136:2218–2220
265. Liu K, Zhang J-J, Wang C, Zhu J-J (2011) Graphene-assisted dual amplification strategy for the fabrication of sensitive amperometric immunosensor. Biosens Bioelectron 26:3627–3632

266. Wang G, Huang H, Zhang G, Zhang X, Fang B, Wang L (2010) Gold nanoparticles/L-cysteine/graphene composite based immobilization strategy for an electrochemical immunosensor. Anal Methods 2:1692–1697
267. Ohno Y, Maehashi K, Inoue K, Matsumoto K (2011) Label-Free Aptamer-Based Immunoglobulin Sensors Using Graphene Field-Effect Transistors. Jpn J Appl Phys 50:070120
268. Ohno Y, Maehashi K, Matsumoto K (2010) Label-Free Biosensors Based on Aptamer-Modified Graphene Field-Effect Transistors. J Am Chem Soc 132:18012–18013
269. Mao S, Lu G, Yu K, Bo Z, Chen J (2010) Specific Protein Detection Using Thermally Reduced Graphene Oxide Sheet Decorated with Gold Nanoparticle-Antibody Conjugates. Adv Mater 22:3521–3526
270. Shih C-J, Paulus GLC, Wang QH, Jin Z, Blankschtein D, Strano MS (2012) Understanding Surfactant/Graphene Interactions Using a Graphene Field Effect Transistor: Relating Molecular Structure to Hysteresis and Carrier Mobility. Langmuir 28:8579–8586
271. Ohno Y, Maehashi K, Yamashiro Y, Matsumoto K (2009) Electrolyte-Gated Graphene Field-Effect Transistors for Detecting pH and Protein Adsorption. Nano Lett 9:3318–3322
272. Pei H, Li J, Lv M, Wang J, Gao J, Lu J, Li Y, Huang Q, Hu J, Fan C (2012) A Graphene-Based Sensor Array for High-Precision and Adaptive Target Identification with Ensemble Aptamers. J Am Chem Soc 134:13843–13849
273. Kasry A, Afzali AA, Oida S, Han S-J, Menges B, Tulevski GS (2011) Detection of Biomolecules via Benign Surface Modification of Graphene. Chem Mater 23:4879–4881
274. Wang J, Zhao W-W, Li X-R, Xu J-J, Chen H-Y (2012) Potassium-doped graphene enhanced electrochemiluminescence of SiO2@CdS nanocomposites for sensitive detection of TATA-binding protein. Chem Commun 48:6429–6431
275. Qu F, Lu H, Yang M, Deng C (2011) Electrochemical immunosensor based on electron transfer mediated by graphene oxide initiated silver enhancement. Biosens Bioelectron 26:4810–4814
276. Chen Y, Vedala H, Kotchey GP, Audfray A, Cecioni S, Imberty A, Vidal S, Star A (2012) Electronic Detection of Lectins Using Carbohydrate-Functionalized Nanostructures: Graphene versus Carbon Nanotubes. ACS Nano 6:760–770

277. Shi Y, Huang WT, Luo HQ, Li NB (2011) A label-free DNA reduced graphene oxide-based fluorescent sensor for highly sensitive and selective detection of hemin. Chem Commun 47:4676–4678
278. Qin H, Liu J, Chen C, Wang J, Wang E (2012) An electrochemical aptasensor for chiral peptide detection using layer-by-layer assembly of polyelectrolyte-methylene blue/polyelectrolyte-graphene multilayer. Anal Chim Acta 712:127–131
279. Du Y, Guo S, Qin H, Dong S, Wang E (2011) Target-induced conjunction of split aptamer as new chiral selector for oligopeptide on graphene–mesoporous silica–gold nanoparticle hybrids modified sensing platform. Chem Commun 48:799–801
280. Liu S-J, Wen Q, Tang L-J, Jiang J-H (2012) Phospholipid–Graphene Nanoassembly as a Fluorescence Biosensor for Sensitive Detection of Phospholipase D Activity. Anal Chem 84:5944–5950
281. Wang H, Zhang Q, Chu X, Chen T, Ge J, Yu R (2011) Graphene Oxide–Peptide Conjugate as an Intracellular Protease Sensor for Caspase-3 Activation Imaging in Live Cells. Angew Chem Int Ed 50:7065–7069
282. Feng D, Zhang Y, Feng T, Shi W, Li X, Ma H (2011) A graphene oxide–peptide fluorescence sensor tailor-made for simple and sensitive detection of matrix metalloproteinase 2. Chem Commun 47:10680–10682
283. Chen C, Zhao J, Jiang J, Yu R (2012) A novel exonuclease III-aided amplification assay for lysozyme based on graphene oxide platform. Talanta 101:357–361
284. Arya SK, Datta M, Malhotra BD (2008) Recent advances in cholesterol biosensor. Biosens Bioelectron 23:1083–1100
285. Li J, Peng T, Peng Y (2003) A Cholesterol Biosensor Based on Entrapment of Cholesterol Oxidase in a Silicic Sol-Gel Matrix at a Prussian Blue Modified Electrode. Electroanalysis 15:1031–1037
286. Jiang H, Ju H (2007) Enzyme–quantum dots architecture for highly sensitive electrochemiluminescence biosensing of oxidase substrates. Chem Commun 404–406
287. Ekanayake EMIM, Preethichandra DMG, Kaneto K (2007) Polypyrrole nanotube array sensor for enhanced adsorption of glucose oxidase in glucose biosensors. Biosens Bioelectron 23:107–113
288. Dey RS, Raj CR (2010) Development of an Amperometric Cholesterol Biosensor Based on Graphene−Pt Nanoparticle Hybrid Material. J Phys Chem C 114:21427–21433

289. Saini D, Chauhan R, Solanki PR, Basu T (2012) Gold-Nanoparticle Decorated Graphene-Nanostructured Polyaniline Nanocomposite-Based Bienzymatic Platform for Cholesterol Sensing. ISRN Nanotechnol. 2012:
290. Aravind SSJ, Baby TT, Arockiadoss T, Rakhi RB, Ramaprabhu S (2011) A cholesterol biosensor based on gold nanoparticles decorated functionalized graphene nanoplatelets. Thin Solid Films 519:5667–5672
291. Manjunatha R, Shivappa Suresh G, Savio Melo J, D'Souza SF, Venkatarangaiah Venkatesha T (2012) An amperometric bienzymatic cholesterol biosensor based on functionalized graphene modified electrode and its electrocatalytic activity towards total cholesterol determination. Talanta 99:302–309
292. Zhang M, Yuan R, Chai Y, Chen S, Zhong X, Zhong H, Wang C (2012) A cathodic electrogenerated chemiluminescence biosensor based on luminol and hemin-graphene nanosheets for cholesterol detection. RSC Adv 2:4639–4641
293. Banks CE, Crossley A, Salter C, Wilkins SJ, Compton RG (2006) Carbon Nanotubes Contain Metal Impurities Which Are Responsible for the "Electrocatalysis" Seen at Some Nanotube-Modified Electrodes. Angew Chem Int Ed 45:2533–2537
294. Zhiguo G, Shuping Y, Zaijun L, Xiulan S, Guangli W, Yinjun F, Junkang L (2011) An ultrasensitive hydrogen peroxide biosensor based on electrocatalytic synergy of graphene–gold nanocomposite, CdTe–CdS core–shell quantum dots and gold nanoparticles. Anal Chim Acta 701:75–80
295. Zhang Q, Qiao Y, Hao F, Zhang L, Wu S, Li Y, Li J, Song X-M (2010) Fabrication of a Biocompatible and Conductive Platform Based on a Single-Stranded DNA/Graphene Nanocomposite for Direct Electrochemistry and Electrocatalysis. Chem – Eur J 16:8133–8139
296. Li M, Xu S, Tang M, Liu L, Gao F, Wang Y (2011) Direct electrochemistry of horseradish peroxidase on graphene-modified electrode for electrocatalytic reduction towards H2O2. Electrochimica Acta 56:1144–1149
297. Shan C, Yang H, Han D, Zhang Q, Ivaska A, Niu L (2009) Water-Soluble Graphene Covalently Functionalized by Biocompatible Poly-l-lysine. Langmuir 25:12030–12033
298. Sheng Q, Wang M, Zheng J (2011) A novel hydrogen peroxide biosensor based on enzymatically induced deposition of polyaniline on the functionalized graphene–carbon nanotube hybrid materials. Sens Actuators B Chem 160:1070–1077

299. Cui Y, Zhang B, Liu B, Chen H, Chen G, Tang D (2011) Sensitive detection of hydrogen peroxide in foodstuff using an organic–inorganic hybrid multilayer-functionalized graphene biosensing platform. Microchim Acta 174:137–144
300. Lu Q, Dong X, Li L-J, Hu X (2010) Direct electrochemistry-based hydrogen peroxide biosensor formed from single-layer graphene nanoplatelet–enzyme composite film. Talanta 82:1344–1348
301. Feng X-M, Li R-M, Ma Y-W, Chen R-F, Shi N-E, Fan Q-L, Huang W (2011) One-Step Electrochemical Synthesis of Graphene/Polyaniline Composite Film and Its Applications. Adv Funct Mater 21:2989–2996
302. Zhang L, Cheng H, Zhang H, Qu L (2012) Direct electrochemistry and electrocatalysis of horseradish peroxidase immobilized in graphene oxide–Nafion nanocomposite film. Electrochimica Acta 65:122–126
303. Zeng Q, Cheng J, Tang L, Liu X, Liu Y, Li J, Jiang J (2010) Self-Assembled Graphene–Enzyme Hierarchical Nanostructures for Electrochemical Biosensing. Adv Funct Mater 20:3366–3372
304. Zhang Q, Qiao Y, Zhang L, Wu S, Zhou H, Xu J, Song X-M (2011) Direct Electrochemistry and Electrocatalysis of Horseradish Peroxidase Immobilized on Water Soluble Sulfonated Graphene Film via Self-assembly. Electroanalysis 23:900–906
305. Zhou K, Zhu Y, Yang X, Li C (2011) Preparation and Application of Mediator-Free H2O2 Biosensors of Graphene-Fe3O4 Composites. Electroanalysis 23:862–869
306. Zhou K, Zhu Y, Yang X, Luo J, Li C, Luan S (2010) A novel hydrogen peroxide biosensor based on Au–graphene–HRP–chitosan biocomposites. Electrochimica Acta 55:3055–3060
307. Palanisamy S, Unnikrishnan B, Chen S-M (2012) An amperometric biosensor based on direct immobilization of horseradish peroxidase on electrochemically reduced graphene oxide modified screen printed carbon electrode. Int J Electrochem Sci 7:7935–7947
308. Schäferling M, Grögel DBM, Schreml S (2011) Luminescent probes for detection and imaging of hydrogen peroxide. Microchim Acta 174:1–18
309. Moiroux J, Elving PJ (1978) Effects of adsorption, electrode material, and operational variables on the oxidation of dihydronicotinamide adenine dinucleotide at carbon electrodes. Anal Chem 50:1056–1062

310. Álvarez-González MI, Saidman SB, Lobo-Castañón MJ, Miranda-Ordieres AJ, Tuñón-Blanco P (2000) Electrocatalytic Detection of NADH and Glycerol by NAD+-Modified Carbon Electrodes. Anal Chem 72:520–527
311. Guo K, Qian K, Zhang S, Kong J, Yu C, Liu B (2011) Bio-electrocatalysis of NADH and ethanol based on graphene sheets modified electrodes. Talanta 85:1174–1179
312. Shan C, Yang H, Han D, Zhang Q, Ivaska A, Niu L (2010) Electrochemical determination of NADH and ethanol based on ionic liquid-functionalized graphene. Biosens Bioelectron 25:1504–1508
313. Wang X, Wang J, Cheng H, Yu P, Ye J, Mao L (2011) Graphene as a Spacer to Layer-by-Layer Assemble Electrochemically Functionalized Nanostructures for Molecular Bioelectronic Devices. Langmuir 27:11180–11186
314. Kumar SP, Manjunatha R, Nethravathi C, Suresh GS, Rajamathi M, Venkatesha TV (2011) Electrocatalytic Oxidation of NADH on Functionalized Graphene Modified Graphite Electrode. Electroanalysis 23:842–849
315. Gao W, Chen Y, Xi J, Lin S, Chen Y, Lin Y, Chen Z (2013) A novel electrochemiluminescence ethanol biosensor based on tris(2,2'-bipyridine) ruthenium (II) and alcohol dehydrogenase immobilized in graphene/bovine serum albumin composite film. Biosens Bioelectron 41:776–782
316. Lim CX, Hoh HY, Ang PK, Loh KP (2010) Direct Voltammetric Detection of DNA and pH Sensing on Epitaxial Graphene: An Insight into the Role of Oxygenated Defects. Anal Chem 82:7387–7393
317. Sun Z, Fu H, Deng L, Wang J (2013) Redox-active thionine–graphene oxide hybrid nanosheet: One-pot, rapid synthesis, and application as a sensing platform for uric acid. Anal Chim Acta 761:84–91
318. Cheng R, Liu Y, Ou S, Pan Y, Zhang S, Chen H, Dai L, Qu J (2012) Optical Turn-On Sensor Based on Graphene Oxide for Selective Detection of d-Glucosamine. Anal Chem 84:5641–5644
319. Deng S, Lei J, Cheng L, Zhang Y, Ju H (2011) Amplified electrochemiluminescence of quantum dots by electrochemically reduced graphene oxide for nanobiosensing of acetylcholine. Biosens Bioelectron 26:4552–4558
320. Wu X, Hu Y, Jin J, Zhou N, Wu P, Zhang H, Cai C (2010) Electrochemical Approach for Detection of Extracellular Oxygen Released from Erythrocytes Based on Graphene Film Integrated with Laccase and 2,2-Azino-bis(3-ethylbenzothiazoline-6-sulfonic acid). Anal Chem 82:3588–3596

321. Bai J, Lai Y, Jiang D, Zeng Y, Xian Y, Xiao F, Zhang N, Hou J, Jin L (2012) Ultrasensitive electrochemical immunoassay based on graphene oxide–Ag composites for rapid determination of clenbuterol. Analyst 137:4349–4355
322. Huang Y, Dong X, Liu Y, Li L-J, Chen P (2011) Graphene-based biosensors for detection of bacteria and their metabolic activities. J Mater Chem 21:12358–12362
323. Wan Y, Wang Y, Wu J, Zhang D (2011) Graphene Oxide Sheet-Mediated Silver Enhancement for Application to Electrochemical Biosensors. Anal Chem 83:648–653
324. Feng L, Chen Y, Ren J, Qu X (2011) A graphene functionalized electrochemical aptasensor for selective label-free detection of cancer cells. Biomaterials 32:2930–2937
325. Jung JH, Cheon DS, Liu F, Lee KB, Seo TS (2010) A Graphene Oxide Based Immuno-biosensor for Pathogen Detection. Angew Chem Int Ed 49:5708–5711
326. Ajjampur SSR, Rajendran P, Ramani S, et al (2008) Closing the diarrhoea diagnostic gap in Indian children by the application of molecular techniques. J Med Microbiol 57:1364–1368
327. Cao L, Cheng L, Zhang Z, Wang Y, Zhang X, Chen H, Liu B, Zhang S, Kong J (2012) Visual and high-throughput detection of cancer cells using a graphene oxide-based FRET aptasensing microfluidic chip. Lab Chip 12:4864–4869
328. Xu C, Wang X, Zhu J (2008) Graphene−Metal Particle Nanocomposites. J Phys Chem C 112:19841–19845
329. Chen S, Zhu J, Wu X, Han Q, Wang X (2010) Graphene Oxide−MnO2 Nanocomposites for Supercapacitors. ACS Nano 4:2822–2830
330. Li X, Niu J, Zhang J, Li H, Liu Z (2003) Labeling the Defects of Single-Walled Carbon Nanotubes Using Titanium Dioxide Nanoparticles. J Phys Chem B 107:2453–2458
331. Wang S, Chia P-J, Chua L-L, et al (2008) Band-like Transport in Surface-Functionalized Highly Solution-Processable Graphene Nanosheets. Adv Mater 20:3440–3446
332. Zhu J, Zeng G, Nie F, Xu X, Chen S, Han Q, Wang X (2010) Decorating graphene oxide with CuO nanoparticles in a water–isopropanol system. Nanoscale 2:988–994
333. Kudin KN, Ozbas B, Schniepp HC, Prud'homme RK, Aksay IA, Car R (2008) Raman Spectra of Graphite Oxide and Functionalized Graphene Sheets. Nano Lett 8:36–41
334. Ferrari AC, Robertson J (2000) Interpretation of Raman spectra of disordered and amorphous carbon. Phys Rev B 61:14095–14107
335. Tuinstra F, Koenig JL (1970) Raman Spectrum of Graphite. J Chem Phys 53:1126–1130

336. Tapas Kuila SB (2012) Chemical functionalization of graphene and its applications. Prog Mater Sci 57:1061–1105
337. Heydrich S, Hirmer M, Preis C, Korn T, Eroms J, Weiss D, Schüller C (2010) Scanning Raman spectroscopy of graphene antidot lattices: Evidence for systematic p-type doping. Appl Phys Lett 97:043113
338. Jin E, Lu X, Cui L, Chao D, Wang C (2010) Fabrication of graphene/prussian blue composite nanosheets and their electrocatalytic reduction of H2O2. Electrochimica Acta 55:7230–7234
339. Li L, Du Z, Liu S, Hao Q, Wang Y, Li Q, Wang T (2010) A novel nonenzymatic hydrogen peroxide sensor based on MnO2/graphene oxide nanocomposite. Talanta 82:1637–1641
340. Liu S, Tian J, Wang L, Li H, Zhang Y, Sun X (2010) Stable Aqueous Dispersion of Graphene Nanosheets: Noncovalent Functionalization by a Polymeric Reducing Agent and Their Subsequent Decoration with Ag Nanoparticles for Enzymeless Hydrogen Peroxide Detection. Macromolecules 43:10078–10083
341. Fu L, Lai G, Jia B, Yu A (2014) Preparation and Electrocatalytic Properties of Polydopamine Functionalized Reduced Graphene Oxide-Silver Nanocomposites. Electrocatalysis 6:72–76
342. Maji SK, Sreejith S, Mandal AK, Ma X, Zhao Y (2014) Immobilizing Gold Nanoparticles in Mesoporous Silica Covered Reduced Graphene Oxide: A Hybrid Material for Cancer Cell Detection through Hydrogen Peroxide Sensing. ACS Appl Mater Interfaces 6:13648–13656
343. Jung I, Field DA, Clark NJ, et al (2009) Reduction Kinetics of Graphene Oxide Determined by Electrical Transport Measurements and Temperature Programmed Desorption. J Phys Chem C 113:18480–18486
344. Zhi M, Xiang C, Li J, Li M, Wu N (2012) Nanostructured carbon–metal oxide composite electrodes for supercapacitors: a review. Nanoscale 5:72–88
345. Gautam M, Jayatissa AH (2011) Gas sensing properties of graphene synthesized by chemical vapor deposition. Mater Sci Eng C 31:1405–1411
346. Yuan W, Liu A, Huang L, Li C, Shi G (2013) High-Performance NO2 Sensors Based on Chemically Modified Graphene. Adv Mater 25:766–771
347. Yoon HJ, Jun DH, Yang JH, Zhou Z, Yang SS, Cheng MM-C (2011) Carbon dioxide gas sensor using a graphene sheet. Sens Actuators B Chem 157:310–313

348. Ghosh A, Subrahmanyam KS, Krishna KS, Datta S, Govindaraj A, Pati SK, Rao CNR (2008) Uptake of H2 and CO2 by Graphene. J Phys Chem C 112:15704–15707
349. Wang C, Yin L, Zhang L, Xiang D, Gao R (2010) Metal Oxide Gas Sensors: Sensitivity and Influencing Factors. Sensors 10:2088–2106
350. Kim H-J, Lee J-H (2014) Highly sensitive and selective gas sensors using p-type oxide semiconductors: Overview. Sens Actuators B Chem 192:607–627
351. Miller DR, Akbar SA, Morris PA (2014) Nanoscale metal oxide-based heterojunctions for gas sensing: A review. Sens Actuators B Chem 204:250–272
352. Debbichi L, Marco de Lucas MC, Pierson JF, Krüger P (2012) Vibrational Properties of CuO and Cu4O3 from First-Principles Calculations, and Raman and Infrared Spectroscopy. J Phys Chem C 116:10232–10237
353. Kohl C-D, Wagner T (eds) (2014) Gas Sensing Fundamentals. Springer Berlin Heidelberg, Berlin, Heidelberg
354. Roy BN, Wright T (1996) Electrical Conductivity in Polycrystalline Copper Oxide Thin Films. Cryst Res Technol 31:1039–1044
355. (2008) Gesundheitliche Bewertung von Kohlendioxid in der Innenraumluft. Bundesgesundheitsblatt - Gesundheitsforschung - Gesundheitsschutz 51:1358–1369
356. http://download.maritex.com.pl/pdfs/se/FIGCDM4161.pdf Technical Information for Figaro CDM4161, 01.06.2015.

Eidesstattliche Erklärung

Ich erkläre hiermit an Eides statt, dass ich die vorliegende Arbeit ohne unzulässige Hilfe Dritter und ohne Benutzung anderer als der angegebenen Hilfsmittel angefertigt habe; die aus anderen Quellen direkt oder indirekt übernommenen Daten und Konzepte sind unter Angabe des Literaturzitats gekennzeichnet.

Weitere Personen waren an der inhaltlich-materiellen Herstellung der vorliegenden Arbeit nicht beteiligt. Insbesondere habe ich hierfür nicht die entgeltliche Hilfe eines Promotionsberaters oder anderer Personen in Anspruch genommen. Niemand hat von mir weder unmittelbar noch mittelbar geldwerte Leistungen für Arbeiten erhalten, die im Zusammenhang mit dem Inhalt der vorgelegten Dissertation stehen.

Die Arbeit wurde bisher weder im In- noch im Ausland in gleicher oder ähnlicher Form einer anderen Prüfungsbehörde vorgelegt.

_____

Ort, Datum Unterschrift